Oxidative Medicine and Cellular Longevity

Antioxidants and Cancer: Theories, Techniques, and Trials in Preventing Cancer

Lead Guest Editor: Gloria M. Calaf
Guest Editors: Angeles Juarranz, Debasish Roy, Consolato M. Sergi, and Francisco Aguayo

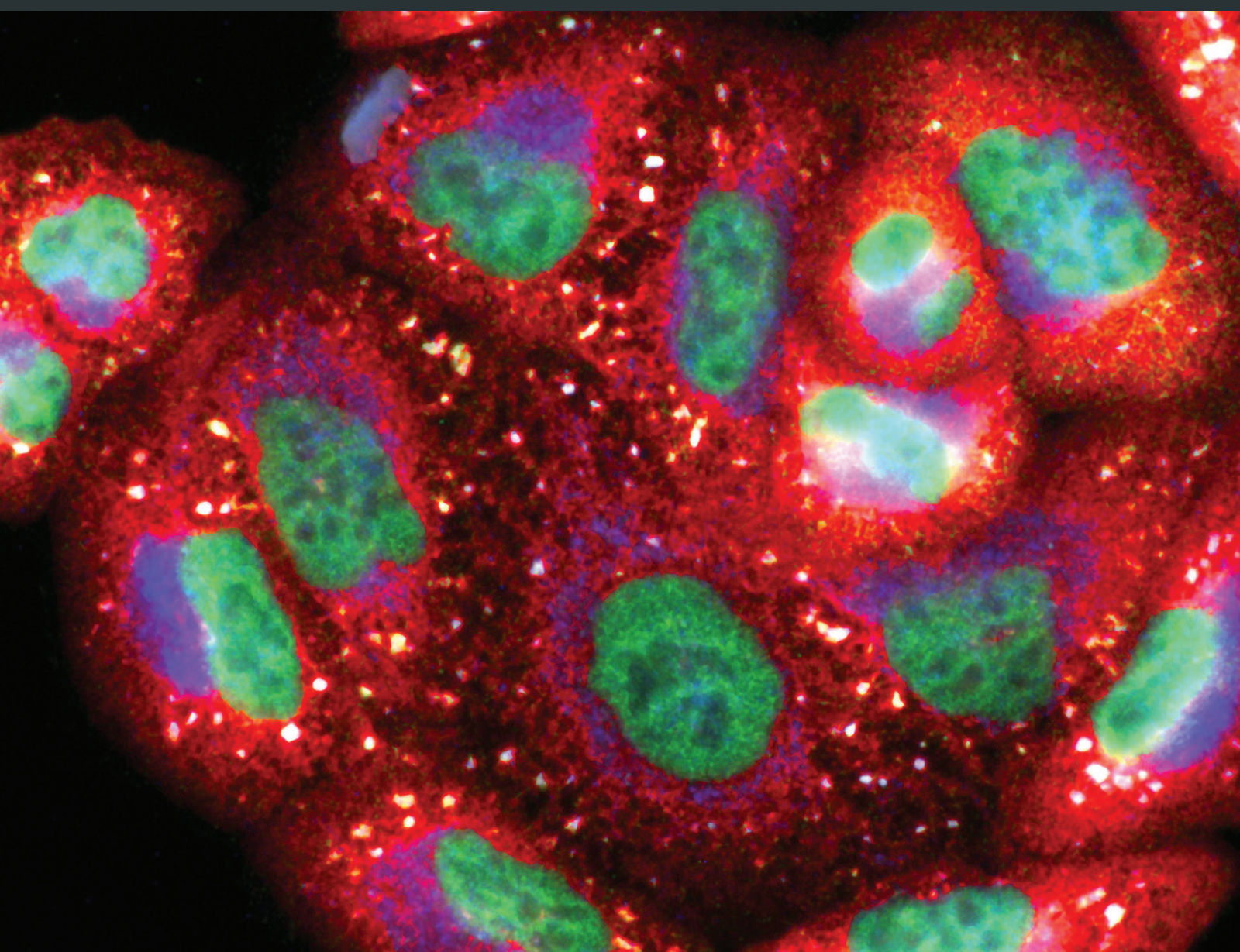

Antioxidants and Cancer: Theories, Techniques, and Trials in Preventing Cancer

Oxidative Medicine and Cellular Longevity

Antioxidants and Cancer: Theories, Techniques, and Trials in Preventing Cancer

Lead Guest Editor: Gloria M. Calaf
Guest Editors: Angeles Juarranz, Debasish Roy, Consolato M. Sergi, and Francisco Aguayo

Editorial Board

Contents

Hindawi
Oxidative Medicine and Cellular Longevity
Volume 2018, Article ID 5363064, 2 pages
https://doi.org/10.1155/2018/5363064

Editorial

Antioxidants and Cancer: Theories, Techniques, and Trials in Preventing Cancer

Gloria M. Calaf,[1,2] **Francisco Aguayo**,[3] **Consolato M. Sergi**,[4] **Angeles Juarranz**,[5,6] **and Debasish Roy**[7]

[1]*Instituto de Alta Investigación, Universidad de Tarapacá, Arica, Chile*
[2]*Center for Radiological Research, Columbia University Medical Center, New York City, NY, USA*
[3]*Departamento de Oncología Básico Clínica, Facultad de Medicina, Universidad de Chile, Santiago, Chile*
[4]*Department of Laboratory Medicine and Pathology, University of Alberta, Edmonton, AB, Canada*
[5]*Laboratory of Photocarcinogenesis, Department of Biology, Faculty of Sciences, Autonomous University of Madrid, Madrid, Spain*
[6]*Instituto Ramón y Cajal de Investigación Sanitaria (IRYCIS), Madrid, Spain*
[7]*Laboratory of Molecular Carcinogenesis, Department of Natural Science, Shirley J. Hinds Allied Health Science Complex, Hostos Community College of the City University of New York, Bronx, NY, USA*

Correspondence should be addressed to Gloria M. Calaf; gmc24@columbia.edu

Received 20 March 2018; Accepted 20 March 2018; Published 20 May 2018

Compounds of natural origin and their derivatives play an increasingly important role in medicine and pharmacology. Approximately 60% of therapeutic drugs used in the treatment of cancer are compositions comprising natural compounds and/or their derivatives.

C. G. Vazhappilly and H. P. Vasantha Rupasinghe demonstrated that an apple flavonoid fraction (AF4) can protect oxidative DNA damage *in vitro* and facilitate repair mechanisms in normal human bronchial epithelial cells exposed to carcinogen-induced DNA damage as nicotine-derived nitrosamine ketones, nitrosamine ketones-acetate, methotrexate, and cisplatin. When DNA damage and repair mechanisms were evaluated, it was found that AF4 pretreated cells showed lower cytotoxicity, total ROS generation, and DNA fragmentation along with consequent inhibition of DNA tail moment after phosphorylation of histone (γ-H2AX).

A. Ortiz-Espín et al. evaluated an extract of an Antarctic plant *Deschampsia antarctica* (EDA) in young human fibroblasts exposed to H_2O_2 to survive in extreme conditions. They measured cell proliferation, viability, and senescence-associated β-galactosidase (SA-β-Gal). They found that EDA per se promoted cell proliferation and viability and increased the expression of antisenescence-related markers. They also tested the expression of several senescence-associated proteins including redox protein thioredoxin, sirtuin 1, and lamin A/C and the replicative protein PCNA. Then, they induced senescence in human fibroblasts and they found that an EDA treatment significantly inhibited the increase in SA-β-Gal levels induced by H_2O_2 and promoted the expression of sirtuin 1 and lamin A/C proteins. The results suggest that EDA protects human fibroblasts from cellular senescence, pointing to this compound as a potential therapeutic agent to treat or prevent skin senescence.

G. Carrasco-Torres et al. used quercetin, a flavonoid considered as chemopreventive agent in different types of cancer. They demonstrated that quercetin was able to prevent and reverse rat liver preneoplastic lesions when using the modified resistant hepatocyte model by downregulating the expression of EGFR and phosphorylating the status of Src-1, STAT5, and Sp-1. Then, they concluded that quercetin reversed preneoplastic lesions and had a chemopreventive effect on the liver of rats. Plant-based compounds are still researched for their anticancer activity and for their quantity in plants. Therefore, the modern chromatographic methods are applied to quantify them

in plants, as the ultraperformance liquid chromatography-tandem mass spectrometry.

T. Kubrak et al. studied the effect of 20 coumarin derivatives on the cytotoxicity and expression of encoding proteins responsible for multidrug resistance (MDR) and genes involved in such resistance in cancer cells. Such genes are considered as the major cause of failure of cancer chemotherapy, demonstrated as overexpression of membrane transporters primarily from the ABC family which actively remove cytostatics from the tumor cell. They studied proteins as *MDR1*, *MRP*, and *LRP* and genes as *BCRP* in the presence and absence of mitoxantrone in 5 cell lines derived from the human hematopoietic system and found that leukemia cells exhibited a multidrug resistance phenotype.

M. Mehdi et al. evaluated glutamate and glucose metabolism through GDH and LDH enzyme activity, oxidant, and antioxidative status among breast cancer patients from Addis Ababa, Ethiopia. Catalytic activities of glutamate dehydrogenase, lactate dehydrogenase, and oxidative stress index were significantly increased both in serum and cancerous tissues of breast cancer patients as compared to control groups of breast cancer patients. They concluded that catalytic activities of GDH and LDH among breast cancer patients were significantly higher than control groups and noncancerous tissues of breast cancer patient. A problem of cancer chemotherapy is the high cytotoxicity toward normal rapidly proliferating cells, especially the bone marrow. In order to mitigate side effects, modified therapeutic regimens such as combination therapy have been introduced.

A. Och et al. studied the content of alkaloids as sanguinarine, berberine, protopine, and chelidonine, unidentified in plant species known for their anticancer activity. Plant-based compounds are still researched for their anticancer activity and for their quantity in plants. Therefore, the modern chromatographic methods are applied to quantify them in plants, for example, UPLC-MS/MS (ultraperformance liquid chromatography-tandem mass spectrometry).

Gloria M. Calaf
Francisco Aguayo
Consolato M. Sergi
Angeles Juarranz
Debasish Roy

Hindawi
Oxidative Medicine and Cellular Longevity
Volume 2018, Article ID 6039453, 13 pages
https://doi.org/10.1155/2018/6039453

Research Article

Blood and Tissue Enzymatic Activities of GDH and LDH, Index of Glutathione, and Oxidative Stress among Breast Cancer Patients Attending Referral Hospitals of Addis Ababa, Ethiopia: Hospital-Based Comparative Cross-Sectional Study

Mohammed Mehdi,[1] **M. K. C. Menon**,[1] **Nebiyou Seyoum**,[2] **Mahteme Bekele**,[3] **Wondimagegn Tigeneh**,[4] **and Daniel Seifu**[1]

[1]*Department of Biochemistry, College of Health Sciences, School of Medicine, Addis Ababa University, Addis Ababa, Ethiopia*
[2]*Department of Surgery, College of Health Sciences, School of Medicine, Addis Ababa University, Addis Ababa, Ethiopia*
[3]*Department of Surgery, St. Paul Hospital, Millennium Medical College, Addis Ababa, Ethiopia*
[4]*Department of Oncology, College of Health Sciences, School of Medicine, Addis Ababa University, Addis Ababa, Ethiopia*

Correspondence should be addressed to Mohammed Mehdi; mohammed.mehdi@aau.edu.et

Received 25 July 2017; Accepted 29 January 2018; Published 26 March 2018

Academic Editor: Gloria M. Calaf

The exact cause of breast cancer is unknown; it is a multifactorial disease. It is the most diagnosed and the second killer cancer among women. Breast cancer can be originated from tissues of breast or secondary from other organs via metastasis. Generally, cancer cells show aberrant metabolism and oxidative stress when compared to noncancerous tissues of breast cancer patients. The current study aims at evaluating glutamate and glucose metabolism through GDH and LDH enzyme activities, oxidant, and antioxidative status among breast cancer patients attending referral hospitals of Addis Ababa, Ethiopia. *Result.* Catalytic activities of glutamate dehydrogenase, lactate dehydrogenase, and oxidative stress index were significantly increased in both serum (4.2 mU/ml, 78.6 mU/ml, and 3.3 : 1, resp.) and cancerous tissues (1.4 mU/ml, 111.7 mU/ml, and 2.15 : 1, resp.) of breast cancer patients as compared to those in serum of control group (3.15 mU/ml, 30.4 mU/ml, and 2.05 : 1, resp.) and noncancerous tissues of breast cancer patients (0.92 mU/ml, 70.5 mU/ml, and 1.1 : 1, resp.) ($P \leq 0.05$). Correspondingly, ratios of reduced to oxidized glutathione were significantly decreased in both serum (20 : 1) and cancerous tissues (23.5 : 1) of breast cancer patients when compared to those in serum of control group (104.5 : 1) and noncancerous tissues of breast cancer patients (70.9 : 1) ($P \leq 0.05$). *Conclusion.* Catalytic activities of GDH and LDH, ratios of GSH to GSSG, and concentration of TOS among breast cancer patients were significantly higher than were those among control group and noncancerous tissues of breast cancer patients, while TAC of breast cancer patients is significantly lower than that of control group and normal tissues of breast cancer patients.

1. Background

Breast cancer is a multifactorial and devastating disease. It is characterized by its uncontrolled growth and spread of atypical breast cells [1, 2]. Globally among women, breast cancer is the most frequently diagnosed and second leading cause of cancer death. As the global burden of breast cancer and its comorbidities has increased, it is evident that novel diagnostic and therapeutic approaches will be necessary to address the breast cancer epidemic. According to the report of American Cancer Society, from 2009 to 2013 in the USA, the incident rate of breast cancer was 123.3/100,000 and death rate from 2010 to 2014 was 21.2/100,000. In 2017, it is estimated to diagnose new 252,710 invasive and 63,410 in situ cases and 40,610 death of breast cancer patients. Considering incidence trend of breast cancer from 2004 to 2013,

invasive breast cancer seems to be stable in white women, but in black women, it was increased by 0.5% [3].

Otto Warburg and his coworkers were the first to study the metabolism of cancer in the 1920s. According to their thought, cancer is a metabolic disease. When normal cells are deprived 35% of their oxygen supply, they will either die or turn into cancer cells. Cancer cells are not like a normal cell, lack the "intelligence" as a result of their division and will be uncontrolled. Such uncontrolled oncogene-driven proliferation of cancer cells and the absence of an efficient vascular bed cause low oxygen tension (hypoxia), forced cancer cells to live in conditions of aerobic glycolysis. Under aerobic conditions, tumor tissues can metabolize approximately tenfold more glucose to lactate in a given time than can normal tissues. Such acidic condition favors tumor invasion and suppresses anticancer immune effectors. Lactate that is produced by tumor cells can be taken up by stromal cells, to regenerate pyruvate that either can be squeezed out to refuel the cancer cell or can be used for oxidative phosphorylation [4–8].

Additional to the Warburg effect, intermediates of glycolysis in cancer cells can be used for the synthesis of protein, nucleotides, and fatty acids [9–11]. Shunting of glucose into aerobic glycolysis causes a reduction in Krebs cycle intermediates "pulls" glutamate through GDH generating α-ketoglutarate (αKG). This is proved by the higher steady state of NH_4^+/Gln ratio greater than 1. Ammonium to alanine produced ratio will be increased. This will indicate the increased GDH and decreased ALT flux results in reduced intramitochondrial pyruvate (metabolized in the cytosol to lactate). Thus, the increased glutamate flux through GDH generates αKG while sparing ketoacid consumption (reduced transamination) [12].

Sparing of glutamate for Krebs cycle intermediates may cause oxidative stress in cancer patients; this may be due to the decreased synthesis of glutathione (major internal antioxidant). All in all, oxidative stress occurs as a result of an imbalance or state of oxidation exceeds the antioxidant systems of the body [13]. Reducing substances in the human body controls the status of over oxidation, and a continuing imbalance in support of oxidation causes different problems when it beats the limit of such control. Free radicals and antioxidant can reinforce differing impacts on cells according to their concentration. Reactive oxygen species may participate in carcinogenesis through induction of gene mutations that result in cell damage and the consequences of signal transduction and transcription factors, and the redox status of cancer cells usually differs from that of normal cells [14]. Because of metabolic and signaling aberrations, cancer cells exhibit elevated ROS levels and it is balanced by an increased antioxidant capacity, which suggests that high ROS levels may constitute a barrier to tumorigenesis [15].

The present study aimed at identifying early metabolic biomarkers for diagnosis, prognosis, and therapeutic targets for breast cancer diseases. This might be possible through evaluation of GDH and LDH enzyme activities, reduced and oxidized glutathione, and oxidative stress index (TOS/TAC) of cancerous tissues and serum of breast cancer patients as compared to serum of control group and adjacent noncancerous tissues of the same patients attending referral hospitals of Addis Ababa, Ethiopia.

1.1. Methodology. A comparative cross-sectional study was conducted at five major referral hospitals [Tikur Anbessa Specialized Hospital, Zewditu Memorial Hospital, St. Paul Specialized Hospital, Menelik the Second Hospital, and Yekatit 12 Hospital] and one health center of Addis Ababa, Ethiopia. The study was conducted from July 2015 to May 2017; accordingly, 27 breast cancer patients and 27 normal individuals as control group were included.

1.2. Blood and Tissue Sample Collection Procedure. Before surgery, the patients were well informed and made aware of the aim of the study. Then, blood samples and their responses to questionnaires were collected by professional nurses. After surgery, the cancerous tissue and adjacent noncancerous tissue samples were collected from the patients.

1.3. Tissue Samples. A total of 54 tissue samples (27 tumor tissues and 27 normal tissues) were collected from 27 breast cancer patients. The collection and fixation of cancerous tissue and adjacent noncancerous tissue was done by attending surgeons of the Surgery Department at the operation room using cold phosphate buffer saline (PBS) and dimethyl sulfoxide (DMSO) and then stored at −80°C of the deep freezer until analysis. During the actual process, portions of the solid tumor, free of fat, connective tissue, necrotic debris, and blood, were cut into pieces of approximately $3 \times 3 \times 3$ mm and frozen quickly (Figure 1). The staging of breast cancer was done by pathologist, and it was based on tumor size, nodal involvement, and metastasis (TNM) staging method.

1.4. Blood Samples. A total of 54 blood samples (27 breast cancer patients and 27 control group) with a volume of 3–5 ml were collected using serum separator tube (SST). Serum samples were harvested into Eppendorf tube after the blood samples were centrifuged at 4000 rpm for five minutes and stored at −80°C deep freezer until the laboratory analysis.

1.5. Homogenization of Tissue Sample. Tissue samples were thawed and sliced into five, approximately 50 to 100 mg wet weight. Each aliquot was homogenized in cold 0.05 M KPE buffer (pH 7.4), 0.1 M phosphate buffer (pH 7.4), 0.1 M Tris-HCl buffer (pH 9.0), and 0.1 M phosphate buffer saline (pH 7.4) for the analysis of GSH and GSSG, LDH, GDH, TOS, and TAC, respectively. Then, the supernatant of the homogenates was taken for determinations of GSH and GSSG, LDH, GDH, TOS, and TAC after centrifugation in 10,000 rpm for 10 min (Figure 1).

1.6. Chemicals and Equipment Used. Glutamate dehydrogenase (GDH), lactate dehydrogenase (LDH), reduced form glutathione (GSH), oxidized form glutathione (GSSG), total protein, total oxidative status (TOS), and total antioxidant capacity (TAC) were determined using the following kits and chemicals bought from Sigma-Aldrich, Merck, and BDH Chemical Company: potassium dihydrogen orthophosphate (KH_2PO_4), dipotassium hydrogen orthophosphate (K_2HPO_4), EDTA sodium salt, sulfosalicylic acid, Triton

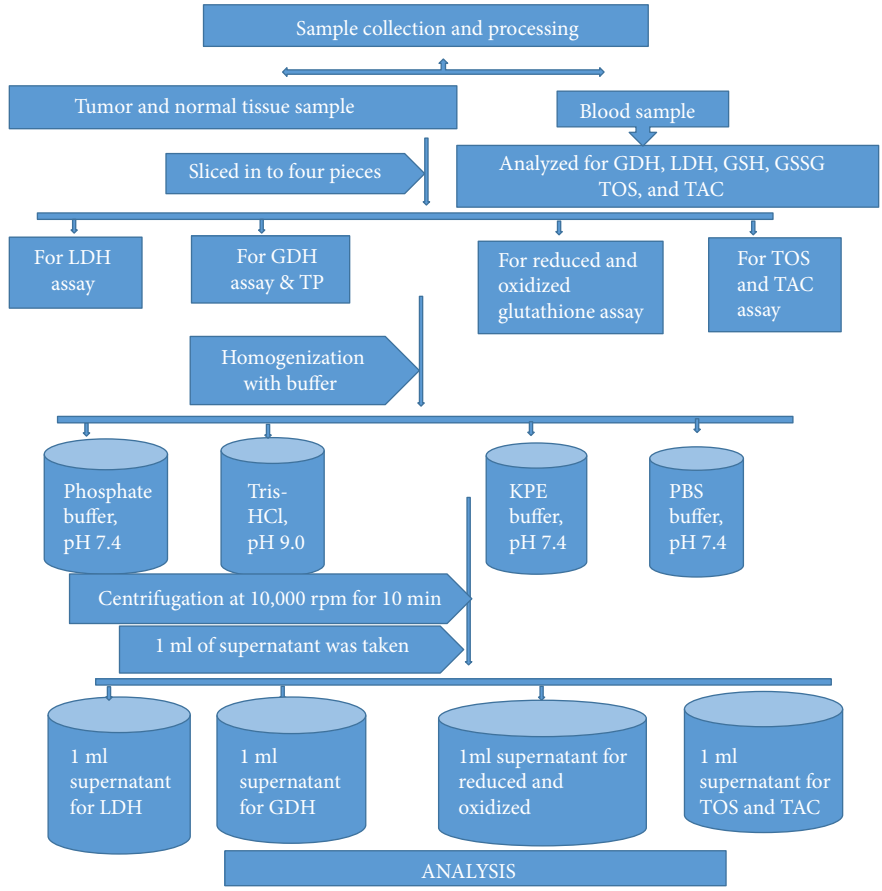

Figure 1: Chart showing the workflow of sample processing, Addis Ababa, Ethiopia, 2015–2017.

X-100, DTNB, β-NADPH, glutathione reductase, reduced form glutathione (GSH), glutathione (disulfide form) (GSSG), triethanolamine and 2-vinylpyridine, xylenol orange, bovine serum albumin (BSA) (Sigma-Aldrich), BCA protein assay reagents, sodium chloride (NaCl), sulfuric acid (H_2SO_4), glycerol, ferrous ammonium sulfate, *o*-dianisidine dihydrochloride, sodium acetate (CH_3COONa), glacial acetic acid, 35%, H_2O_2 solution, 2,2′-azino-bis(3-ethylbenzthiazoline-6-sulfonic acid) (ABTS), and Trolox (6-hydroxy-2,5,7,8-tetramethylchroman-2-carboxylic acid). The equipment used was Eppendorf tube and Falcon centrifuge tube (Multifuge), ultraviolet/visible spectrophotometer (Jenway, 6705, UK), ELISA plate reader (Biotest, 2001, Austria), homogenizer (Heidolph, RZR 2100), water path (GFL, 1002, Germany), and magnetic stirrer.

1.7. Glutamate Dehydrogenase (GDH) Assay Principle. The change of NAD^+ to NADH is measured spectrophotometrically at 340 nm and is relative to the activity of glutamate dehydrogenase [16]. The test results were expressed as mU/l.

$$\text{Glutamate} + \text{NAD}^+ \overset{\text{GDH}}{\rightleftarrows} \alpha\text{-Ketoglutaric acid} + \text{NADH}. \quad (1)$$

1.8. Lactate Dehydrogenase (LDH) Assay Principle. It was determined based on the principles of Vassault. The consumption of NADH was measured using spectrophotometer at 340 nm [17].

$$\text{NADH} + \text{H}^+ + \text{Pyruvate} \overset{\text{LDH}}{\rightleftarrows} \text{Lactate} + \text{NAD}^+. \quad (2)$$

1.9. Total Glutathione (GSH) Assay Principle. It was determined based on the principles of Rahman et al. [18]. The assay depends on the reaction of GSH with DTNB that produces the TNB chromophore and oxidized glutathione–TNB adduct (GS–TNB). The rate of formation of TNB, measured at 412 nm, is proportional to the concentration of GSH in the sample. The disulfide product (GS–TNB) is then reduced by GR in the presence of NADPH, recycling GSH back into the reaction. Because GR reduces the GSSG formed into 2GSH, the amount of glutathione measured represents the sum of reduced and oxidized glutathione in the sample ([GSH] total = [GSH] + 2 × [GSSG]) [18].

$$\begin{aligned} 2\text{GSH} + \text{DTNB} &\overset{\text{GR}}{\rightarrow} \text{TNB} + \text{GS-TNB}, \\ \text{GS-TNB} + \text{NADPH} &\overset{\text{GR}}{\rightarrow} 2\text{GSH} + \text{NADP}^+. \end{aligned} \quad (3)$$

1.10. Oxidized Glutathione (GSSG) Assay Principle. It was determined based on the principles of Rahman et al. [18]. The principle used GSSG reductase recycling method. By monitoring NADPH spectrophotometrically at a wavelength of 340 nm, the amount of GSSG was determined. The

samples are treated with 2-vinylpyridine, which covalently reacts with GSH (but not GSSG). The excess 2-vinylpyridine is neutralized with triethanolamine [18].

$$\text{GSSG} + \text{NADPH} \xrightarrow{\text{GR}} 2\text{GSH} + \text{NADP}^{+}. \quad (4)$$

1.11. Total Protein Assay Method and Principle. Determination of total protein in serum and tissue of the study participants was done based on the method of Smith et al. [19]. The principle of this method is that proteins in the sample reduce Cu^{+2} to Cu^{+1} in an alkaline solution (the biuret reaction) and result in a purple color formation by bicinchoninic acid (BCA). The absorbance was read at wavelength of 562 nm.

1.12. Total Oxidant Status (TOS) Assay Principle. It was determined based on the principles of Erel [20]. In this process, oxidants present in the sample oxidize the ferrous particle *o*-dianisidine complex to the ferric particle. The oxidation reaction is upgraded by glycerol molecules, which are richly present in the reaction medium. A colored compound is formed when the ferric ion reacts with xylenol orange in an acidic medium. The color strength, which can be measured spectrophotometrically at 560 nm wavelength, is correlated to the total quantity of oxidant molecules present in the plasma. The assay is aligned with hydrogen peroxide, and the outcomes are expressed as far as μmolar hydrogen peroxide equivalent per liter (μmol H_2O_2 Eq/l) [20].

1.13. Total Antioxidant Capacity (TAC) Assay Principle. It was determined based on the principles of Koracevic et al. [21]. In this technique, the hydroxyl radical, the most powerful natural radical, is generated by the Fenton reaction and it responds with the colorless substrate *o*-dianisidine to create the dianisyl radical, which is splendid yellowish brown in color. Upon the addition of sample, the oxidative responses started by the hydroxyl radicals present in the reaction are scavenged by the antioxidant agents present in the sample, keeping the color change and consequently giving a viable estimation of TAC [21]. The test results were expressed as mmol Trolox Eq/l.

1.14. Determination of Oxidative Stress Index (OSI). It was calculated based on the method of Erel [20]. The proportion of TOS to TAC is acknowledged as the oxidative stress index (OSI). For estimation, the subsequent unit of TAC is changed over to mmol/l, and the OSI value is computed [20].

$$\text{OSI (subjective unit)} = \frac{\text{TOS}(\mu\text{mol } H_2O)}{\text{TAC}(\text{mmol TroloxEq/l})} \times 100. \quad (5)$$

1.15. Data Processing and Software Used in Statistical Analysis. All data were checked, cleared and fed into EpiData (version 3.5.1, 2008), and then exported to SPSS (version 22.0, 2012, America) software for statistical analysis. Descriptive analysis, Spearman correlation, linear regression, independent sample *t*-test, and one-way ANOVA followed by post hoc analysis were used for this study. All data were expressed in mean ± SD, and $P \leq 0.05$ was considered as statistically significant.

1.16. Ethical Approval. The study was ethically approved from the Ethical Review Committee of Biochemistry Department College of Health Sciences, Addis Ababa University, with protocol number 09/15 and meeting number DRERC 09/15.

2. Results

2.1. Socio-Demographic Profile. A total of 54 (27 breast cancer patients and 27 normal individuals as control group) participants were recruited. These were from five major referral hospitals of Addis Ababa, Ethiopia, and one health center. These were Tikur Anbessa Specialized Hospital (TASH), St. Paul Specialized Hospital (SPH), Zewditu Memorial Hospital (ZMH), Yekatit 12 Hospital (YH), Menelik the Second Hospital (MH), and Teklehaimanot Health Center (THC). Most of the participants were from Tikur Anbessa Specialized Hospital (13 patients, 48.1%) and St. Paul Specialized Hospital (6 patients, 22.2%).

Socio-demographic profiles of participants are presented in Table 1. All participants were female, and their mean age was 44.93 with a minimum age of 25 to a maximum age of 68. Thirteen of them were less than or equal to 40 years old, and fourteen of them were greater than 40 years old. Consecutively, sex- and age-matched control samples were also collected.

Out of the 27 breast cancer patients, 17 (63.0%) were living in urban areas and 10 (37.0%) were living in rural areas. Twelve of breast cancer patients (44.5%) were illiterate, 17 (63.0%) of them were married, 15 (55.6%) of them gave birth, had at least 1 and at most 4 children, 15 (55.6%) of them feed their children with breast milk, 14 (51.9%) of them used birth control, 16 (59.3%) of them were premenopausal, and 3 (11.1%) of them were obese (Table 1).

2.2. Clinical and Histopathological Findings. Clinical and histopathological results of all breast cancer patients were studied and tabulated in Table 2. From each breast cancer patient, tumor tissue, noncancerous tissue (5 cm away from cancerous tissue), and blood sample were collected. Histology of tumor tissues was graded as low-grade or well-differentiated (9 patients, 33.3%), intermediate grade (intermediately differentiated) (10 patients, 37.0%), and high-grade (poorly differentiated) (8 patients, 29.6%) cases. Staging of tumor tissues was done based on tumor size; all tumor tissues were classified into five stages. Out of which, 5 patients (18.5%) were in stage zero, 4 patients (14.8%) were in stage one, 7 patients (25.9%) were in stage two, 8 patients (29.6%) were in stage three, and 3 patients (11.1%) were in stage four. Based on invasiveness, tumor tissues were categorized into invasive ductal carcinoma (11 patients, 40.7%), invasive lobular carcinoma (5 patients, 18.5%), ductal carcinoma in situ (8 patients, 29.6%), and lobular carcinoma in situ (3 patients, 11.1%) (Table 2).

2.3. Biochemical Analysis

2.3.1. Serum and Tissue Enzymatic Activity of Glutamate Dehydrogenase (GDH). Glutamate dehydrogenase (GDH) activity was determined and normalized by dividing with

Table 1: Descriptive analysis of socio-demographic profile of breast cancer (BCA) patients and control group at the five referral hospitals and one health center of Addis Ababa, Ethiopia, 2015–2017.

Socio-demographic data of BCA and control group		BCA patients ($N = 27$) N (%)	Control group ($N = 27$) N (%)
Age (yr.)	≤40	13 (48.1)	14 (51.9)
	>40	14 (51.9)	13 (48.1)
Residence	Urban	17 (63.0)	19 (70.4)
	Rural	10 (37.0)	8 (29.6)
Education level	Illiterate	12 (44.5)	0 (0.0)
	High school or less	11 (40.7)	14 (51.9)
	College and above	4 (14.8)	13 (48.1)
Marital status	Single	7 (25.9)	18 (66.7)
	Married	17 (63.0)	9 (33.3)
	Widowed	3 (11.1)	0 (0.0)
Child birth	Yes	15 (55.6)	7 (25.9)
	No	12 (44.4)	20 (74.1)
No. of children	0	12 (44.4)	20 (74.1)
	1–4	14 (51.9)	7 (25.9)
	≥5	1 (3.7)	0 (0.0)
Breast feeding	Yes	15 (55.6)	7 (25.9)
	No	12 (44.4)	20 (74.1)
Birth control	Yes	14 (51.9)	5 (18.5)
	No	13 (48.1)	22 (81.5)
Menopausal status	Pre	16 (59.3)	21 (77.8)
	Post	11 (40.7)	6 (22.2)
Body mass index (kg/m^2)	Under weight (<18.5)	4 (14.8)	2 (7.4)
	Normal weight (18.5–24.9)	14 (51.9)	18 (66.7)
	Over weight (25–29.9)	6 (22.2)	4 (14.8)
	Obese (≥30)	3 (11.1)	3 (11.1)

total protein in serum and tissues of the study participants. The catalytic activities of GDH in serum samples of breast cancer patients and control group were significantly different ($P < 0.05$) (95% CI (0.8–1.3)). Glutamate dehydrogenase in serum samples of breast cancer patients were 4.20 ± 0.72 mU/l, whereas in control group, it was 3.15 ± 0.69 mU/l. Similarly, catalytic activities of GDH in cancerous and noncancerous tissues of breast cancer patients were assessed and were significantly different ($P < 0.05$) (95% CI (0.12–0.82)). The cancerous tissues had enzymatic activities of GDH in comparison with noncancerous tissues (0.92 ± 0.73 and 1.4 ± 0.88 mU/l, resp.) (Tables 3 and 4).

2.4. Serum and Tissue Enzymatic Activities of Lactate Dehydrogenase (LDH). Enzymatic activities of LDH in serum and tissue samples from breast cancer patients were investigated in comparison to those in serum samples from control group and normal tissues of breast cancer patients. Results were normalized by the amount of total protein in serum and tissue of the study participants. Serum LDH activities of breast cancer patients were significantly higher than were those of control group (78.6 ± 113 and 30.4 ± 32.6 mU/l, resp.) ($P < 0.05$) (95% CI (3.4–92.9)) (Table 4). Similarly, cancerous tissues had a higher LDH activities than had noncancerous tissues (111.7 ± 23.2 and 70.5 ± 10.7 mU/l), and it was statistically significant ($P < 0.05$) (95% CI (−7.5–89.9)) (Tables 3 and 4).

2.5. Serum and Tissue Levels of Glutathione. The concentration of reduced and oxidized glutathione in serum and tissue samples of breast cancer patients was examined (Tables 3 and 4). Results were normalized by the amount of total protein in serum and tissue of the study participants. Oxidized glutathione in serum of breast cancer patients was significantly ($P \leq 0.05$) higher than was that of control group (0.51 ± 0.2 and 0.2 ± 0.1 μM/μg of total protein, resp.). Similarly, cancerous tissues of breast cancer patients showed a significantly ($P \leq 0.05$) higher oxidized glutathione than did noncancerous tissues of breast cancer patients (0.47 ± 0.3 and 0.21 ± 0.1 μM/μg of total protein, resp.).

Consecutively, serum of breast cancer patients was significantly lower in reduced glutathione as compared to serum of control group (10.2 ± 2.9 and 20.9 ± 2.6 μM/μg

Table 2: Descriptive analysis of clinical and pathological profiles of breast cancer (BCA) patients attending referral hospitals of Addis Ababa, Ethiopia, 2015–2017.

Clinicopathological profile of BCA ($N = 27$)		N (%)
Family history of BCA	Yes	7 (25.9)
	No	20 (74.1)
Location of breast cancer	Right breast	17 (63)
	Left breast	10 (37)
Tumor size	pT1 (0.1–2 cm)	9 (33.3)
	pT2 (2–5 cm)	8 (29.6)
	pT3 (>5 cm)	3 (11.1)
	pT4 (extension to the chest wall/skin)	7 (25.9)
Nodal status	pN0	10 (37.0)
	pN1	12 (44.4)
	pN2	3 (11.1)
	pN3	2 (7.4)
Metastasis	Mx	2 (7.4)
	M0	23 (85.2)
	M1	2 (7.4)
Stage of BCA	0	5 (18.5)
	I	4 (14.8)
	II	7 (25.9)
	III	8 (29.6)
	IV	3 (11.1)
Grading	Low grade (well differentiated)	9 (33.3)
	Intermediate grade (moderately–differentiated)	10 (37.1)
	High grade (poorly–differentiated)	8 (29.6)
Histology of cancer	Invasive ductal carcinoma	11 (40.7)
	Invasive lobular carcinoma	5 (18.5)
	Ductal carcinoma in situ	8 (29.6)
	Lobular carcinoma in situ	3 (11.1)

Table 3: Comparative mean analysis of serum enzymatic activities of GDH and LDH, concentration of glutathione, and the oxidative stress index of breast cancer (BCA) patients ($N = 27$) and control group ($N = 27$), Addis Ababa, Ethiopia, 2015–2017.

Serum parameters	Control group	BCA patients	Mean diff.	P value	95% CI
GDH (mU/l)	3.15 ± 0.69	4.20 ± 0.72	1.04	≤0.001	(0.8–1.3)
LDH (mU/l)	30.4 ± 32.6	78.6 ± 113	48.2	0.036*	(3.4–92.9)
GSH (μM per μg of protein)	20.9 ± 2.6	10.2 ± 2.9	−10.7	≤0.001	(4.3–6.0)
GSSG (μM per μg of protein	0.2 ± 0.1	0.51 ± 0.2	0.31	≤0.001	(0.8–1.2)
TOS (μmol H_2O_2 Eq/l)	2.32 ± 1.0	2.75 ± 1.1	0.43	≤0.001	(0.39–1.27)
TAC (mmol Trolox Eq/l)	100.9 ± 29.8	83.5 ± 30.3	−13.65	0.017*	(−24.7 to −2.6)
OSI (ratio of TOS/TAC*100)	2.3 ± 1.5	3.3 ± 1.7	1.0	0.006*	(0.32–1.67)
Total protein (μg/ml)	59.7 ± 29.3	208 ± 11.8	148.22	0.001*	(143.56–152.87)

*The mean difference is significant at P value ≤ 0.05.

of total protein, resp.) ($P < 0.05$). Correspondingly, reduced glutathione in cancerous tissue and noncancerous tissue of breast cancer patients was statistically different ($P \leq 0.05$); tumor tissues had a lower reduced glutathione than had normal tissues (11.03 ± 2.0 and 14.9 ± 2.7 μM/μg of total protein, resp.). Furthermore, ratios of reduced (GSH) to oxidized glutathione (GSSG) in serum and cancerous tissues of breast cancer patients (19.9 : 1 and 32.3 : 1, resp.) were significantly ($P \leq 0.05$) decreased as compared to those in serum samples of control group and noncancerous

Table 4: Comparative mean analysis of tissue enzymatic activities of GDH and LDH, concentration of glutathione, and the oxidative stress index of noncancerous tissues ($N = 27$) and cancerous tissues ($N = 27$), Addis Ababa, Ethiopia, 2015–2017.

Tissue parameters	Normal tissue	Tumor tissue	Mean diff.	P value	95% CI
GDH (mU/l)	0.92 ± 0.73	1.40 ± 0.88	0.5	0.011*	(0.12–0.82)
LDH (mU/l)	70.5 ± 10.7	111.7 ± 23.2	41.2	0.009*	(−7.5 to 89.9)
GSH (μM per μg of protein)	14.9 ± 2.7	11.03 ± 2.0	−3.87	0.029*	(−0.2 to 0.8)
GSSG (μM per μg of protein)	0.21 ± 0.1	0.47 ± 0.3	0.26	0.003*	(0.09–0.02)
TOS (μmol H_2O_2 Eq/l)	2.1 ± 0.9	3.5 ± 1.1	1.4	≤0.001	(0.33–1.22)
TAC (mmol Trolox Eq/l)	188.9 ± 26.7	161.6 ± 50.8	−27.32	0.01*	(−47.42 to −7.2)
OSI (ratio of TOS/TAC*100)	1.1 ± 0.5	2.15 ± 1.8	1.05	0.002*	(0.3–1.22)
Total protein (μg/ml)	149.4 ± 54.2	194.9 ± 27.4	45.5	0.001*	(34.7–56.4)

*The mean difference is significant at P value ≤ 0.05.

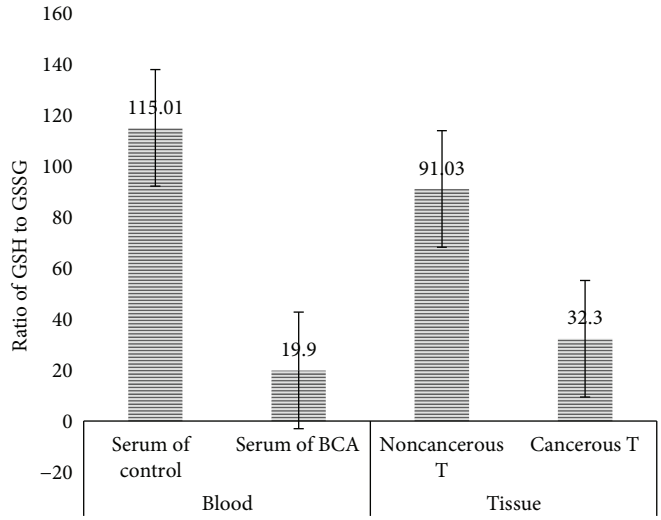

Figure 2: A bar graph showing glutathione index in serum and cancerous tissues of breast cancer (BCA) patients in comparison to serum of control group and noncancerous tissues of breast cancer patients, Addis Ababa, Ethiopia, 2015–2017.

tissue of breast cancer patients (30.7 : 1 and 75 : 1, resp.) (Figure 2).

2.6. Serum and Tissue Levels of TOS and TAC. The concentration of total oxidative status (TOS) of breast cancer patients and control group was examined (refer to Tables 4 and 5). Total oxidative status in serum of breast cancer patients (3.3 ± 1.7 μmol H_2O_2 Eq/l) was significantly ($P \leq 0.05$) higher than was that of control group (2.3 ± 2.0 μmol H_2O_2 Eq/l) (Tables 3 and 4). Within tissue samples of breast cancer patients, total oxidative status in tumor tissues (2.15 ± 1.8 μmol H_2O_2 Eq/l) was significantly ($P \leq 0.05$) higher than was that in normal tissues (1.1 ± 0.5 μmol H_2O_2 Eq/l) (Tables 3 and 4).

In serum sample of breast cancer patients, there was a significantly ($P \leq 0.05$) lower amount of TAC concentration (83.5 ± 30.3 mmol Trolox Eq/l) than that of control group (100.9 ± 29.8 mmol Trolox Eq/l). In tissue sample of breast cancer patients, TAC in tumor tissues was significantly ($P \leq 0.05$) lower in the concentration of TAC (161.6 ± 50.8 mmol Trolox Eq/l) than that in normal tissues (188.9 ± 26.7 mmol Trolox Eq/l) and their mean difference among tissue samples of breast cancer patients was statistically significant (Tables 3 and 4).

2.7. Oxidative Stress Index (OSI). Likewise, OSI in serum and tissue samples of breast cancer patients and control group was explored. Serum samples of breast cancer patients had a significantly higher OSI value (3.3 ± 1.7) than control group (2.3 ± 2.0), and the difference was statistically significant ($P = 0.006$). Within tissues of breast cancer patients, cancerous tissues had a higher OSI (2.15 ± 1.8) value than noncancerous tissues (1.1 ± 0.5) ($P = 0.002$) (Tables 3 and 4 and Figure 3).

2.8. Comparison of Different Parameters of Serum and Tissues within the Numerous Stages Identified in Breast Cancer Patients. Blood and tissue parameters of GDH, LDH, GSH,

Table 5: A one-way ANOVA (post hoc) analysis of serum and tissue parameters in control subjects and pathologically confirmed breast cancer patients participated from five hospitals of Addis Ababa, Ethiopia ($N = 27$), 2015–2017.

Serum and tissue parameters of BCA	Sample	Stages of breast cancer patients				
		Stage 0 ($N = 5$)	Stage I ($N = 4$)	Stage II ($N = 7$)	Stage III ($N = 8$)	Stage IV ($N = 3$)
GDH	S	4.6 ± 0.4	4.1 ± 0.5	4.13 ± 0.91	4.2 ± 0.9	3.7 ± 0.45
	T	0.7 ± 0.2[a]	1.2 ± 0.6	1.24 ± 0.71	1.9 ± 1.1[a]	1.78 ± 1.15
LDH	S	77.7 ± 27.1	80.9 ± 38.7	138.7 ± 61.9	57.6 ± 5.4	90.0 ± 11.7
	T	42.4 ± 4.1[b]	63.8 ± 5.1[b]	67.7 ± 3.1[b]	131.3 ± 8.4[b]	341.8 ± 41.4[b]
GSH	S	5.4 ± 2.4	5.9 ± 0.5	5.8 ± 1.8	7.0 ± 3.3	6.3 ± 0.6
	T	1.0 ± 0.3	1.2 ± 0.5	2.0 ± 1.9	1.4 ± 1.5	1.5 ± 0.7
GSSG	S	1.1 ± 0.5	1.2 ± 0.1	1.1 ± 0.4	1.4 ± 0.6	1.2 ± 0.1
	T	0.3 ± 0.1	0.3 ± 0.04	0.2 ± 0.1	0.3 ± 0.1	0.2 ± 0.03
TOS	S	1.4 ± 0.4[c]	3.4 ± 1.3[c]	2.4 ± 0.7	3.2 ± 1.16[c]	2.8 ± 0.6[c]
	T	3.2 ± 0.3	2.3 ± 0.4	3.3 ± 1.6	2.5 ± 1.2	2.4 ± 0.8
TAC	S	0.90 ± 0.29	0.84 ± 0.14	0.87 ± 0.21	0.90 ± 0.34	0.77 ± 0.47
	T	1.84 ± 0.23	1.44 ± 0.33	1.86 ± 0.40	1.46 ± 0.59	1.12 ± 0.83
OSI	S	2.47 ± 0.87	2.15 ± 1.29	2.96 ± 1.8	3.57 ± 2.06	3.98 ± 1.23
	T	2.1 ± 0.87	1.13 ± 0.84[d]	1.78 ± 0.4	1.69 ± 0.83	3.03 ± 2.9[d]
Total protein	S	212.1 ± 14.4	209.7 ± 8.6	197.3 ± 8.6	210.9 ± 11.6	215.3 ± 4.34
	T	175.9 ± 51.9	193.8 ± 30.7	195.1 ± 6.5	200.8 ± 12.8	212.2 ± 27.3

[a]Mean difference of GDH between stages 0 and III of tissue sample ($P \leq 0.05$), [b]mean difference of LDH between stages IV and 0, I, II, and III of tissue sample ($P \leq 0.001$, 0.001, 0.001, and ≤0.05, resp.), [c]mean difference between stages 0 and I, III, and IV ($P \leq 0.05$) of blood sample, and [d]mean difference of OSI among stages I and IV in tissue of BCA ($P \leq 0.05$) were statistically significant. NB: measuring units of GDH and LDH are in mU/l, GSH and GSSG were in μM/μg of total protein, TOS is in μmol H_2O_2 Eq/l, TAC is in mmol Trolox Eq/l, and total protein is in μg/ml.

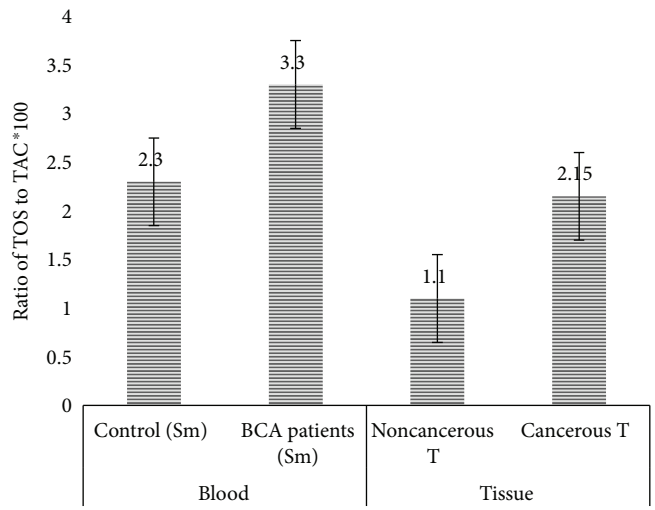

Figure 3: A bar graph showing oxidative stress index in serum and cancerous tissues of breast cancer (BCA) patients in comparison to serum of control group and noncancerous tissue of breast cancer patients, Addis Ababa, Ethiopia, 2015–2017.

GSSG, TOS, TAC, and OSI were compared with the stages of breast cancer patients (refer to Table 5). Even though it was not statistically significant ($P > 0.05$), serum glutamate dehydrogenase enzyme activity was higher in stage zero (4.6 ± 0.4 mU/l) and lower in stage four (3.7 ± 0.45 mU/l), whereas tissue glutamate dehydrogenase enzyme activities were higher in stage three (1.9 ± 1.1 mU/l) and lower in stage zero (0.7 ± 0.2 mU/l) and it was statistically significant ($P \leq 0.05$).

The catalytic activities of serum lactate dehydrogenase were higher in stage four (341.8 ± 41.4 mU/l) and lower in stage one (42.4 ± 4.1 mU/l), and the mean difference of stage four with stages zero, one, two, and three was statistically significant ($P \leq 0.05$) (Table 5). The catalytic activities of tissue lactate dehydrogenase were higher in stage two (138.7 ± 61.9 mU/l) and lower in stage zero (77.7 ± 27.1 mU/l); however, their mean difference was not statistically significant ($P > 0.05$).

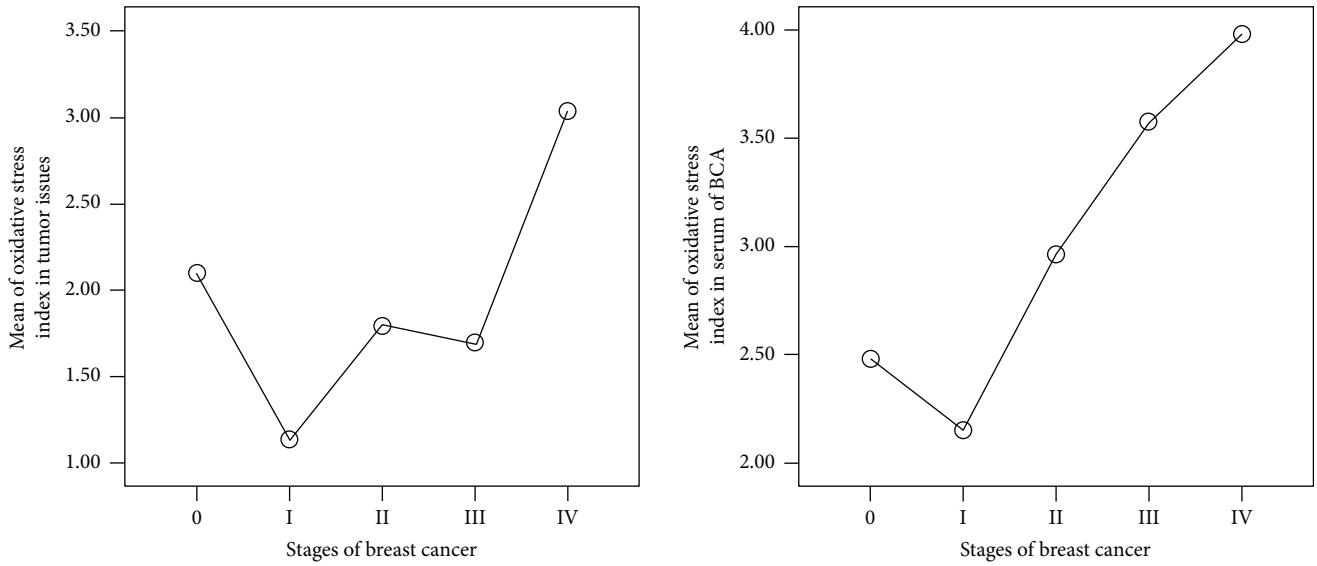

Figure 4: Mean plots of oxidative stress index in serum and tumor tissue samples of breast cancer patients, Addis Ababa, Ethiopia, 2015–2017.

Serum and tissue levels of total antioxidant capacity were lower in stages zero and four, whereas in stages two and three, there was a higher value but it was not statistically significant ($P > 0.05$). Similarly, serum and tissue levels of total oxidative status were not consistent and fluctuate among the stages of breast cancer patients. The mean difference of total oxidative status in serum of stage zero of breast cancer patients was significantly different in comparison to the other stages one, three, and four ($P = 0.003$, 0.002, and 0.045, resp.) (Table 5).

The oxidative stress index of breast cancer patients was analyzed and correlated with stage of cancer (Figure 4). There was significantly higher oxidative stress in stage four of breast cancer patients than in the other stages ($P < 0.05$), whereas it was lower in stage one.

3. Discussion

Currently, the prevalence of cancer has grown into a major public anxiety, as it is becoming the major cause of morbidity and mortality worldwide. More than 60% of cancer cases occur in Africa, Asia, Central, and South America. According to the International Agency for Research on Cancer [22], about 715,000 new cancer cases and 542,000 cancer deaths occurred in 2008 in Africa. In Ethiopia, there is no country-wide cancer registry; however, based on Addis Ababa cancer registry, a total of 5701 cancer cases were registered from September 2011 to August 2014. Among those 3820 (67%) were females and 1881 (33%) were males. The most common type of cancers among females were cancers of the breast (33%), cervix (17%), and ovary (6%), while among male cancers of colorectal (19%), leukemia (18%), and prostate (11%) [23]. Hence, an early biomarker for diagnosis, prognosis, and a potential treatment target for breast cancer is required.

In the present study, serum and tissue levels of glutamate dehydrogenase (GDH), lactate dehydrogenase (LDH), reduced glutathione (GSH), oxidized glutathione (GSSG), total oxidative status (TOS), and total antioxidant capacity (TAC) were determined in search of a potential biomarker for diagnosis, prognosis, and treatment target for breast cancer disease. Those serum and tissue parameters were studied on 54 (27 breast cancer patients and 27 age- and sex-matched apparently healthy control group) participants.

As current study revealed, significantly higher enzymatic activities of GDH and LDH, ratios of TOS to TAC (OSI), and lower ratios of GSH to GSSG in serum and tissue samples from breast cancer patients were observed as compared to noncancerous tissue of the same patients and serum samples of control group.

Activities of GDH were significantly ($P = 0.011$) increased (almost 1.5 times) in both serum and tumor tissues of breast cancer patients as compared to adjacent noncancerous tissues of the same patient or serum samples of control group. Furthermore, between stages of breast cancer, stage zero has the lowest and stage three has the highest activity of GDH in tumor tissues of breast cancer patients and the mean difference is statistically significant ($P = 0.029$). These findings agreed with the studies of Koppenol et al. [10], Toyokuni et al. [24], Koukourakis et al. [25], Lu et al. [26], Liu et al. [27], and Agrawal et al. [28]. The possible reason for high catalytic activities of GDH in cancer cells may be due to the fact that either it is important for redox homeostasis in cancer cells [29] or overexpression of GDH promoted cell proliferation, migration, and invasion *in vitro*, whereas loss of function of GDH had the opposite effect [27].

Previous works suggest that GDH enzymes are important in cancer cell either for synthesizing Krebs cycle intermediates (α-ketoglutarate and subsequent metabolite fumarate) or for synthesizing protein and fatty acid from citrate which originate from α-ketoglutarate. In addition to that, the

substrate of GDH, glutamate itself is a substrate for antioxidant (GSH) and nucleotide synthesis in the cancer cell. These metabolic changes support the production of intermediates for cell growth and division and are regulated by both oncogenes and tumor suppressor genes, in a number of key cancer-producing pathways [30, 31].

Similarly, the catalytic activities of LDH were significantly increased in both cancerous tissue and serum of breast cancer patients when compared to noncancerous tissues of breast cancer patients and serum of control group. The results of current study showed that mean values of LDH were significantly ($P < 0.05$) lower in noncancerous tissues (70.5 ± 10.7) mU/l than in tumor tissues (111.7 ± 23.2 mU/l) of breast cancer patients. Patients with a higher clinical stage had higher LDH activity than lower stages, and there is a significant difference of mean between stage four (341.8 ± 41.4) and stage zero (42.4 ± 4.1 mU/l), stage one (63.8 ± 5.1 mU/l), stage two (67.7 ± 3.1 mU/l), and stage three (131.3 ± 8.4 mU/l) ($P < 0.05$). These observations were in agreement with the studies of Agrawal et al. [28] and Talaiezadeh et al. [32].

The high activities of LDH in cancer cells may be due to the process of high cell proliferation, migration, or invasion than normal cells. That is to say, large cancer cell population requires a higher and rapid energy source as compared to normal cell population. In order to meet this large and rapid energy demand, cancer cells use LDH activity as one option which is helpful for metabolic requirements and aerobic glycolysis of malignant cells. The possible mechanisms of high LDH activities in the cancer cell may be due to higher expressions of LDH gene in cancer cells as compared to normal cells [28, 32].

Generally, tissues have different rates of metabolic activity and oxygen consumption. When cells have a high production of reactive oxygen species than cellular antioxidant defenses, attempts by the cells to remove these toxic species induce oxidative stress. Oxidative stress has long been implicated in cancer development and progression [33]. The current study examined reduced glutathione (GSH), oxidized glutathione (GSSG), total oxidative status (TOS), and total antioxidant capacity (TAC) of serum and cancerous tissue of breast cancer patients in comparison to serum of control group and noncancerous tissue of breast cancer patients as a tool for assessing oxidative stress. The current study's result showed that concentration of oxidized glutathione in both serum and tissue samples from breast cancer patients was significantly increased as compared to serum of control group and noncancerous tissues of breast cancer patients ($P < 0.05$). Cancerous tissues ($0.47 \pm 0.3\ \mu$M/μg of total protein) have a higher mean value than noncancerous tissues ($0.21 \pm 0.1\ \mu$M/μg of total protein). Whereas, the counterpart, concentration of reduced glutathione in both serum and cancerous tissue was significantly decreased when compared to serum of control group and noncancerous tissues of breast cancer patients ($P < 0.05$), tumor tissues ($11.03 \pm 2.0\ \mu$M/μg of total protein) have lower mean value than normal tissues ($14.9 \pm 2.7\ \mu$M/μg of total protein).

In the same way, ratios of reduced (GSH) to oxidized glutathione (GSSG) in serum and cancerous tissues of breast cancer patients (19.9 : 1 and 32.3 : 1, resp.) were decreased as compared to those in serum samples of control group and noncancerous tissues of breast cancer patients (30.7 : 1 and 75 : 1, resp.) (Figure 4). These observations agreed with the report of Perry et al. [34] and Gamcsik et al. [35]. Perry and his colleagues [34] reported that GSSG levels in primary breast tumors were more than twice the levels found in normal breast tissue and levels in lymph node metastases were more than four times the levels found in normal breast tissue. Another group Gamcsik and his colleagues [35] reported that oxidized glutathione levels in breast tumors are higher than in disease-free breast tissue.

The possible justification for these results may be due to unusual levels of oxidative stress in breast cancer as oxidized glutathione in healthy tissue normally is below 5% of the reduced from. This might be due to the content of GSH in some tumor cells that is typically associated with higher levels of GSH-related enzymes, such as γ-glutamylcysteine ligase (GCL) and γ-glutamyltranspeptidase (GGT) activities, as well as a higher expression of GSH-transporting export pumps [34, 35]. Barranco and his colleagues [36] reported that the larger ratios of tumor glutathione to normal tissue glutathione, the poorer prognosis of cancer and less survival.

Moreover, the concentration of total oxidative status (TOS) and total antioxidant capacity (TAC) and their ratios (OSI) in breast cancer patients and control group were also investigated. The results revealed that TOS was significantly elevated in both serum and tumor tissues of breast cancer patients than serum of control group and noncancerous tissues of breast cancer patients ($2.6 \pm 1.1\ \mu$mol H_2O_2 Eq/l in the serum of breast cancer patients and $1.8 \pm 1.0\ \mu$mol H_2O_2 Eq/l in serum control group) ($P = 0.001$). Similarly, it was $2.8 \pm 1.1\ \mu$mol H_2O_2 Eq/l in tumor tissues of breast cancer patients and $2.0 \pm 0.9\ \mu$mol H_2O_2 Eq/l in normal tissues of the same breast cancer patients ($P \leq 0.001$).

Correspondingly, breast cancer patients have a significantly lower concentration of total antioxidant capacity (TAC) in both serum (0.83 ± 0.3 mmol Trolox Eq/l) and tumor tissue (1.61 ± 0.5 mmol Trolox Eq/l) than serum samples of control group (1.09 ± 0.3 mmol Trolox Eq/l) and in adjacent normal tissues (1.88 ± 0.26 mmol Trolox Eq/l) of breast cancer patients ($P < 0.05$).

These findings agreed with the study of others finding [37–40]. Erten Şener and his colleagues [37] found that TAC was 2.01 ± 0.01 mmol Trolox Eq/l in patients with breast cancer and 2.07 ± 0.03 mmol Trolox Eq/l in control group ($P < 0.05$), and Zowczak-Drabarczyk and his colleagues [38] found that TAC in breast cancer patients was 1.35 mmol Trolox Eq/l and in control group was 1.61 mmol Trolox Eq/l ($P < 0.05$). The findings of TAC were also in lined with the study of former whom found a significantly higher value of oxidative status, as compared to control group [39, 40]. Furthermore, oxidative status in other types of cancer patients such as thyroid cancer and colorectal cancer patients reported increased concentration of TOS [37, 38, 41, 42].

Consistently, ratios of TOS to TAC (OSI) in serum and tissue samples from breast cancer patients were significantly different as compared to those in serum samples from

control group and noncancerous tissue of the same breast cancer patients. Serum samples of breast cancer patients have had a significantly higher ratio of total oxidative status to total antioxidant capacity (OSI) value (3.3 ± 1.7) than control group (2.3 ± 1.5) ($P = 0.006$). Likewise, tumor tissues of breast cancer patients had significantly higher value of OSI (2.15 ± 1.8) than noncancerous tissue (1.1 ± 0.5) ($P = 0.002$). This finding agreed with the study of Feng and his colleagues. They found a significantly higher values of OSI in breast cancer patients when compared to control group [43].

Surprisingly, even within the different stages of breast cancer patients, OSI values were different. Lower stages (0 and one) have lower values of OSI than the higher stages (two to four) of breast cancer patients. Mean difference of OSI between stages one and four in tumor tissue of breast cancer patients was significantly ($P = 0.037$) different. These results are supported by the study of Zarrini and his colleagues [44]. They reported that patients in advanced stages had lower serum antioxidant capacity and higher lipid peroxidation levels than control group [44].

The possible reason for high oxidative stress in breast cancer cells may be due to oxygen radical production by the macrophages. In addition, tumor necrosis factor-α is secreted by tumor-associated macrophages and is known to induce cellular oxidative stress. Determination of oxidative stress in cancer cells is useful either to detect the increase of the mutation rate during accelerated tumor progression or to activate growth-promoting signaling pathways. It is also helpful to adapt oxidative stress which results in increased resistance to therapy or to increase blood supply to tumor cells. It was also useful in evaluating the risk of invasion and metastasis of cancerous cells [45, 46].

Reczek and Chandel explained the dual role of reactive oxygen species (ROS) in cancer. ROS can promote protumorigenic signaling, facilitating cancer cell proliferation, survival, and adaptation to hypoxia. Conversely, ROS can promote antitumorigenic signaling and trigger oxidative stress-induced cancer cell death [47].

Furthermore, oxygen radicals are powerful DNA damaging agents, either ROS causes strand breaks or alterations in guanine and thymine bases or sister chromatid exchanges. This may inactivate additional tumor suppressor genes within tumor cells or further increase expression of proto-oncogenes. Genetic instability due to persistent carcinoma cell oxidative stress will, therefore, increase the malignant potential of the tumor [45].

4. Conclusion

Enzymatic activities of glutamate dehydrogenase and lactate dehydrogenase, the concentration of reduced and oxidized glutathione, and the ratio of total oxidative status and total antioxidant capacity (OSI) in serum and tumor tissues of breast cancer patients were determined. In conclusion, enzymatic activities of glutamate dehydrogenase and lactate dehydrogenase as well as ratios of total oxidative status to total antioxidant capacity were significantly increased in serum and tumor tissues of breast cancer patients as compared to serum of control group and noncancerous tissues of breast cancer. However, ratios of reduced to oxidized glutathione were significantly decreased in both serum and cancerous tissues of patients as compared to serum of control group and noncancerous tissues of the same breast cancer patients. Furthermore, marital status, bearing a child, and breast feeding have a lower risk for breast cancer than unmarried women who never bore a child and who did not breast feed, whereas birth control has a higher risk for breast cancer than nonuser women. Therefore, glutamate dehydrogenase, lactate dehydrogenase, and oxidative stress play a critical role in breast cancer progression and may be an ideal therapeutic target for regulation of breast cancer disease.

Abbreviations

GDH: Glutamate dehydrogenase
GSH: Reduced glutathione
GSSG: Oxidized glutathione
LDH: Lactate dehydrogenase
TAC: Total antioxidant capacity
TOS: Total oxidative stress.

Conflicts of Interest

The authors declare that there are no conflicts of interest regarding the publication of this paper.

Acknowledgments

The authors would like to acknowledge the study participants for their cooperation and willingness. Furthermore, they would like to extend their deepest gratitude to the Biochemistry Department of Addis Ababa University for their administrative support and adding (posting) the thesis on the AAU digital library (http://etd.aau.edu.et/handle/123456789/17041). The authors are grateful to Addis Ababa University, College of Health Sciences, School of Medicine, for their financial support.

References

[1] A. E. Fard, A. Zarepour, A. Zarrabi, A. Shanei, and H. Salehi, "Synergistic effect of the combination of triethylene-glycol modified Fe_3O_4 nanoparticles and ultrasound wave on MCF-7 cells," *Journal of Magnetism and Magnetic Materials*, vol. 394, pp. 44–49, 2015.

[2] Genetic home reference, "Breast cancer," 2015, October 2015, http://ghr.nlm.nih.gov/glossary=malignancy.

[3] American Cancer Society, *Cancer Facts & Figures 2017*, American Cancer Society, Atlanta, 2017.

[4] M. I. Koukourakis, A. Giatromanolaki, A. L. Harris, and E. Sivridis, "Comparison of metabolic pathways between cancer cells and stromal cells in colorectal carcinomas: a metabolic survival role for tumor-associated stroma," *Cancer Research*, vol. 66, no. 2, pp. 632–637, 2006.

[5] N. M. Mazure, "Hypoxia signalling in cancer and approaches to enforce tumour regression," *Nature*, vol. 441, no. 7092, pp. 437–443, 2006.

[6] K. Fischer, P. Hoffmann, S. Voelkl et al., "Inhibitory effect of tumor cell–derived lactic acid on human T cells," *Blood*, vol. 109, no. 9, pp. 3812–3819, 2007.

[7] P. Swietach, R. D. Vaughan-Jones, and A. L. Harris, "Regulation of tumor pH and the role of carbonic anhydrase 9," *Cancer and Metastasis Reviews*, vol. 26, no. 2, pp. 299–310, 2007.

[8] K. L. Eales, K. E. Hollinshead, and D. A. Tennant, "Hypoxia and metabolic adaptation of cancer cells," *Oncogenesis*, vol. 5, no. 1, article e190, 2016.

[9] G. Kroemer and J. Pouyssegur, "Tumor cell metabolism: cancer's Achilles' heel," *Cancer Cell*, vol. 13, no. 6, pp. 472–482, 2008.

[10] W. H. Koppenol, P. L. Bounds, and C. V. Dang, "Otto Warburg's contributions to current concepts of cancer metabolism," *Nature Reviews Cancer*, vol. 11, no. 5, pp. 325–337, 2011.

[11] O. Warburg and T. Nguyen, *The Prime Cause of Cancer*, 2015, http://EnCognitive.com.

[12] E. Friday, R. Oliver, T. Welbourne, and F. Turturro, "Glutaminolysis and glycolysis regulation by troglitazone in breast cancer cells: relationship to mitochondrial membrane potential," *Journal of Cellular Physiology*, vol. 226, no. 2, pp. 511–519, 2011.

[13] Y. Naito and T. Yoshikawa, "What is oxidative stress?," *Japan Medical Association Journal*, vol. 45, no. 7, pp. 271–276, 2002.

[14] A. F. Yücel, Ö. Kemik, A. S. Kemik, S. Purisa, and İ. S. Tüzün, "Relationship between the levels of oxidative stress in mesenteric and peripheral serum and clinicopathological variables in colorectal cancer," *Balkan Medical Journal*, vol. 29, no. 2, pp. 144–147, 2012.

[15] C. Gorrini, I. S. Harris, and T. W. Mak, "Modulation of oxidative stress as an anticancer strategy," *Nature Reviews. Drug Discovery*, vol. 12, no. 12, pp. 931–947, 2013.

[16] D. Botman, W. Tigchelaar, and C. J. Van Noorden, "Determination of glutamate dehydrogenase activity and its kinetics in mouse tissues using metabolic mapping (quantitative enzyme histochemistry)," *Journal of Histochemistry & Cytochemistry*, vol. 62, no. 11, pp. 802–812, 2014.

[17] A. Vassault, "Lactate dehydrogenase, UV-method with pyruvate and NADH," *Methods in Enzymatic Analysis*, vol. 3, p. 118, 1983.

[18] I. Rahman, A. Kode, and S. K. Biswas, "Assay for quantitative determination of glutathione and glutathione disulfide levels using enzymatic recycling method," *Nature Protocols*, vol. 1, no. 6, pp. 3159–3165, 2006.

[19] P. K. Smith, R. I. Krohn, G. T. Hermanson et al., "Measurement of protein using bicinchoninic acid," *Analytical Biochemistry*, vol. 150, no. 1, pp. 76–85, 1985.

[20] O. Erel, "A new automated colorimetric method for measuring total oxidant status," *Clinical Biochemistry*, vol. 38, no. 12, pp. 1103–1111, 2005.

[21] D. Koracevic, G. Koracevic, V. Djordjevic, S. Andrejevic, and V. Cosic, "Method for the measurement of antioxidant activity in human fluids," *Journal of Clinical Pathology*, vol. 54, no. 5, pp. 356–361, 2001.

[22] J. Ferlay, H. R. Shin, F. Bray, D. Forman, C. Mathers, and D. M. Parkin, "Estimates of worldwide burden of cancer in 2008: GLOBOCAN 2008," *International Journal of Cancer*, vol. 127, no. 12, pp. 2893–2917, 2010.

[23] Addis Ababa City Cancer Registry2014, May 2017, http://afcrn.org/membership/members/100-Addisababa.

[24] S. Toyokuni, K. Okamoto, J. Yodoi, and H. Hiai, "Persistent oxidative stress in cancer," *FEBS Letters*, vol. 358, no. 1, pp. 1–3, 1995.

[25] M. I. Koukourakis, E. Kontomanolis, A. Giatromanolaki, E. Sivridis, and V. Liberis, "Serum and tissue LDH levels in patients with breast/gynaecological cancer and benign diseases," *Gynecologic and Obstetric Investigation*, vol. 67, no. 3, pp. 162–168, 2009.

[26] W. Lu, H. Pelicano, and P. Huang, "Cancer metabolism: is glutamine sweeter than glucose?," *Cancer Cell*, vol. 18, no. 3, pp. 199-200, 2010.

[27] G. Liu, J. Zhu, M. Yu et al., "Glutamate dehydrogenase is a novel prognostic marker and predicts metastases in colorectal cancer patients," *Journal of Translational Medicine*, vol. 13, no. 1, p. 144, 2015.

[28] A. Agrawal, M. B. Gandhe, D. Gupta, and M. V. Reddy, "Preliminary study on serum lactate dehydrogenase (LDH)-prognostic biomarker in carcinoma breast," *Journal of Clinical and Diagnostic Research*, vol. 10, no. 3, article BC06, 2016.

[29] L. Jin, D. Li, G. N. Alesi et al., "Glutamate dehydrogenase 1 signals through antioxidant glutathione peroxidase 1 to regulate redox homeostasis and tumor growth," *Cancer Cell*, vol. 27, no. 2, pp. 257–270, 2015.

[30] D. M. Miller, S. D. Thomas, A. Islam, D. Muench, and K. Sedoris, "c-Myc and cancer metabolism," *Clinical Cancer Research*, vol. 18, no. 20, 2012.

[31] B. J. Altman, Z. E. Stine, and C. V. Dang, "From Krebs to clinic: glutamine metabolism to cancer therapy," *Nature Reviews Cancer*, vol. 16, no. 10, pp. 619–634, 2016.

[32] A. Talaiezadeh, A. Shahriari, M. R. Tabandeh, P. Fathizadeh, and S. Mansouri, "Kinetic characterization of lactate dehydrogenase in normal and malignant human breast tissues," *Cancer Cell International*, vol. 15, no. 1, p. 19, 2015.

[33] J. Limón-Pacheco and M. E. Gonsebatt, "The role of antioxidants and antioxidant-related enzymes in protective responses to environmentally induced oxidative stress," *Mutation Research/Genetic Toxicology and Environmental Mutagenesis*, vol. 674, no. 1–2, pp. 137–147, 2009.

[34] R. R. Perry, J. Mazetta, M. Levin, and S. C. Barranco, "Glutathione levels and variability in breast tumors and normal tissue," *Cancer*, vol. 72, no. 3, pp. 783–787, 1993.

[35] M. P. Gamcsik, M. S. Kasibhatla, S. D. Teeter, and O. M. Colvin, "Glutathione levels in human tumors," *Biomarkers*, vol. 17, no. 8, pp. 671–691, 2012.

[36] S. C. Barranco, R. R. Perry, M. E. Durm et al., "Relationship between colorectal cancer glutathione levels and patient survival: early results," *Diseases of the Colon & Rectum*, vol. 43, no. 8, pp. 1133–1140, 2000.

[37] D. Erten Şener, A. Gönenç, M. Akıncı, and M. Torun, "Lipid peroxidation and total antioxidant status in patients with breast cancer," *Cell Biochemistry & Function*, vol. 25, no. 4, pp. 377–382, 2007.

[38] M. M. Zowczak-Drabarczyk, D. Murawa, L. Kaczmarek, K. Połom, and M. Litwiniuk, "Total antioxidant status in plasma of breast cancer patients in relation to ERβ expression," *Contemporary Oncology*, vol. 17, no. 6, p. 499, 2013503, 2013.

[39] A. L. Júnior, M. F. Paz, L. I. Silva et al., "Serum oxidative stress markers and genotoxic profile induced by chemotherapy in

patients with breast cancer: a pilot study," *Oxidative Medicine and Cellular Longevity*, vol. 2015, Article ID 212964, 11 pages, 2015.

[40] C. Panis, V. J. Victorino, A. C. Herrera et al., "Can breast tumors affect the oxidative status of the surrounding environment? A comparative analysis among cancerous breast, mammary adjacent tissue, and plasma," *Oxidative Medicine and Cellular Longevity*, vol. 2015, Article ID 6429812, 9 pages, 2015.

[41] D. Wang, J. F. Feng, P. Zeng, Y. H. Yang, J. Luo, and Y. W. Yang, "Total oxidant/antioxidant status in sera of patients with thyroid cancers," *Endocrine-Related Cancer*, vol. 18, no. 6, pp. 773–782, 2011.

[42] R. Wu, J. Feng, Y. Yang et al., "Significance of serum total oxidant/antioxidant status in patients with colorectal cancer," *PLoS One*, vol. 12, no. 1, article e0170003, 2017.

[43] J. F. Feng, L. Lu, P. Zeng et al., "Serum total oxidant/antioxidant status and trace element levels in breast cancer patients," *International Journal of Clinical Oncology*, vol. 17, no. 6, pp. 575–583, 2012.

[44] A. S. Zarrini, D. Moslemi, H. Parsian, M. Vessal, A. Mosapour, and Z. S. Kelagari, "The status of antioxidants, malondialdehyde and some trace elements in serum of patients with breast cancer," *Caspian Journal of Internal Medicine*, vol. 7, no. 1, p. 31, 2016.

[45] N. S. Brown and R. Bicknell, "Hypoxia and oxidative stress in breast cancer oxidative stress—its effects on the growth, metastatic potential and response to therapy of breast cancer," *Breast Cancer Research*, vol. 3, no. 5, p. 323, 2001.

[46] A. Jezierska-Drutel, S. A. Rosenzweig, and C. A. Neumann, "Role of oxidative stress and the microenvironment in breast cancer development and progression," *Advances in Cancer Research*, vol. 119, pp. 107–125, 2013.

[47] C. R. Reczek and N. S. Chandel, "The two faces of reactive oxygen species in cancer," *Annual Review of Cancer Biology*, vol. 1, no. 1, pp. 79–98, 2017.

Hindawi
Oxidative Medicine and Cellular Longevity
Volume 2017, Article ID 5647281, 13 pages
https://doi.org/10.1155/2017/5647281

Research Article

Modulation of Multidrug Resistance Gene Expression by Coumarin Derivatives in Human Leukemic Cells

Tomasz Kubrak,[1] Anna Bogucka-Kocka,[2] Łukasz Komsta,[3] Daniel Załuski,[4] Jacek Bogucki,[5] Dariusz Galkowski,[6] Robert Kaczmarczyk,[7] Marcin Feldo,[8] Maria Cioch,[9] and Janusz Kocki[10]

[1]*Centre for Innovative Research in Medical and Natural Sciences, Faculty of Medicine, University of Rzeszow, Rzeszow, Poland*
[2]*Department of Biology and Genetics, Medical University of Lublin, Lublin, Poland*
[3]*Department of Medicinal Chemistry, Medical University of Lublin, Lublin, Poland*
[4]*Department of Pharmacognosy, Ludwik Rydygier Collegium Medicum, Nicolaus Copernicus University, 9 Marie Curie-Skłodowska Street, 85-094 Bydgoszcz, Poland*
[5]*Warsaw Higher Humanistic School, Warsaw, Poland*
[6]*Praesum Healthcare Services, Lake Worth, FL 33461, USA*
[7]*Department of Neurosurgery and Paediatric Neurosurgery, Medical University of Lublin, Lublin, Poland*
[8]*Department of Vascular Surgery and Angiology, Medical University of Lublin, Lublin, Poland*
[9]*Department of Hemato-Oncology and Bone Marrow Transplantation, Medical University of Lublin, Lublin, Poland*
[10]*Department of Clinical Genetics, Medical University of Lublin, Lublin, Poland*

Correspondence should be addressed to Anna Bogucka-Kocka; anna.bogucka-kocka@umlub.pl

Received 6 July 2017; Accepted 6 November 2017; Published 13 December 2017

Academic Editor: Gloria M. Calaf

The presence of multidrug resistance (MDR) in tumor cells is considered as the major cause of failure of cancer chemotherapy. The mechanism responsible for the phenomenon of multidrug resistance is explained, among others, as overexpression of membrane transporters primarily from the ABC family which actively remove cytostatics from the tumor cell. The effect of 20 coumarin derivatives on the cytotoxicity and expression of *MDR1*, *MRP1*, *BCRP*, and *LRP* genes (encoding proteins responsible for multidrug resistance) in cancer cells was analyzed in the study. The aim of this research included determination of IC10 and IC50 values of selected coumarin derivatives in the presence and absence of mitoxantrone in leukemia cells and analysis of changes in the expression of genes involved in multidrug resistance: *MDR1*, *MRP*, *LRP*, and *BCRP* after 24-hour exposure of the investigated cell lines to selected coumarins in the presence and absence of mitoxantrone in IC10 and IC50 concentrations. The designed research was conducted on 5 cell lines derived from the human hematopoietic system: CCRF/CEM, CEM/C1, HL-60, HL-60/MX1, and HL-60/MX2. Cell lines CEM/C1, HL-60/MX1, and HL-60/MX2 exhibit a multidrug resistance phenotype.

1. Introduction

Compounds of natural origin and their derivatives play an increasingly important role in medicine and pharmacology. Approximately 60% of therapeutic drugs used in the treatment of cancer are compositions comprising natural compounds and/or their derivatives [1]. The main problem of cancer chemotherapy is the adverse effects resulting in high cytotoxicity toward normal rapidly proliferating cells, especially the bone marrow and gastrointestinal tract. In order to mitigate the side effects, modified therapeutic regimens such as combination therapy have been introduced [2–4]. Several hundred membrane transporters in two major protein superfamilies ATP-binding cassette (ABC) and solute carrier (SLC) can be found in humans. The transporters may represent the rate determining step in pharmacokinetics and drug-drug interactions [5, 6]. ABC transporters, among other functions, use the energy of ATP binding and

hydrolysis to actively transport chemicals across extra- and intracellular membranes.

Subfamilies of multidrug resistance proteins (MDRs and ABCB), multidrug resistance-associated proteins (MRPs and ABCC), and breast cancer resistance protein (BCRP and ABCG2) also belong to the human ABC transporter family [5].

The phenomenon of multidrug resistance caused by overexpression of these ABC drug transporters in cancer cells confers cross-resistance to a multitude of drugs and presents a significant obstacle limiting the effectiveness of cancer chemotherapy. In recent years, a number of natural, plant-derived compounds have been found to inhibit proliferation, induce apoptosis, suppress angiogenesis, retard metastasis, and enhance chemotherapy exhibiting anticancer potential both in vitro and in vivo. Many researchers point to the use of natural products as inhibitors of multidrug resistance and often call them "fourth generation modulators" [7, 8].

The occurrence of multidrug resistance was first described by Biedler and Riehm in 1970 during incubation of leukemia cells from a *Syrian hamster* and mice in an increasing concentration of actinomycin D. They encountered not only resistance to this particular drug but also to many others including daunorubicin and vinblastine [9]. However, the real breakthrough occurred in 1976 when Juliano and Ling described for the first time the now classical P-glycoprotein (ABCB; P-gp), which is the first known human protein responsible for the occurrence of the multidrug resistance [10]. Numerous studies showed a close relationship between overexpression of P-gp and a lower rate of cancer remission with a higher incidence of resistance to treatment. This observation underlines the importance of the mechanism of multidrug resistance-related P-gp in cancer. In addition, some studies provided evidence that expression of P-gp may be a factor the clinical outcome of therapy in certain tumors such as breast cancer and neuroblastoma or sarcoma in children [11, 12]. Based on these observations and findings, we can state that the future success of anticancer therapy is insignificant degree dependent on the results of research targeted to overcome multidrug resistance [13–15]. Mitoxantrone is a synthetic anthracenedione that has been used in the clinical treatment of various cancers. The anticancer mechanisms of mitoxantrone are believed to be related to its capacity to bind DNA and inhibit DNA topoisomerase II in the nuclear compartment of cells. In addition, the action of its metabolites in the intracellular cytosolic compartment may also contribute to the antineoplastic activities of mitoxantrone [16, 17].

It was reported that plant-derived polyphenolic compounds, mainly flavonoids and stilbenes or their synthetic derivatives, can modulate the main ABC transporters responsible for cancer drug resistance, including P-gp, multidrug resistance-associated protein 1 (MRP1), and breast cancer resistance protein (BCRP) [18]. The coumarins are secondary plant metabolites that are characterized by enormous structural diversity. They have very diverse mechanisms of action. Their biological activity is determined by their lactone structure, whereas pharmacological properties are determined by the structure of compounds [19].

Some of the coumarins, such as aesculetin, aesculin, and fraxin, also possess antioxidant activity. It was confirmed that acute lymphocytic leukemia (ALL) and acute nonlymphocytic leukemia (ANLL) have increased levels of various reactive oxygen (ROS) such as superoxide radicals, H_2O_2, and decreased levels of enzymatic (SOD and CAT) and nonenzymatic antioxidants compared to healthy individuals [20–22].

There are many publications about relationships that modulate multidrug resistance that are not used in the clinic due to weak action or side effects. There is also a need to look for substances that overcome the drug resistance phenomenon of tumor cells. Therefore, testing effective compounds such as coumarins which can reverse drug resistance is warranted [23].

In our previous papers, coumarin derivatives were screened for their cytotoxic activity against human tumor cells and several were found to exhibit potent cytotoxic activity [24–31]. These studies led to this analysis of the impact of coumarin derivatives to reverse drug resistance in five human leukemic cell lines via multidrug resistance genes expression. In a continuing search for potent and selective cytotoxic coumarin derivatives as antitumor agents, we analyzed 20 coumarin derivatives and evaluated their cytotoxic effects against human leukemic cells and the impact on *MDR1*, *MRP1*, *BCRP*, and *LRP* gene expression.

2. Materials and Methods

2.1. Cell Lines and Cell Culture. Human acute promyelocytic leukemia cell lines HL60, HL60/MX1, and HL60/MX2 and acute lymphoblastic leukemia cell lines CEM/C1 and CCRF/CEM were used. Cell lines were obtained from the American Type Culture Collection (ATCC) 10801, University Boulevard Manassas, VA 20110, USA. HL-60 (CCL 240) is a promyelocytic cell line derived by Collins (1987). The peripheral blood leukocytes were obtained by leukopheresis from a 36-year-old Caucasian female with acute promyelocytic leukemia. HL-60/MX1 (CRL–2258), a mitoxantrone-resistant derivative of the HL-60 cell line, was obtained from peripheral blood leukocytes obtained by leukopheresis from a patient with acute promyelocytic leukemia. HL-60/MX2 (CRL–2257) is also a mitoxantrone resistant derivative of the HL-60 cell line. HL-60/MX2 cells display atypical multidrug resistance (MDR) with the absence of P-gp overexpression and altered topoisomerase II catalytic activity and reduced levels of topoisomerase II alpha and beta proteins. CCRF/CEM (CCL–119) was derived from human lymphoblasts from the peripheral blood of a child with acute leukemia. CEM/C1 is a camptothecin- (CPT-) resistant derivative of the human T cell leukemia cell line CCRF/CEM. The cell line was selected and subcloned in 1991 for resistance to CPT (http://www.lgcstandarts-atcc.org/). The cells were maintained in RPMI 1640 medium (PAA Laboratories, Linz, Austria) supplemented with 10% fetal bovine serum (FBS) (PAA Laboratories) for HL60/MX1, HL60/MX2, CEM/C1, and CCRF/CEM cell lines and 20% FBS for HL60 cells, penicillin-streptomycin (100 U/mL PAA Laboratories), and

amphotericin (PAA Laboratories) at 37°C in a humidified atmosphere of 5% CO_2.

2.2. Analysis of Cell Viability. Cells were seeded on 12-well plates (Sarstedt, Wiener. Neudorf, Austria) at an initial density of 1×10^6 cells/ml. After 24 hours, the cell suspension was stimulated with coumarin derivatives at concentrations ranging from 10 μM to 1000 μM. After 24 hours, 1 mL of cell suspension was centrifuged at 1000 rpm for 5 minutes and the supernatant was discarded. The cells were resuspended in 50 μL PBS. From each tube, a 10 μL cell suspension was taken and mixed with 10 μL of Trypan blue reagent (Bio-Rad, Hercules, CA, USA). The sample was incubated for 5 minutes. Cell viability was measured by TC20 Automated Cell Counter (Bio-Rad). Each experiment was repeated three times.

2.3. Standards and Reagents. Isopimpinellin (ISO), bergapten (BER), xanthotoxol (XOL), xanthotoxin (XIN), byakangelicin (BIN), byakangelicol (BOL), heraclenin (HEC), phellopterin (FEL), herniarine (HER), aesculetin (AET), dihydrocoumarin (DHD), coumarin (COU), aesculin (AEL), umbelliferone (UMB), 4-methylo-7-methoxycoumarin (4,7M), 4-methylo-7-ethoxycoumarin (4,7E), 7-methylocoumarin (7ME), 6-methylocoumarin (6ME), 0,0-dimethylofraxetin (OOD), and scoparone (SCO) were purchased from ChromaDex® (ChromaDex, Irvine, CA, USA).

2.4. Determination of Gene Expression. Relative gene expression of *MDR1*, *MRP1*, *BCRP*, and *LRP* was assessed by real-time quantitative PCR and $2^{-\Delta\Delta C}{}_T$ method. Genes were quantitatively assessed in each sample taken from the research group and referred to gene expression determined in the corresponding samples in the control group 1 : 1.

2.4.1. Cell Preparation. Cells were seeded on 12-well plates (Sarstedt, Wiener. Neudorf, Austria) at an initial density of 1×10^6 cells/ml. After 24 hours, the cell suspension was stimulated with coumarin derivatives separately at IC10 and IC50 concentrations. Another group of cells was stimulated with coumarin derivative sat IC10 and IC50 concentration with mitoxantrone (+M) at a concentration of 0.02 μM. We used two controls—cell cultures without stimulators and cell cultures with mitoxantrone at a concentration of 0.02 μM. After 24 hours, the cell suspension (from each well) was centrifuged at 800 rpm for 5 minutes, and the supernatant was discarded.

2.4.2. Isolation of Total Cellular RNA. To isolate total cellular RNA, we followed the method of Kocki et al. with modification, using a TRI-Reagent Solution (Ambion, USA) [32]. During this process, samples of cells were mixed with 250 μl TRI-Reagent buffer (Ambion, USA) to obtain a homogenous suspension. Samples were then incubated for 5 min at room temperature until complete dissociation. At the next stage, 50 μl chloroform (Sigma-Aldrich, USA) was added to the sample and shaken for 15 s. Next, the samples were left for 15 min to incubate at room temperature after which they were centrifuged for 15 min at 14,000 rpm at 4°C in 5415R Eppendorf centrifuges. The aqueous phase was placed in a new tube and 250 μl 2-propanol (Sigma-Aldrich, USA) was added. The samples were thoroughly mixed and incubated for 20 min at room temperature. Following that, the mixtures were centrifuged for 20 min at 14,000 rpm at 4°C in 5415R Eppendorf centrifuges. Aqueous phase was removed from the above precipitate. The RNA precipitate was washed in cool 80% ethanol and obtained RNA samples were stored in 80% ethanol at −80°C for further analysis.

2.4.3. Quantitative and Qualitative Analysis of RNA. The RNA concentration and purity were measured by spectrophotometry on a NanoDrop2000 (Thermo Scientific, USA). Precipitate of RNA in 80% ethanol was taken out at −20°C and next centrifuged for 15 min at 14,000 rpm at 4°C in 5415R Eppendorf centrifuges. The liquid part was removed, and RNA pellets were left to dry at room temperature. Subsequently, the precipitate was dissolved in DNase-, RNase-, and protease-free water (Sigma-Aldrich, USA) at 4°C, the volume depending on RNA concentration.

2.4.4. cDNA Synthesis. The cDNA was synthesized using High-Capacity cDNA Reverse Transcription Kit, according to manufacturer's instructions [33]. Each reactive mixture contained the following set of reagents: 1 × RT buffer, 20 U RNase inhibitor, 50 U reverse transcriptase (MultiScribe Reverse Transcriptase), 1 × RT random primers, and 4 mM of each deoxynucleotide: dATP, dGTP, dTTP, and dCTP plus examined 1 μg RNA in DNase-, RNase-, and protease-free water (Sigma-Aldrich, USA) to complete the volume required for reaction. Final volume of the reactive mixture was 20 μl. Afterwards, the reactive components were thoroughly mixed and centrifuged to fuse them well. The cDNA was synthesized on Veriti Dx (Applied Biosystems, USA) under the following conditions: stage I, 25°C (10 min); stage II, 37°C (120 min); stage III, 85°C (5 min); and stage IV, 4°C.

2.4.5. The qPCR Protocol. The cDNA, which was obtained by reverse transcription (RT) procedure, was amplified by real-time gene expression analysis (qPCR) on a 7900HT Real-Time Fast System [33], using the manufacturer's SDS software. Triplicate qPCR reactions were conducted for each sample. To exclude reagent contamination by foreign DNA, a blind trial was always performed without a DNA target. Reaction components included 11.25 μl mixture of cDNA probe and 1.25 μl oligonucleotide starters specific for genes examined and 12.5 μl buffer TaqMan Universal PCR Master Mix. The reaction was performed on an optic reaction plate in required reactive volume 25 μl, using probe sets of TaqMan Gene Expression Assays [33] with FAM-NFQ markers and oligonucleotide starters for human genes *MDR1*, *MRP1*, *BCRP*, and *LRP* and the housekeeping gene *GAPDH* was used as an internal control gene. Amplification protocol included in the following cycles: initial denaturation: 95°C, 10 min; and 40 cycles each composed of two temperatures: 95°C, 15 s and 60°C, 1 min. The number of copies of DNA molecules was monitored and calculated on a 7900HT Real-Time Fast System [33] in each amplification cycle. To calculate the number of examined DNA

Table 1: IC10 values for line cells CEM/C1, CCRF/CEM, HL-60, HL-60/MX1, and HL-60/MX2 (μM). SD: standard deviation.

	CEM/C1 IC10 ± SD	CCRF/CEM IC10 ± SD	HL-60 IC10 ± SD	HL-60/MX1 IC10 ± SD	HL-60/MX2 IC10 ± SD
ISO	13.0 ± 2.5	6.9 ± 1.0	4.6 ± 0.6	13.8 ± 2.2	16.4 ± 2.1
BER	12.1 ± 2.0	8.8 ± 1.7	4.6 ± 1.1	15.8 ± 2.6	11.4 ± 2.4
XOL	11.7 ± 3.1	7.6 ± 1.0	4.6 ± 1.1	13.4 ± 2.0	11.1 ± 2.5
XIN	12.8 ± 2.1	5.7 ± 3.6	9.3 ± 3.1	11.7 ± 2.6	10.5 ± 2.0
BIN	15.5 ± 2.6	8.5 ± 3.1	4.6 ± 2.6	3.0 ± 2.5	12.9 ± 1.7
BOL	15.5 ± 2.5	6.4 ± 2.0	9.2 ± 2.5	11.5 ± 2.5	10.5 ± 1.0
HEC	12.7 ± 2.5	6.0 ± 3.1	9.2 ± 2.0	15.0 ± 3.2	18.2 ± 2.0
FEL	21.4 ± 3.5	5.9 ± 0.4	9.8 ± 3.1	14.5 ± 2.8	16.4 ± 2.0
HER	4.4 ± 1.2	4.3 ± 1.2	3.4 ± 1.9	18.2 ± 2.5	5.9 ± 0.9
AET	4.5 ± 0.8	3.6 ± 2.2	9.0 ± 3.1	11.1 ± 4.4	5.9 ± 1.5
DHD	5.3 ± 0.6	5.0 ± 1.5	4.8 ± 1.0	4.0 ± 4.3	5.9 ± 1.1
COU	5.3 ± 0.5	1.0 ± 3.1	5.0 ± 1.5	4.0 ± 4.2	4.3 ± 2.0
AEL	4.2 ± 1.1	4.2 ± 0.5	5.9 ± 4.2	2.5 ± 3.5	8.3 ± 1.1
UMB	5.0 ± 0.6	4.0 ± 1.1	5.5 ± 1.5	13.3 ± 2.2	8.3 ± 1.0
4,7M	3.6 ± 0.2	5.5 ± 0.5	2.3 ± 1.1	16.7 ± 2.8	6.7 ± 1.5
4,7E	1.9 ± 1.0	4.5 ± 0.8	1.7 ± 1.6	16.7 ± 2.6	7.7 ± 1.4
7ME	2.8 ± 1.0	3.6 ± 1.1	7.7 ± 2.1	14.3 ± 4.2	8.3 ± 1.6
6ME	2.6 ± 1.0	5.9 ± 2.1	6.2 ± 2.0	18.2 ± 3.8	5.5 ± 1.6
0,0D	2.6 ± 0.3	4.3 ± 1.4	2.9 ± 0.8	11.1 ± 3.4	8.3 ± 2.2
SCO	2.7 ± 0.5	6.2 ± 0.7	3.6 ± 0.3	22.2 ± 3.2	7.1 ± 1.9

molecules present in the mixture at the onset of reaction, the number of PCR cycles after which the level of fluorescence exceeded the defined threshold cycle (CT) RQ Study Software [33] was used. The CT value for each sample of the endogenous control gene (*GAPDH*) was used to normalize the level of the interesting gene expression. The relative level of gene expression was calculated according to [34].

The RQ defines the expression of an examined gene in a stimulated cell sample with reference to the gene expression in the control cell sample calibrator (without stimulation). Finally, the RQs were analyzed after their logarithmic conversion into logarithm of RQ (LogRQ) [33]. Thus, the obtained results were more legible. LogRQ takes value greater, equal to or less than zero. LogRQ = O means that gene expression in the calibrated sample and the stimulated one are the same. LogRQ < 0 points to decreased gene expression in the stimulated cell sample, whereas LogRQ > 0 points to signal increased gene expression in the stimulated cell sample compared to the calibrated one.

2.4.6. Statistical Analysis. The results obtained for stem cells were statistically analyzed by STATISTICA software by means of the nonparametric Mann–Whitney *U* test, Spearman rho correlation analysis, and Kruskal–Wallis test. The results obtained for cell lines were analyzed by chemometric techniques: cluster analysis based on Euclidean distance and Parallel Factor Analysis (PARAFAC). Data were presented as means ± SEM. The level of statistical significance was set at $p < 0.05$.

3. Results

3.1. Analysis of Cytotoxicity. The cytotoxicity of the examined coumarins was estimated using trypan blue vital staining in the presence of mitoxantrone M(+) and absence of mitoxantrone. The experiment was performed in triplicate and the mean values were calculated from the given values (Tables 1, 2, 3, and 4).

The cells of the 5 cancer cell lines exposed to coumarin derivatives presented diverse cytotoxicity dependent on the dose of IC10, IC10M(+), IC50, and IC50 M(+).

Cytotoxicity depends on both the type of relationship and the type of cell line. It turned out that the most sensitive cell lines to the IC10 dose were CCRF/CEM > HL-60 > CEM/C1 > HL-60/MX2 > HL-60/MX1 and to the IC50 dose without mitoxantrone were CCRF/CEM > CEM/C1 > HL-60 > HL-60/MX1 > HL-60/MX2.

It appeared that the most sensitive cell lines to the IC10 dose were CCRF/CEM > HL-60 > CEM/C1 > HL-60/MX2 > HL-60/MX1 and to the IC50 dose with mitoxantrone were CEM/C1 > CCRF/CEM > HL-60 > HL-60/MX2 > HL-60/MX1, respectively.

3.2. Analysis of Gene Expression Using Chemometry. In a preliminary statistical analysis of data results, descriptive statistics, minimal and maximal values, and means and standard variances were used.

To investigate a similarity between the behavior of investigated compounds, cell lines, and gene expression changes connected with multidrug resistance after exposition to investigated coumarin derivatives, a dimensionality reduction was

Table 2: IC10 + M values for line cells CEM/C1, CCRF/CEM, HL-60, HL-60/MX1, and HL-60/MX2 (μM). SD: standard deviation.

	CEM/C1 IC10 ± SD	CCRF/CEM IC10 ± SD	HL-60 IC10 ± SD	HL-60/MX1 IC10 ± SD	HL-60/MX2 IC10 ± SD
ISO	12.8 ± 2.5	8.0 ± 0.5	5.6 ± 0.5	14.0 ± 1.5	16.8 ± 2.5
BER	12.3 ± 2.0	7.7 ± 1.0	5.2 ± 0.4	13.4 ± 1.8	12.7 ± 2.0
XOL	13.0 ± 2.1	9.1 ± 1.1	5.6 ± 0.6	10.3 13.1	10.7 ± 1.4
XIN	14.7 ± 2.1	10.2 ± 2.1	9.4 ± 1.1	12.0 ± 2.1	10.2 ± 1.3
BIN	15.0 ± 2.6	8.2 ± 1.6	6.6 ± 0.6	11.8 ± 2.6	11.1 ± 2.6
BOL	12.0 ± 2.5	7.1 ± 0.8	14.7 ± 2.5	13.0 ± 2.5	11.0 ± 2.5
HEC	14.3 ± 2.5	6.6 ± 2.1	10.2 ± 2.5	14.0 ± 2.5	15.9 ± 2.5
FEL	17.3 ± 3.5	6.4 ± 2.6	11.0 ± 3.5	12.2 ± 3.5	15.7 ± 3.5
HER	4.2 ± 0.6	5.1 ± 0.5	4.2 ± 0.4	17.3 ± 2.5	6.4 ± 0.5
AET	5.3 ± 0.5	4.3 ± 1.0	10.0 ± 2.0	10.2 ± 2.0	6.2 ± 1.0
DHD	5.1 ± 0.6	5.6 ± 1.1	5.8 ± 0.7	3.8 ± 0.5	6.2 ± 1.1
COU	5.0 ± 0.4	1.2 ± 0.1	6.2 ± 0.5	4.2 ± 0.5	4.8 ± 0.6
AEL	4.8 ± 0.6	4.0 ± 0.6	6.4 ± 2.6	2.3 ± 2.6	7.6 ± 2.6
UMB	5.2 ± 0.5	4.2 ± 0.5	6.8 ± 2.5	13.0 ± 2.5	7.8 ± 1.5
4,7M	3.2 ± 0.5	6.3 0.7	4.1 ± 2.5	14.8 ± 2.5	6.2 ± 0.5
4,7E	1.7 ± 0.2	5.2 ± 0.5	2.3 ± 3.5	14.8 ± 3.5	7.2 ± 1.5
7ME	4.1 ± 0.5	4.2 ± 0.5	8.2 ± 2.5	13.8 ± 2.5	7.6 ± 1.5
6ME	3.2 ± 0.8	6.2 ± 1.0	6.8 ± 2.0	16.2 ± 2.0	4.8 ± 2.0
0,0D	2.2 ± 0.6	4.8 ± 1.1	4.0 ± 0.5	10.4 ± 2.1	7.4 ± 1.1
SCO	2.4 ± 0.2	6.8 ± 2.1	4.2 ± 2.1	20.2 ± 2.1	6.4 ± 2.1

Table 3: IC50 values for line cells CEM/C1, CCRF/CEM, HL-60, HL-60/MX1, and HL-60/MX2 (μM). SD: standard deviation.

	CEM/C1 IC50 ± SD	CCRF/CEM IC50 ± SD	HL-60 IC50 ± SD	HL-60/MX1 IC50 ± SD	HL-60/MX2 IC50 ± SD
ISO	21.5 ± 4.5	10.0 ± 4.2	21.5 ± 2.5	21.0 ± 4.2	26.0 ± 5.7
BER	28.5 ± 7.5	15.5 ± 4.5	16.5 ± 3.6	16.0 ± 4.9	36.5 ± 3.6
XOL	15.5 ± 4.5	12.5 ± 4.5	28.0 ± 5.0	19.0 ± 6.1	45.0 ± 9.0
XIN	24.0 ± 5.0	23.0 ± 7.6	61.0 ± 7..0	36.0 ± 5.1	46.5 ± 5.5
BIN	13.0 ± 4.5	5.5 ± 4.5	22.0 ± 3.6	8.0 ± 1.0	29.0 ± 4.0
BOL	19.0 ± 4.0	15.5 ± 4.0	43.0 ± 6.1	19.5 ± 2.6	34.5 ± 5.5
HEC	22.0 ± 5.3	18.0 ± 4.2	45.0 ± 10.1	18.0 ± 6.4	29.5 ± 5.0
FEL	8.0 ± 4.0	15.5 ± 4.5	42.0 ± 5.0	31.0 ± 8.0	40.5 ± 4.5
HER	25.0 ± 4.0	25.0 ± 4.0	25.0 ± 4.6	56.6 ± 4.1	30.0 ± 4.0
AET	25.0 ± 3.5	20.0 ± 2.6	25.0 ± 3.6	67.6 ± 7.7	30.0 ± 6.5
DHD	25.0 ± 4.0	20.0 ± 2.5	20.0 ± 3.2	47.2 ± 5.5	30.0 ± 4.6
COU	25.0 ± 5.0	30.0 ± 4.7	20.0 ± 3.0	43.8 ± 4.9	40.0 ± 4.9
AEL	25.0 ± 6.6	25.0 ± 3.5	20.0 ± 4.2	47.2 ± 4.6	40.0 ± 6.2
UMB	25.0 ± 3.2	25.0 ± 3.3	20.0 ± 2.1	42.8 ± 4.9	40.0 ± 4.0
4,7M	30.0 ± 3.8	20.0 ± 3.6	20.0 ± 4.2	30.0 ± 3.5	30.0 ± 5.3
4,7E	10.0 ± 1.5	25.0 ± 4.6	10.0 ± 2.5	32.4 ± 3.1	40.0 ± 3.8
7ME	15.0 ± 2.6	25.0 ± 3.1	25.0 ± 4.5	36.8 ± 3.1	40.0 ± 6.2
6ME	30.0 ± 5.7	30.0 ± 4.9	25.0 ± 2.1	39.5 ± 6.7	30.0 ± 4.3
0,0D	25.0 ± 3.5	30.0 ± 3.6	25.0 ± 4.0	35.7 ± 4.2	40.0 ± 5.5
SCO	20.0 ± 4.2	30.0 ± 4.6	25.0 ± 3.5	42.8 ± 4.8	40.0 ± 3.5

Table 4: IC50 + M values for line cells CEM/C1, CCRF/CEM, HL-60, HL-60/MX1, and HL-60/MX2 (μM). SD: standard deviation. *The survival of line cells after exposure to compounds at 50 μmol concentration drops to about 20%.

	CEM/C1 IC50 ± SD	CCRF/CEM IC50 ± SD	HL-60 IC50 ± SD	HL-60/MX1 IC50 ± SD	HL-60/MX2 IC50 ± SD
ISO	15.5 ± 4.5	10.5 ± 4.2	29.0 ± 2.5	28.0 ± 4.2	28.5 ± 5.7
BER	15.5 ± 7.5	14.0 ± 4.5	18.5 ± 3.6	24.0 ± 4.9	23.0 ± 3.6
XOL	15.5 ± 4.5	12.0 ± 4.5	42.0 ± 5.0	28.0 ± 6.1	37.5 ± 9.0
XIN	25.0 ± 5.0	16.0 ± 7.6	60.5 ± 10.0	31.0 ± 5.1	37.5 ± 5.5
BIN	13.0 ± 4.5	11.0 ± 4.5	27.0 ± 3.6	25.5 ± 4.0	23.0 ± 6.0
BOL	12.0 ± 4.0	*	19.0 ± 6.1	17.0 ± 2.6	30.0 ± 5.5
HEC	28.0 ± 5.3	*	46.5 ± 10.1	16.0 ± 6.4	36.0 ± 5.0
FEL	10.5 ± 4.0	*	36.0 ± 5.0	18.0 ± 8.0	42.0 ± 4.5
HER	23.2 ± 4.5	28.2 ± 4.5	28.1 ± 4.5	61.0 ± 4.5	28.2 ± 4.5
AET	23.6 ± 7.5	24.1 ± 7.5	22.6 ± 7.5	68.4 ± 7.5	29.4 ± 7.5
DHD	23.6 ± 4.5	23.2 ± 4.5	22.8 ± 4.5	52.3 ± 4.5	28.6 ± 4.5
COU	23.2 ± 5.0	34.0 ± 5.0	23.1 ± 5.0	47.8 ± 5.0	38.2 ± 5.0
AEL	24.0 ± 4.5	22.4 ± 4.5	21.4 ± 4.5	49.2 ± 4.5	38.8 ± 4.5
UMB	23.8 ± 4.0	22.6 ± 4.0	21.2 ± 4.0	44.8 ± 4.0	38.6 ± 4.0
4,7M	26.2 ± 5.3	23.6 ± 5.3	8.2 ± 5.3	34.0 ± 5.3	32.4 ± 5.3
4,7E	12.2 ± 4.0	27.6 ± 4.0	28.2 ± 4.0	34.2 ± 4.0	41.8 ± 4.0
7ME	13.8 ± 4.5	27.2 ± 4.5	27.6 ± 4.5	40.1 ± 4.5	37.6 ± 4.5
6ME	26.4 ± 7.5	34.0 ± 7.5	26.4 ± 7.5	42.0 ± 7.5	28.2 ± 7.5
0,0D	22.3 ± 4.5	32.2 ± 4.5	27.2 ± 4.5	38.2 ± 4.5	37.2 ± 4.5
SCO	18.7 ± 5.0	31.4 ± 5.0	27.4 ± 5.0	44.6 ± 5.0	36.4 ± 5.0

applied using the chemometric techniques: cluster analysis and Parallel Factor Analysis (PARAFAC).

To investigate a distribution of similarities of coumarin derivative action, a total chemometric analysis (of all expression change values) was also performed.

The results of the cluster analysis were presented as dendrograms (Figures 1 and 2). As the investigated data were continuous variables, Euclidean distance was chosen as an appropriate similarity measure.

The data was organized as a tensor of dimensions: four genes (*MDR1*, *MRP*, *LRP*, and *BCRP2*), five cell lines (HL-60, HL-60/X1, HL-60/MX2, CEM/C1, and CCRF/CEM), and 8 furanocoumarin derivatives: isopimpinellin (ISO), bergapten (BER), xanthotoxol (XOL), xanthotoxin (XIN), byakangelicin (BIN), byakangelicol (BOL), heraclenin (HEC), phellopterin (FEL), and 12 simple coumarins derivatives: herniarine (HER), aesculetin (AET), dihydrocoumarin (DHD), coumarin (COU), aesculin (AEL), umbelliferone (UMB), 4-methylo-7-methoxycoumarin (4,7M), 4-methylo-7-ethoxycoumarin (4,7E), 7-methylocoumarin (7ME), 6-methylocoumarin (6ME), 0,0-dimethylofraxetin (OOD), and scoparone (SCO).

3.3. Coumarin Derivative Dataset

3.3.1. Analysis of Similarity of the Investigated Coumarin Derivatives on the Level of Gene Expression. The cutoff height of the dendrogram (Figure 1(a)) was set to 12. Two visible clusters were observed. The first consists of furanocoumarins: isopimpinellin (ISO), bergapten (BER), xanthotoxol (XOL), xanthotoxin (XIN), byakangelicin (BIN), byakangelicol (BOL), heraclenin (HEC), and phellopterin (FEL); the second consists of coumarins: herniarine (HER), aesculetin (AET), dihydrocoumarin (DIH), coumarin (COU), aesculin (AEL), umbelliferone (UMB), 4-methylo-7-methoxycoumarin (4,7M), 4-methylo-7-ethoxycoumarin (4,7E), 7-methylocoumarin (7ME), 6-methylocoumarin (6ME), 0,0-dimethylofraxetin (OOD), and Scoparone (SCO).

The PARAFAC analysis of aforementioned data tensor explained 61.56% with an optimal number of two factors. The results grouped in two clusters. First, as previously, contains furanocoumarin derivatives, whereas the second contains the other coumarins (Figure 1(b)).

3.3.2. Analysis of Similarity of Genes Expression in Cell Lines Stimulated with Coumarin Derivatives. Optimal cutoff height for clustering was chosen to be 14 (Figure 1(c)). Genes are divided into two distinct clusters: *LRP* + *MRP* and *BCRP2* + *MDR1*. PARAFAC results (Figure 1(d)) do not show any clustering tendency.

3.3.3. Analysis of Similarity of Cell Lines Specific Gene Expression Stimulated with Coumarin Derivatives. The optimal cutoff height was set to 20 (Figure 1(e)). First cluster is created by HL-60, HL-60/MX2, and HL-60/MX1 lines, not strictly similar. The rest of lines are much more similar to themselves. In PARAFAC results (Figure 1(f)), the HL-60/MX2 cell line is a visible outlier and the other lines are much more similar to themselves.

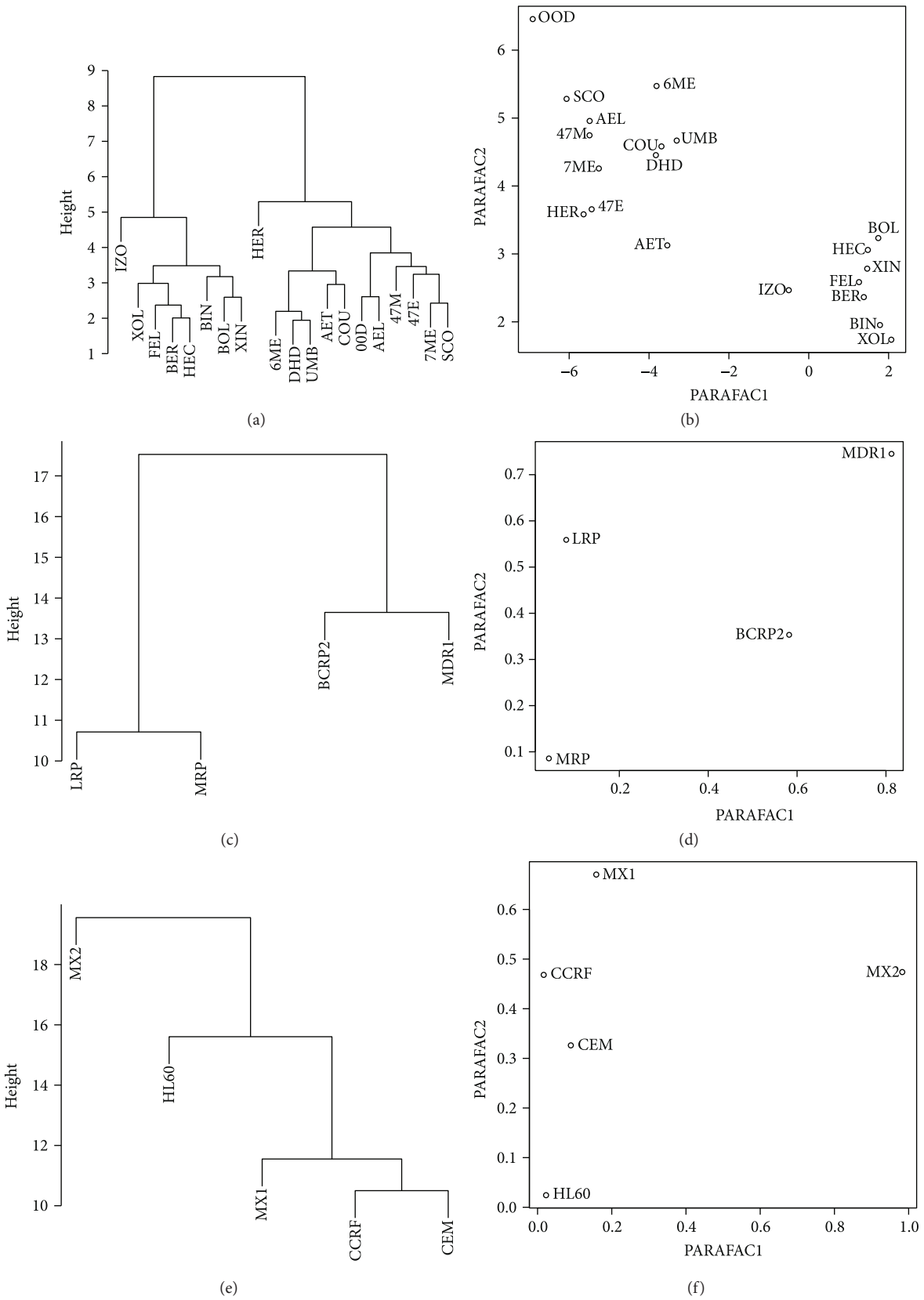

Figure 1: Comparison of similarities between coumarin derivatives (a, b), genes (c, d) and cell lines (e, f) by cluster analysis with Euclidean distance (a, c, e) and PARAFAC (b, d, f).

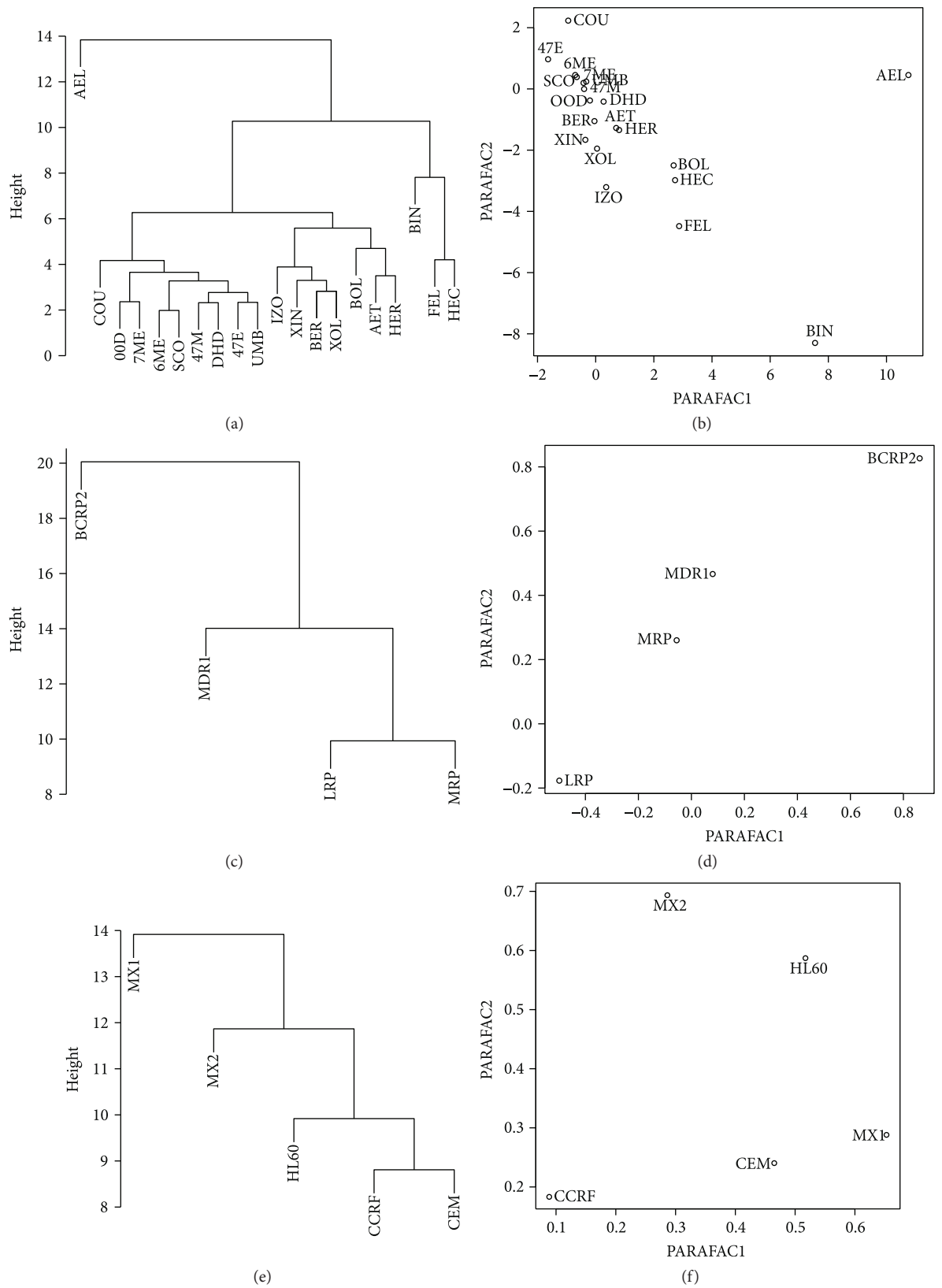

Figure 2: Similarity between furanocoumarin compounds (a, b), genes (c, d) and cell lines (e, f) analyzed by cluster analysis with Euclidean distance (a, c, e) and PARAFAC (b, d, f) while the mitoxantrone action.

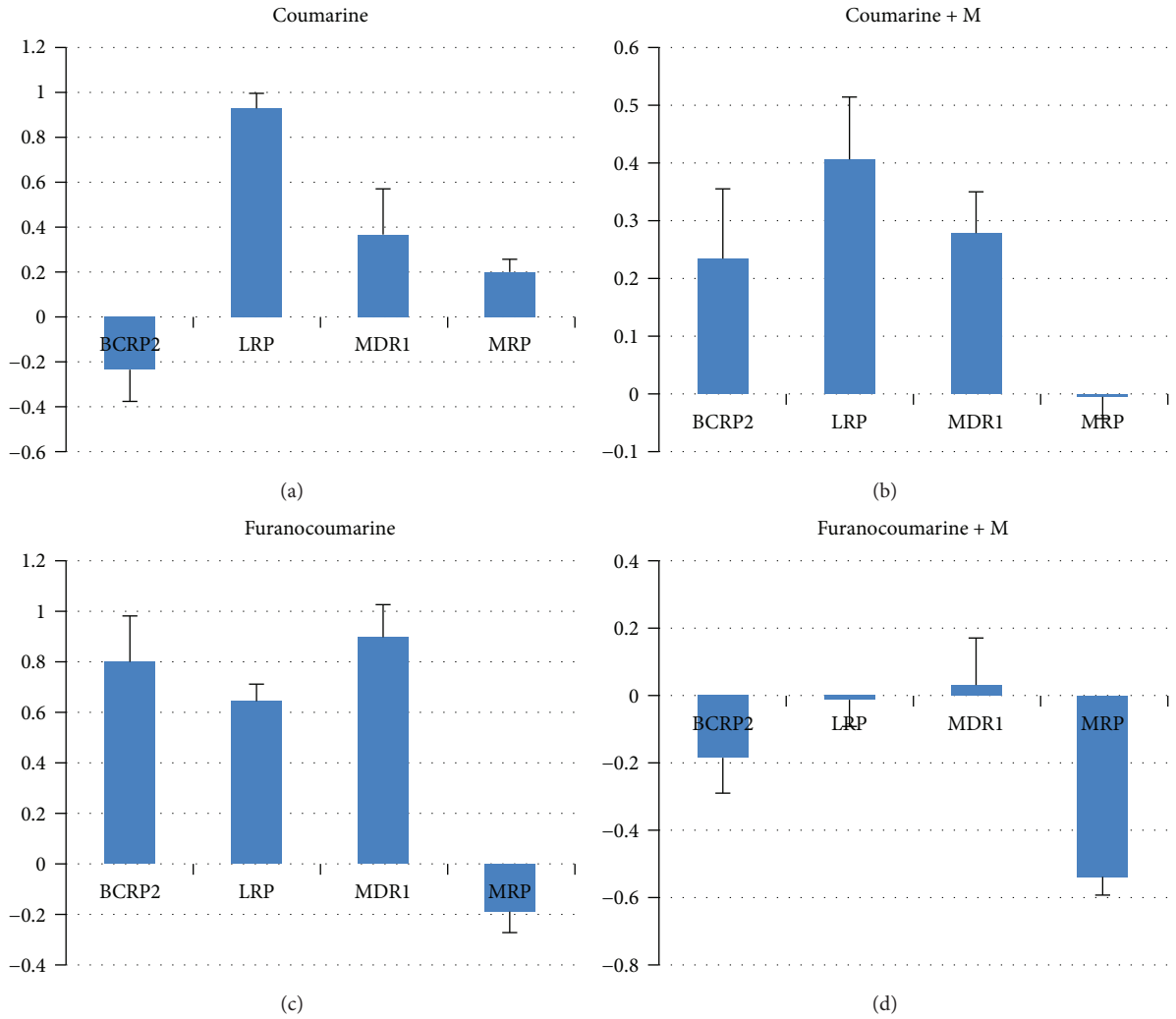

Figure 3: The mean *BCRP*, *LRP*, *MDR1*, and *MRP1* gene expression level in the cell lines CCRF/CEM, CEM/C1, HL-60, HL-60/MX1, and HL-60/MX2 after 24 h exposition on: coumarin (a), coumarin with mitoxantrone (b), furanocoumarins (c), and furanocoumarins without mitoxantrone (d) derivatives.

3.4. Coumarin Derivatives + Mitoxantrone Dataset

3.4.1. Analysis of Similarity of the Investigated Coumarin Derivatives on the Level of Gene Expression—Mitoxantrone Exposed Cells. Aesculin (AEL) was found to be an outlier during cluster analysis (Figure 2(a)). Phellopterin (FEL) and heraclenin (HEC) were similar to themselves but were slightly different than byakangelicin (BIN). Umbelliferone (UMB), 0,0-dimethylofraxetin (OOD), scoparone (SCO), 7-methylocoumarin (7ME), 6-methylocoumarin (6ME), 4-methylo-7-methoxycoumarin (4,7M), 4-methylo-7-ethoxycoumarin (4,7E), and dihydrocoumarin (DIH) formed visible cluster; however, they differ to coumarine (COU).

In the next cluster, a strong similarity was found between bergaptene (BER) and xanthotoxol (XOL), which were different than xanthotoxin (XIN) and isopimpinellin (ISO).

Two-factor PARAFAC decomposition explained 45.89% of whole data (Figure 2(b)). Aesculin (AEL) and byakangelicin (BIN) were identified as outliers during this analysis.

3.4.2. Analysis of Similarity of Cell Line-Specific Gene Expression Stimulated with Coumarin Derivatives and Mitoxantrone. Expression levels of *LRP* and *MRP1* genes were found to be similar (Figure 2(c)), whereas the other genes are not clustered. No clustering tendency was also observed with PARAFAC (Figure 2(d)).

3.5. Cell Line Similarity. CCRF/CEM and CEM/C1 cell lines were found to be most similar (Figure 2(e)), whereas the other cell lines are not clustered. No visible clustering tendency is observed with PARAFAC (Figure 2(f)).

3.5.1. Changes in Gene Expression of BCRP2, LRP, MDR1, and MRP in Cell Lines after 24 h Exposition on Coumarine Derivatives (Figure 3(a)). We observed a decrease in *BCRP* gene expression to minimum −3.392 (MX2/HL-60; 4,7M; IC50) and increased gene expression to a maximum *LRP* to 2.005-fold (MX1/HL-60; OOD; IC50), *MDR1* to 2.761-fold

(MX1/HL-60; 4,7M; IC50), *MRP1* to 1.407-fold (CCRF/CEM; OOD; IC50).

The mean expression levels of genes were *BCRP* −0.2346 (SD 1.06), *LRP* 0.933 (SD 0.50), *MDR1* 0.3664 (SD 1.56), and *MRP* 0.204 (SD 0.41).

3.5.2. Changes in Gene Expression of BCRP, LRP, MDR1, and MRP1 in Cell Lines after 24 h Exposition on Coumarine Derivatives with Mitoxantrone (Figure 3(b)). We observed increased gene expression to a maximum *BCRP* to 3.652-fold (CEM/C1; AEL; IC50), *LRP* to 1.790-fold (MX2/HL-60; 7ME; IC50), *MDR1* to 1.973-fold (MX1/HL-60; 6ME; IC50) and a decrease of *MRP1* gene expression to a minimum −0.822 (MX1/HL-60; HER; IC50).

The mean expression levels of genes were *BCRP* 0.234 (SD 0.92), *LRP* 0.406 (SD 0.82), *MDR1* 0.278 (SD 0.53), and *MRP1*-0.006 (SD 0.26).

3.5.3. Changes in Gene Expression of BCRP, LRP, MDR1, and MRP1 in Cell Lines after 24 h Exposition on Furanocoumarin Derivatives (Figure 3(c)). We observed an increase of gene expression to a maximum *BCRP* to 2.850-fold (MX1/HL-60; FEL; IC50), *LRP* to 1.358-fold (MX1/HL-60; BOL; IC50), *MDR1* to 2.513-fold (MX2/HL-60; BOL; IC50), and *MRP* 0.841-fold (CCRF/CEM; BER; IC50).

The mean expression levels of genes were *BCRP 2*0.800 (SD 1.13), *LRP* 0.647 (SD 0.37), *MDR1* 0.896 (SD 0.83), and *MRP1* −0.189 (SD 0.51).

3.5.4. Changes in Gene Expression of BCRP, LRP, MDR1, and MRP1 in Cell Lines after 24 h Exposition on Furanocoumarin Derivatives with Mitoxantrone (Figure 3(d)). We observed decreased gene expression to a minimum *BCRP* to −1.6571-fold (MX1/HL-60; IZO; IC50), *LRP* to −1.176-fold (CEM/C1; BIN; IC50), and *MRP1* to −1.213-fold (CEM/C1; BOL; IC50) and increase of *MDR1* gene expression to a maximum 2.325-fold (CEM/C1; BIN; IC50).

The mean expression levels of genes were *BCRP* −0.186 (SD 0.94), *LRP* −0.012 (SD 0.48), *MDR1* 0.029 (SD 0.87), and *MRP1* −0.541 (SD 0.30).

4. Discussion

Multidrug resistance is one of the main causes of failure in anticancer therapy. For over 40 years, research targeted at searching for compounds that abolish the multidrug resistance effect has been conducted by many research teams all over the world. The mechanism of multidrug resistance can be explained by overexpression of membrane transporters, mainly from the ABC family, which remove drugs from the cancer cell in an active way.

The cytotoxicity of the examined coumarins was estimated using trypan blue vital staining in the presence of M(+) and absence of mitoxantrone M. The IC10, IC10M(+), IC50, and IC50 M(+) values were determined. The cells of the five cancer cell lines exposed to coumarin derivatives presented diverse cytotoxicity dependent on the dose of IC10, IC10M(+), IC50, and IC50M(+).

Received dose values the IC10, IC10M(+), IC50, and IC50M(+) of coumarin compounds show high cytotoxicity for all tested cell lines. IC50 doses of coumarin compounds were lower than those for furanocoumarins, indicating more toxic effects on tumor cells. A similar conclusion was made by Yang et al. [35], in which ostol—a representative of simple coumarin—showed much higher cytotoxicity than the furanocoumarins investigated.

Against the background of the results, it can be concluded that lines without resistance phenotype are more susceptible to the effects of coumarin compounds. The least sensitive cell line is HL-60/MX1 and HL-60/MX2 derived from promyelocytic leukemia.

Coumarin substances, both natural and synthetic, are often screened for cancer toxicity in various cancer cell lines [36–39]. A literature review shows that the most commonly studied leukemia is HL-60.

Yang et al. [35] isolated five coumarin substances from *Cnidium monnieri* L. fruits and then examined their toxicity towards HL-60 cells. IC50 values have been established on a level not more than 50 μM for isopimpinellin (ISO), bergapten (BER), and xanthotoxin (XIN). Similar values were obtained in our work for isopimpinellin (ISO) and bergapten (BER) but were slightly higher for xanthotoxin (XIN) 61 μM/ml.

Cluster analysis with the Euclidean distance measure based on the MDR gene expression divided the examined compounds into two groups. The first group comprises furanocoumarin derivatives and the second one comprises coumarin derivatives. Such a division shows that these compounds have different mechanisms of action on the transcriptome of cancer cells.

Most of the investigators in the work of coumarin compounds induce increased expression of *MDR1*, *BCRP*, *LRP*, and *MRP* genes in leukemia cells [40–42]. This phenomenon can be explained by the correct detection by defense mechanisms of cells in response to coumarin compounds, which are recognized by the cell as xenobiotics.

However, to our knowledge, this is the first report describing the study of the effect of coumarin compounds with mitoxantrone on the expression of multidrug resistance genes. Our research show, in the case of furanocoumarin compounds in the presence of mitoxantrone, the expression of the *MDR1*, *BCRP*, *LRP*, and *MRP* genes was reduced, which may be of interest in a therapeutic context.

Studying the level of gene expression in the ABC family is often used in clinical practice. The levels of gene expression in the ABC family are examined in patients prior to initiation of treatment. The result is determined by further therapy. Evaluation of ABC gene expression in leukemia diagnostics may contribute to the early identification of patients at risk for treatment failure who require individual therapy [40, 41, 43].

On the basis of the results of the analysis of the ABC family gene expression in leukemia cells exposed to the examined compounds and statistical analysis, it is concluded that the furanocoumarin compounds are more promising in terms of their mechanism of action.

The high activity of coumarin compounds seems to be a basis for the design of new analogues characterized by increased activity and safety of use. The challenge for

researchers is to create new drugs based on the design and synthesis of highly active derivatives and the elucidation of their mechanism of action. Recent advances in the design of new union structures may lead to the discovery of novel anticancer drugs. Increased cancer mortality and high medical costs are the incentive to continually seek for anticancer drugs with increased efficacy.

The obtained results significantly broaden the knowledge about the anticancer effects of coumarin compounds and their effect on the expression of *MDR1*, *BCRP*, *LRP*, and *MRP* multidrug induction genes of tumor cells derived from the human hematopoietic system: CEM/C1, CCRF/CEM, HL-60, HL-60/MX1, and HL-60/MX2.

Overexpression of resistance genes, resulting in cell-induced drug resistance, is of great importance in the treatment of cancer. Often, it is a major factor in the failure of therapy. Therefore, it is important to look for new compounds that will safely modulate the expression of genes that affect multidrug resistance.

5. Conclusions

(1) For a majority of the coumarin compounds, the IC10, IC10M(+), IC50, and IC50M(+) values were estimated for the first time. The values obtained show high cytotoxicity to the examined cell lines, that is, CEM/C1, CCRF/CEM, HL-60, HL-60/MX1, and HL-60/MX2.

(2) It was observed that cell lines without the resistance phenotype are more sensitive to the coumarin compounds. HL-60/MX1 and HL-60/MX2 cell lines derived from promyelocytic leukemia are the least sensitive.

(3) In the case of furanocoumarin compounds, in the presence of mitoxantrone, the expression of the *MDR1*, *BCRP*, *LRP*, and *MRP* genes was reduced, which may be of interest in a therapeutic context.

(4) Cluster analysis conducted based on gene expression clearly divided the examined compounds into two groups. The first group comprises furanocoumarin derivatives, and the second group includes coumarin derivatives. Such a division shows that these compounds have different mechanisms of action on the transcriptome of cancer cells. The PARAFAC analysis confirms this observation.

(5) The obtained results significantly broaden the knowledge about the anticancer effects of coumarin compounds and their effect on the expression of *MDR1*, *BCRP*, *LRP*, and *MRP* genes in tumor cell lines derived from human hematopoietic system: CEM/C1, CCRF/CEM, HL-60, HL-60/MX1, and HL-60/MX2.

Abbreviations

HL-60: Human Caucasian promyelocytic leukemia from the American Type Culture Collection (ATCC CCL-240™)
HL-60/MX1: Human Caucasian acute promyelocytic leukemia from the American Type Culture Collection (ATCC CRL-2258™)
HL-60/MX2: Human Caucasian acute promyelocytic leukemia from the American Type Culture Collection (ATCC CRL-2257™)
CEM/C1: Human Caucasian acute lymphoblastic leukemia from the American Type Culture Collection (ATCC CRL-2265™)
CCRF/CEM: Human Caucasian acute lymphoblastic leukemia from the American Type Culture Collection (ATCC CCL-119™)
ISO: Isopimpinellin
BER: Bergapten
XOL: Xanthotoxol
XIN: Xanthotoxin
BIN: Byakangelicin
BOL: Byakangelicol
HEC: Heraclenin
FEL: Phellopterin
HER: Herniarine
AET: Aesculetin
DHD: Dihydrocoumarin
COU: Coumarin
AEL: Aesculin
UMB: Umbelliferone
4,7M: 4-methylo-7-methoxycoumarin
4,7E: 4-methylo-7-ethoxycoumarin
7ME: 7-methylocoumarin
6ME: 6-methylocoumarin
OOD: 0,0-dimethylofraxetin
SCO: Scoparone.

Conflicts of Interest

The authors declare no competing financial interest.

Acknowledgments

The authors acknowledge support by the Polish National Science Center (NN 405162 639–ABK). The paper was developed using the equipment purchased within the project "The equipment of innovative laboratories doing research on new medicines used in the therapy of civilization and neoplastic diseases" within the Operational Program Development of Eastern Poland 2007–2013, Priority Axis I Modern Economy, Operations I.3 Innovation Promotion (ABK, JK).

Supplementary Materials

Amplification plot. (*Supplementary Materials*)

References

[1] H. Liu, W. Jiang, and M. Xie, "Flavonoids: recent advances as anticancer drugs," *Recent Patents on Anti-Cancer Drug Discovery*, vol. 5, no. 2, pp. 152–164, 2010.

[2] R. Ebermann, G. Alth, M. Kreitner, and A. Kubin, "Natural products derived from plants as potential drugs for the

photodynamic destruction of tumor cells," *Journal of Photochemistry and Photobiology B: Biology*, vol. 36, no. 2, pp. 95–97, 1996.

[3] A. Lacy and R. O'Kennedy, "Studies on coumarins and coumarin-related compounds to determine their therapeutic role in the treatment of cancer," *Current Pharmaceutical Design*, vol. 10, no. 30, pp. 3797–3811, 2004.

[4] J. Pan, Q. Zhang, C. Zhao, and R. Zheng, "Redifferentiation of human hepatoma cells induced by synthesized coumarin," *Cell Biology International*, vol. 28, no. 5, pp. 329–333, 2004.

[5] K. I. Inui, S. Masuda, and H. Saito, "Cellular and molecular aspects of drug transport in the kidney," *Kidney International*, vol. 58, no. 3, pp. 944–958, 2000.

[6] K. M. Morrissey, S. L. Stocker, M. B. Wittwer, L. Xu, and K. M. Giacomini, "Renal transporters in drug development," *Annual Review of Pharmacology and Toxicology*, vol. 53, no. 1, pp. 503–529, 2013.

[7] C.-P. Wu, S. Ohnuma, and S. V. Ambudkar, "Discovering natural product modulators to overcome multidrug resistance in cancer chemotherapy," *Current Pharmaceutical Biotechnology*, vol. 12, no. 4, pp. 609–620, 2011.

[8] S. Karthikeyan and S. Hoti, "Development of fourth generation ABC inhibitors from natural products: a novel approach to overcome cancer multidrug resistance," *Anti-Cancer Agents in Medicinal Chemistry*, vol. 15, no. 5, pp. 605–615, 2015.

[9] J. D. Hayes and C. R. Wolf, "Molecular mechanisms of drug resistance," *Biochemical Journal*, vol. 272, no. 2, pp. 281–295, 1990.

[10] K. Jamroziak, E. Balcerczak, W. Młynarski, M. Mirowski, and T. Robak, "Distribution of allelic variants of functional C3435T polymorphism of drug transporter MDR1 gene in a sample of Polish population," *Polish Journal of Pharmacology*, vol. 54, no. 5, pp. 495–500, 2001.

[11] H. S. L. Chan, G. Haddad, P. S. Thorner et al., "P-glycoprotein expression as a predictor of the outcome of therapy for neuroblastoma," *The New England Journal of Medicine*, vol. 325, no. 23, pp. 1608–1614, 1991.

[12] H. M. Abdallah, A. M. Al-Abd, R. S. El-Dine, and A. M. El-Halawany, "P-glycoprotein inhibitors of natural origin as potential tumor chemo-sensitizers: a review," *Journal of Advanced Research*, vol. 6, no. 1, pp. 45–62, 2015.

[13] H. Thomas and H. M. Coley, "Overcoming multidrug resistance in cancer: an update on the clinical strategy of inhibiting p-glycoprotein," *Cancer Control*, vol. 10, no. 2, pp. 159–165, 2003.

[14] D. Jakoniuk, "Rola transportu blonowego w zjawisku opornosci wielolekowej," *Postępy Biologii Komórki*, vol. 31, pp. 703–715, 2004.

[15] E. Borowski, M. M. Bontemps-Gracz, and A. Piwkowska, "Strategies for overcoming ABC-transporters-mediated multidrug resistance (MDR) of tumor cells," *Acta Biochimica Polonica*, vol. 52, no. 3, pp. 609–627, 2005.

[16] S. Vibet, K. Maheo, J. Gore, P. Dubois, P. Bougnoux, and I. Chourpa, "Differential subcellular distribution of mitoxantrone in relation to chemosensitization in two human breast cancer cell lines," *Drug Metabolism and Disposition*, vol. 35, no. 5, pp. 822–828, 2007.

[17] F. Shen, B. J. Bailey, S. Chu et al., "Dynamic assessment of mitoxantrone resistance and modulation of multidrug resistance by valspodar (PSC833) in multidrug resistance human cancer cells," *The Journal of Pharmacology and Experimental Therapeutics*, vol. 330, no. 2, pp. 423–429, 2009.

[18] K. Michalak and O. Wesolowska, "Polyphenols counteract tumor cell chemoresistance conferred by multidrug resistance proteins," *Anti-Cancer Agents in Medicinal Chemistry*, vol. 12, no. 8, pp. 880–890, 2012.

[19] S. Kohlmünzer, *Farmakognozja*, Lekarskie PZWL, Warszawa, 5th edition, 2003.

[20] E. Hofmann, J. Webster, T. Kidd, R. Kline, M. Jayasinghe, and S. Paula, "Coumarins with xanthine oxidase inhibiting and radical scavenging properties: tools to combat oxidative stress in cells," *International Journal of Bioscience, Biochemistry and Bioinformatics*, vol. 4, no. 4, pp. 234–239, 2014.

[21] K. N. Venugopala, V. Rashmi, and B. Odhav, "Review on natural coumarin lead compounds for their pharmacological activity," *BioMed Research International*, vol. 2013, Article ID 963248, 14 pages, 2013.

[22] U. K. Udensi and P. B. Tchounwou, "Dual effect of oxidative stress on leukemia cancer induction and treatment," *Journal of Experimental & Clinical Cancer Research*, vol. 33, no. 1, pp. 106–115, 2014.

[23] M. Kawase, H. Sakagami, N. Motohashi et al., "Coumarin derivatives with tumor-specific cytotoxicity and multidrug resistance reversal activity," *In Vivo*, vol. 19, no. 4, pp. 705–711, 2005.

[24] A. Bogucka-Kocka, "The analysis of furanocoumarins in fruits of *Heracleum sibiricum* L.," *Acta Poloniae Pharmaceutica*, vol. 56, no. 5, pp. 399–402, 1999.

[25] A. Bogucka-Kocka and J. Kocki, "Influence of 4-methyl-7ethoxycoumarin on apoptosis in leukaemic Jurkat cells," *Annales Universitatis Mariae Curie-Sklodowska, Sectio DDD, Pharmacia*, vol. 17, no. 2, pp. 159–162, 2004.

[26] A. Bogucka-Kocka, J. Kocki, and T. Krzaczek, "The influence of bergapten on apoptosis in human Jurkat leukemic cell line," *Annales Universitatis Mariae Curie-Sklodowska, Sectio DDD, Pharmacia*, vol. 15, no. 2, pp. 187–192, 2002.

[27] A. Bogucka-Kocka, J. Rułka, J. Kocki, P. Kubiś, and E. Buzała, "Bergapten apoptosis induction in blood lymphocytes of cattle infected with bovine leukaemia virus (BLV)," *Bulletin of the Veterinary Institute in Pulawy*, vol. 48, no. 2, pp. 99–103, 2004.

[28] A. Bogucka-Kocka, H. D. Smolarz, M. Cioch, A. Dmoszyńska, and J. Kocki, "Xanthotoxin-induced apoptosis in chronic myelogenous leukemia," *Polish Journal of Environmental Studies*, vol. 14, no. 1, Supplement 2, pp. 44-45, 2005.

[29] A. Bogucka-Kocka, H. D. Smolarz, and J. Kocki, "Apoptotic and cytotoxic effects of selected furanocoumarins on human leukemic t-lymphoblasts," *Polish Journal of Environmental Studies*, vol. 14, no. 2, Supplement 2, pp. 453-454, 2005.

[30] J. Kocki and A. Bogucka-Kocka, "Apoptosis induction of human peripheal blood lymphocytes by naturally occurring coumarins," *Polish Journal of Environmental Studies*, vol. 13, no. 1, Supplement 2, pp. 221–224, 2004.

[31] K. Szewczyk and A. Bogucka-Kocka, "Analytical methods for isolation, separation and identification of selected furanocoumarins in plant material," in *Phytochemicals - a global perspective of their role in nutrition and health*, V. Rao, Ed., pp. 57–92, Intech, Rijeka, 2012.

[32] J. Kocki, M. Ułamek-Kozioł, A. Bogucka-Kocka et al., "Dysregulation of amyloid-β protein precursor, β-secretase, presenilin 1 and 2 genes in the rat selectively vulnerable CA1 subfield of hippocampus following transient global

brain ischemia," *Journal of Alzheimer's Disease*, vol. 47, no. 4, pp. 1047–1056, 2015.

[33] Applied Biosystems, "Relative quantitation using comparative CT: Getting started guide," 2007, https://www3.appliedbiosystems.com/cms/groups/mcb_support/documents/generaldocuments/cms_042115.pdf.

[34] K. J. Livak and T. D. Schmittgen, "Analysis of relative gene expression data using real-time quantitative PCR and the $2^{-\Delta\Delta C}{}_{T}$ method," *Methods*, vol. 25, no. 4, pp. 402–408, 2001.

[35] L.-L. Yang, M.-C. Wang, L.-G. Chen, and C.-C. Wang, "Cytotoxic activity of coumarins from the fruits of *Cnidium monnieri* on leukemia cell lines," *Planta Medica*, vol. 69, no. 12, pp. 1091–1095, 2003.

[36] I. Kostova, "Synthetic and natural coumarins as cytotoxic agents," *Current Medicinal Chemistry-Anti-Cancer Agents*, vol. 5, no. 1, pp. 29–46, 2005.

[37] M. A. Musa, V. L. Badisa, L. M. Latinwo, J. Cooperwood, A. Sinclair, and A. Abdullah, "Cytotoxic activity of new acetoxycoumarin derivatives in cancer cell lines," *Anticancer Research*, vol. 31, no. 6, pp. 2017–2022, 2011.

[38] M. Musa, J. Cooperwood, and M. O. Khan, "A review of coumarin derivatives in pharmacotherapy of breast cancer," *Current Medicinal Chemistry*, vol. 15, no. 26, pp. 2664–2679, 2008.

[39] J. Klenkar and M. Molnar, "Natural and synthetic coumarins as potential anticancer agents," *Journal of Chemical and Pharmaceutical Research*, vol. 7, no. 7, pp. 1223–1238, 2015.

[40] D. D. Ross, "Novel mechanisms of drug resistance in leukemia," *Leukemia*, vol. 14, no. 3, pp. 467–473, 2000.

[41] M. Kourti, N. Vavatsi, N. Gombakis et al., "Expression of multidrug resistance 1 (MDR1), multidrug resistance-related protein 1 (MRP1), lung resistance protein (LRP), and breast cancer resistance protein (BCRP) genes and clinical outcome in childhood acute lymphoblastic leukemia," *International Journal of Hematology*, vol. 86, no. 2, pp. 166–173, 2007.

[42] A. C. R. de Moraes, C. K. Maranho, G. S. Rauber, and M. C. Santos-Silva, "Importance of detecting multidrug resistance proteins in acute leukemia prognosis and therapy," *Journal of Clinical Laboratory Analysis*, vol. 27, no. 1, pp. 62–71, 2013.

[43] A. Sparreboom, R. Danesi, Y. Ando, J. Chan, and W. D. Figg, "Pharmacogenomics of ABC transporters and its role in cancer chemotherapy," *Drug Resistance Updates*, vol. 6, no. 2, pp. 71–84, 2003.

Hindawi
Oxidative Medicine and Cellular Longevity
Volume 2017, Article ID 9369872, 7 pages
https://doi.org/10.1155/2017/9369872

Research Article

UPLC-MS/MS Profile of Alkaloids with Cytotoxic Properties of Selected Medicinal Plants of the *Berberidaceae* and *Papaveraceae* Families

Anna Och,[1] Katarzyna Szewczyk,[1] Łukasz Pecio,[2] Anna Stochmal,[2] Daniel Załuski,[3] and Anna Bogucka-Kocka[1,4]

[1]*Chair and Department of Pharmaceutical Botany, Medical University of Lublin, Chodźki 1, 20-093 Lublin, Poland*
[2]*Institute of Soil Science and Plant Cultivation, 8 Czartoryskich, 24-100 Puławy, Poland*
[3]*Department of Pharmacognosy, Ludwik Rydygier Collegium Medicum, Nicolaus Copernicus University, 9 Marie Curie-Skłodowska Street, 85-094 Bydgoszcz, Poland*
[4]*Chair and Department of Biology and Genetics, Medical University of Lublin, Chodźki 4a, 20-093 Lublin, Poland*

Correspondence should be addressed to Anna Bogucka-Kocka; anna.bogucka-kocka@umlub.pl

Received 1 May 2017; Revised 20 June 2017; Accepted 4 July 2017; Published 30 August 2017

Academic Editor: Angeles Juarranz

Cancer is one of the most occurring diseases in developed and developing countries. Plant-based compounds are still researched for their anticancer activity and for their quantity in plants. Therefore, the modern chromatographic methods are applied to quantify them in plants, for example, UPLC-MS/MS (ultraperformance liquid chromatography tandem mass spectrometry). Therefore, the aim of the present study was to evaluate the content of sanguinarine, berberine, protopine, and chelidonine in *Dicentra spectabilis* (L.) Lem., *Fumaria officinalis* L., *Glaucium flavum* Crantz, *Corydalis cava* L., *Berberis thunbergii* DC., *Meconopsis cambrica* (L.) Vig., *Mahonia aquifolium* (Pursh) Nutt., *Macleaya cordata* Willd., and *Chelidonium majus* L. For the first time, N,N-dimethyl-hernovine was identified in *M. cambrica*, *B. thunbergii*, *M. aquifolium*, *C. cava*, *G. flavum*, and *C. majus*; methyl-hernovine was identified in *G. flavum*; columbamine was identified in *B. thunbergii*; and methyl-corypalmine, chelidonine, and sanguinarine were identified in *F. officinalis* L. The richest source of protopine among all the examined species was *M. cordata* ($5463.64 \pm 26.3\,\mu g/g$). The highest amounts of chelidonine and sanguinarine were found in *C. majus* ($51{,}040.0 \pm 1.8\,\mu g/g$ and $7925.8 \pm 3.3\,\mu g/g$, resp.), while *B. thunbergi* contained the highest amount of berberine ($6358.4 \pm 4.2\,\mu g/g$).

1. Introduction

Different ethnic communities of the world have used plant-based drugs to manage various ailments for centuries. Natural sources of drugs, such as paclitaxel (*Taxus brevifolia*) and *Vinca* alkaloids, are examples for the value of traditionally used plants for modern drug development. Plant-based molecules are used very often as drug precursors being converted into drugs by chemical modification, for example, 10-deacetybaccatin. It is established that about 120 plant-derived compounds are used in western medicine, and about 80% of the world population use medicinal plants in primary health care. Despite the fact that a lot of progress has been made towards the discovery of effective anticancer drugs, many western communities still use the plant-based drugs, including plants from traditional Chinese medicine. The plant-based drugs are used in developed and developing countries separately or together with synthetic drugs [1].

Alkaloids are naturally occurring chemical compounds with the strongest pharmacological activity among substances synthesized by plants. They are responsible for toxic properties of many plant species. High biological activity

made these compounds the subject of study for their use in pharmacy, particularly as anticancer drugs. Sanguinarine, berberine, and protopine are quaternary isoquinoline alkaloids, while chelidonine is a tertiary alkaloid. These compounds are extensively investigated for their antitumor activity. According to literature reports, sanguinarine induces apoptosis of many tumor cell lines [2, 3]. Berberine also possesses antitumor activity against several cell lines [4, 5]. Chelidonine is the main alkaloid of great celandine (*Chelidonium majus* L.). An increased interest in chelidonine was observed at the beginning of the 21st century, when scientists began to focus on its promising anticancer activity, such as against uveal melanoma cells [6], liver cancer [7], leukemia cells [8], or melanoma cells [6]. Protopine is an alkaloid with high pharmacological activity. It inhibits blood platelet aggregation and acts antihistaminically and antibacterially [9]. Regarding its antitumor activity, the fact of great importance is that the compound significantly increases the mRNA levels of CYP1A1 in human liver cells and hepatoma HepG2 cells [10]. In prostate cancer cells, the compound inhibits mitosis and induces apoptosis [11]. These alkaloids are present mainly in plant species of *Papaveraceae*, *Ranunculaceae*, and *Berberidaceae* families.

There are different ways of the anticancer alkaloid action, including an induction and activation of the apoptotic signaling proteins and promotion of apoptosis via an induction of DNA damage, caspase activators, and cell growth inhibitors. Apart from these modes of action, there are the other ones based on the formation of G-quadruplexes. This mode of action can be considered as a novel approach for cancer treatment [12, 13].

C. majus, *M. cordata*, *D. spectabilis*, *F. officinalis*, *G. flavum*, *C. cava*, *B. thunbergii*, *M. cambrica*, and *M. aquifolium* are the sources of alkaloids. The best known among the examined species are *C. majus* and *M. cordata*, characterized by the highest content of chelidonine. Until now, only these two species have been analyzed using a UPLC method [14]. *B. thunbergii* is the species which is currently arousing a great interest in research, particularly in China. It is the plant of the traditional Chinese and Tibetan medicine where it is highly effective in treatment of many inflammatory diseases in this region. Other species are also used as folk medicine in North America and Europe and as Ayurvedic medicine for their very rich chemical composition [15–17]. Until now, the discussed plant species have been analyzed by methods such as nonaqueous capillary electrophoresis-electrospray ion trap mass spectrometry [18], chromatography on a silica-gel column, TLC [19], and HPLC [18]. For the species *F. officinalis* and *G. flavum*, methods of individual substance extraction were mostly developed [14, 20]. *M. aquifolium* was studied mainly in terms of its antimicrobial activity due to the presence of (4-*O*-methyl-α-D-glucurono)-D-xylan possessing potent immunomodulation activity [21].

In this paper, we report on the separation and determination of four isoquinoline alkaloids in nine plant species in order to confirm published data, obtained using other analytical methods. Seven of the investigated species have never been analyzed using UPLC. The study was also conducted in order to identify new alkaloids in the investigated plant species. The UPLC method was chosen as it is precise, accurate, reproducible, and allows the identification of compounds based on their ESI-MS/MS spectra.

2. Experimental

2.1. Materials and Chemicals. *Berberis thunbergii*, *Chelidonium majus*, *Corydalis cava*, *Dicentra spectabilis*, *Fumaria officinalis*, *Glaucium flavum*, *Macleaya cordata*, *Mahonia aquifolium*, and *Meconopsis cambrica* were collected in June 2012 in the Botanical Gardens of Maria-Curie Sklodowska University in Lublin, Poland. These specimens were authenticated by Professor Anna Bogucka-Kocka (voucher specimens: DS-0612, FO-0612, GF-0612, CC-0612, BT-.0612, MeCa-0612, MA-0612, CM-0612, and MaCo-0612). The reference compounds protopine (P), berberine (B), chelidonine (CH), and sanguinarine (S) were of analytical grade from Sigma-Aldrich Company (St. Louis, USA). The purity of each compound was more than 98%, according to the manufacturer. Acetonitrile, ammonium acetate, methanol gradient HPLC grade, and acetic acid (>98%) for LC-UV-MS separations were purchased from J.T. Baker (Phillipsburg, NJ). Water was purified in-house using a Simplicity-185 with the Milli-Q water purification system (Millipore Co.).

2.2. Sample Preparation. Mixed standard stock solutions containing protopine (P) (0.960 mg/ml), berberine (B) (1.105 mg/ml), chelidonine (CH) (1.225 mg/ml), and sanguinarine (S) (1.065 mg/ml) in methanol were prepared and diluted with methanol to six different concentrations within the ranges (P) 4.4–131.5 μg/ml; (B) 6.1–183.8 μg/ml; (CH) 5.5–165.8 μg/ml; and (S) 5.3–159.8 μg/ml for the preparation of calibration curves. The standard solutions were filtered through a 0.22 mm membrane prior to injection. All solutions were stored in a refrigerator at 4°C before analysis.

The extracts were prepared according to the method as described earlier [22]. Five grams of the dried and ground plant materials were macerated with 80 ml of methanol for 3-4 days. Subsequently, methanol was poured off and a new portion was added. This process was repeated nine times. After the last extraction, there was no residue after the evaporation of solvent. The obtained portions of the extracts were combined. The solvent was partially evaporated in the vacuum evaporator UnipanPro Typ 365 to the total volume of 100 ml.

2.3. Ultraperformance Liquid Chromatography-Tandem Mass Spectrometry (UPLC-MS/MS). Chromatographic conditions were based on Lu et al. [12] with some modifications. The UPLC analysis was performed using the Waters ACQUITY UPLC system (Waters Corp., Milford, MA, USA) equipped with a binary pump system, sample manager, column manager, and PDA detector (Waters Corp.). Waters MassLynx software v.4.1 was used for acquisition and data processing. The separation of alkaloids in analyzed extracts was carried out with BEH C18 column (100 mm × 2.1 mm × 1.7 μm), Waters Corp., Milford, MA, USA. Column temperature was maintained at 35°C. The flow

rate was adjusted to 0.40 ml/min. Elution was conducted using mobile phase A (ammonium acetate, 20 mM, adjusted to pH 3.0 with acetic acid in Milli-Q water) and mobile phase B (acetonitrile) with gradient program as follows: 0–0.8 min, 3% B; 0.8–1.0 min, 3–12% B; 1.0–9.5 min, 12% B; 9.5–15.0 min, 12–20% B; 15.0–20.0 min, 20–30% B; 20.0–21.0 min, 30% B; 21.0–21.1 min, 30–80% B; 21.1–22.1 min, 80% B; 22.1–22.2, 80–3% B; and 22.2–25.0 min, 3% B. The samples were kept at 15°C in the sample manager. The injection volume of the sample was 1.0 μl (partial loop with needle overfill mode). A strong needle wash solution (95 : 5, methanol-water, *v*/*v*) and a weak needle wash solution (5 : 95, acetonitrile-water, *v*/*v*) were used. Chromatograms were acquired at 240 nm and 270 nm at a 5-point rate, at 4.8 nm resolution. Peaks were assigned on the basis of their retention times, mass to charge ratio (*m*/*z*), and ESI-MS/MS fragmentation pattern, in comparison to those of the reference compounds and literature data [23]. The MS analyses were carried out on a TQD mass spectrometer (Waters Corp.) equipped with a Z-spray electrospray interface. The parameters for ESI source were capillary voltage 3.0 kV, cone voltage 30 V, desolvation gas N_2 800 L/h, cone gas N_2 80 L/h, source temp. 120°C, desolvation temp. 350°C, dwell time 0.6 s. Analysis was carried out using a full scan mode (mass range of 250–450 amu was scanned). Compounds were analyzed in a positive ion mode. The content of identified compounds was estimated based on the peak area at 270 nm [+/− very low content (below 5% of the total peak area at 270 nm), + low content (below 15% of the total peak are at 270 nm), ++ moderate content (15–30% of the total peak area at 270 nm), and +++ high content (above 30% of the total peak area at 270 nm)]. The protopine, berberine, chelidonine, and sanguinarine were quantified on the basis of their peak areas and comparison with a calibration curve obtained with the corresponding standards.

The methods were validated in terms of accuracy, precision LOD, and LOQ. Moreover, the linear ranges of calibration curves were determined. The stock solution of the four standards was prepared and diluted to six appropriate concentrations for the establishment of calibration curves. The regression equations were achieved after linear regression of the peak areas versus the corresponding concentrations. Limit of detection (LOD) and limit of quantification (LOQ) for each analyte were determined under the chromatographic conditions at a signal-to-noise ratio (S/N) of 3 and 10, respectively. Intraday and interday variations were chosen to determine the precision of the developed assay. Three different concentration solutions (low, medium, and high) of the standards were prepared. The intraday variation was determined by analyzing seven replicates a day. Interday variation was examined in seven days. Repeatability was confirmed with six solutions prepared from sample 1 and one of them was injected into the apparatus at 0, 3, 6, 12, 16, 18, and 24 h to access the stability of the solution. Variations were expressed by RSDs.

3. Results and Discussion

In our experiment, the established analytical method was applied for determination of alkaloids in nine species belonging to *Berberidaceae* and *Papaveraceae* families. The analysis of samples revealed the presence of nineteen alkaloids. For the final identification of B, CH, P, and S, the comparisons of retention times with available chemical standards were made. The identification of alkaloids other than B, CH, P, and S was based on the detected maxima and the shape of the spectra. The results are presented in Table 1. Exemplary UPLC chromatograms of *B. thunbergii* extract are shown in Figure 1.

The least differentiated taxa are *M. cambrica* and *D. spectabilis*—containing two of the identified alkaloids. The richest are *C. majus*—eight identified alkaloids and *C. cava*—seven identified alkaloids.

The lowest level of protopine was detected in *M. cambrica* (74.4 ± 0.4 μg/g), while the highest content of it was detected in *M. cordata* ($54{,}636.4 \pm 2.6$ μg/g). In *M. aquifolium* and *B. thunbergii*, protopine was not detected. Berberine was detected in four of investigated plant species—*C. majus*, *M. cordata*, *B. thunbergii*, and *M. aquifolium*. The lowest level of berberine was detected in *M. cordata* (1401.4 ± 2.4 μg/g), while the highest in *B. thunbergii* (6358.4 ± 4.2 μg/g).

The lowest level of sanguinarine was detected in *C. cava* (69.0 ± 0.1 μg/g), while the highest content of sanguinarine was detected in *C. majus* (7925.8 ± 3.3 μg/g). In *B. thunbergii*, *M. cambrica*, and *M. aquifolium*, sanguinarine was not detected. Chelidonine was detected only in *F. officinalis* (650.0 ± 0.5 μg/g) and *C. majus* ($51{,}040.0 \pm 1.8$ μg/g). *N,N*-Dimethyl-hernovine was not detected earlier in any of the investigated plants. The compound was observed in *M. cambrica*, *B. thunbergii*, *M. aquifolium*, *C. cava*, *G. flavum*, and *C. majus*. Methyl-hernovine was detected for the first time in *G. flavum* and columbamine in *B. thunbergii*. According to literature data, columbamine occurs in *C. cava* [24] and *M. aquifolium* [25] which was not confirmed in this study. Methyl-corypalmine was detected in *F. officinalis* for the first time. In this study, the presence of fumarophycine [26] and corydamine [27] in this plant material was confirmed. The presence of jatrorrhizine in *M. aquifolium* [25] and corydaline in *C. cava* [28, 29] was also confirmed, but not in *F. officinalis* [27]. Corydine and tetrahydropalmatine were found in this study only in *C. cava* but were not in other investigated plant species. Allocryptopine was detected only in *C. majus* and *M. cordata*. The analysis confirmed the presence of cryptopine in *Chelidonium majus* but not in *F. officinalis* [27] nor in *M. cordata* [30]. The study did not confirm the presence of columbamine in *C. cava* [23] and *M. aquifolium* [25] and cryptopine in *F. officinalis* [27], *D. spectabilis* [31], and *M. cordata* [30].

Validation of the UHPLC method was performed in terms of accuracy and precision LOD and LOQ. The results of the regression indicated that all four reference compounds showed good linearity in a relatively wide concentration range. The correlation coefficients of all calibration curves were $R^2 > 0.9992$. The LODs and LOQs of the four analytes were 10.0–47.8 and 33.2–159.6 μg/g, respectively. Parameters of calibration curves together with LOD and LOQ values are presented in Table 2.

The relative standard deviation (RSD%), as a measure of repeatability, was from 0.58% (berberine) to 1.25%

Table 1: The contents (μg/g) of alkaloids in investigated plant species.

Plant species	Compound																		
	Allocryptopine	Berberine*	Chelerythrine	Chelidonine*	Columbamine	Coptisine	Corydaline	Corydamine	Corydine	Cryptopine	*N,N*-Dimethyl-hernovine	Fumarophycine	Glaucine	Jatrorrhizine	Methyl-corypalmine	Methyl-hernovine	Protopine*	Sanguinarine*	Tetrahydropalmatine
Berberis thunbergii	–	6358.4 ± 4.2	–	–	++	–	–	–	–	–	+/–	–	–	–	–	–	–	–	–
Chelidonium majus	+++	5366.6 ± 4.3	+++	51,040.0 ± 1.8	–	–	–	–	–	++	+++	–	–	–	–	–	11,660.6 ± 13.6	7925.8 ± 3.3	–
Corydalis cava	–	–	–	–	–	++	++	–	++	–	++	–	–	–	–	–	1764.0 ± 0.7	69.0 ± 0.1	+/–
Dicentra spectabilis	–	–	–	–	–	–	–	–	–	–	–	–	–	–	–	–	11,899.6 ± 8.6	1105.6 ± 1.0	–
Fumaria officinalis	–	–	–	650.0 ± 0.5	–	–	–	+/–	–	–	–	+/–	–	–	+/–	–	3726.6 ± 0.6	125.4 ± 0.2	–
Glaucium flavum	–	–	–	–	–	–	–	–	–	–	++	–	+++	–	–	+/–	4990.0 ± 1.3	407.4 ± 0.9	–
Macleaya cordata	+++	1401.4 ± 2.4	–	–	–	–	–	–	–	–	–	–	–	–	–	–	54,636.4 ± 2.6	1835.0 ± 4.3	–
Mahonia aquifolium	–	3344.6 ± 3.7	–	–	–	–	–	–	–	–	++	–	–	++	–	–	–	–	–
Meconopsis cambrica	–	–	–	–	–	–	–	–	–	–	+	–	–	–	–	–	74.4 ± 0.4	–	–

*Comparisons with chemical standard have been made; without ∗ indicates tentative assignment based on UV-Vis and MS/MS profile. –: not detected; +/–: tentatively detected, <5% based on the peak area recorded at 270 nm for all identified; +: <15% based on peak area recorded at 270 nm for all identified, ++: 15–30% based on the peak area recorded at 270 nm for all identified; +++: >30% based on the peak area recorded at 270 nm for all identified.

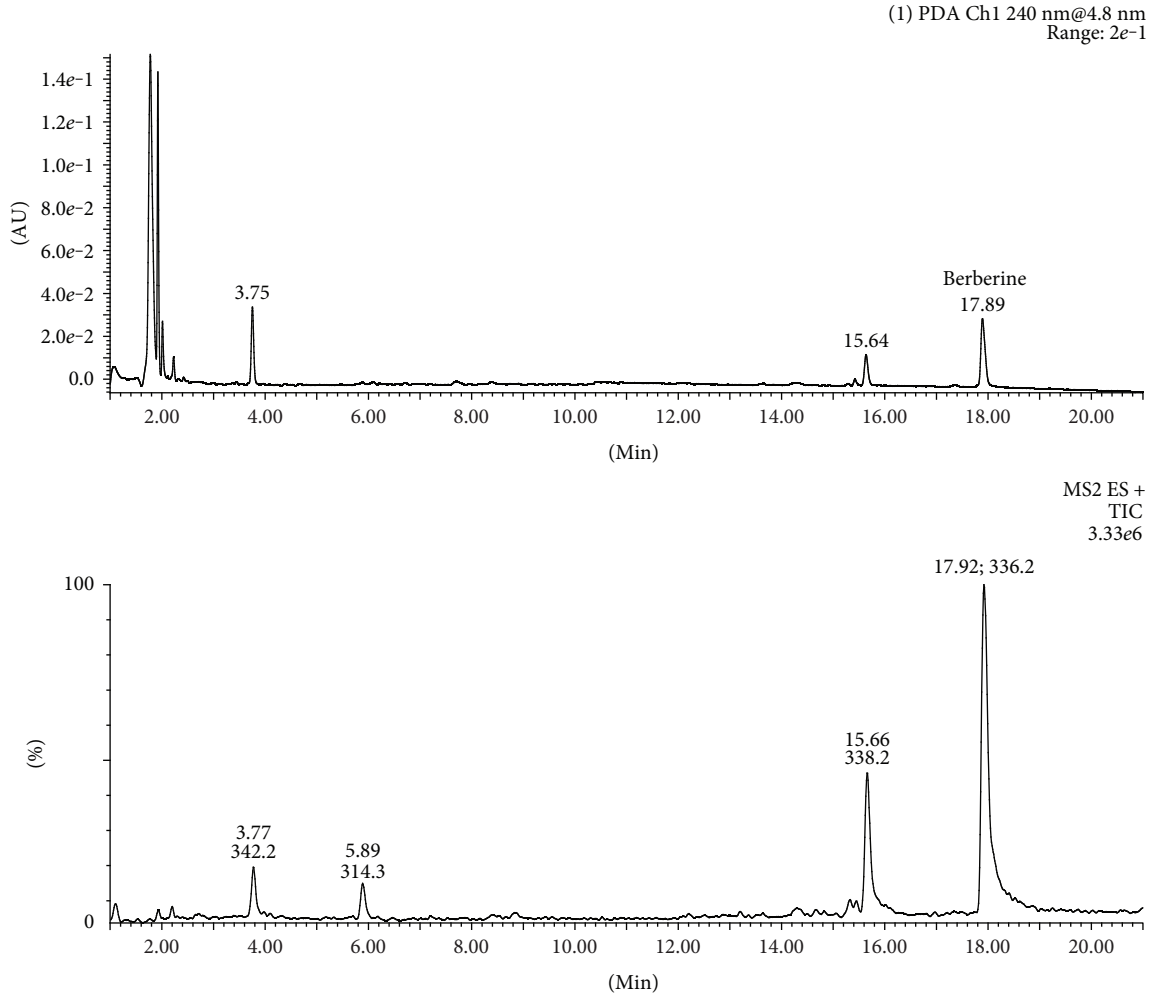

Figure 1: The UPLC-PDA (240 nm) and UPLC-ESI-MS/MS (positive ion mode) chromatograms of *Berberis thunbergii* extract.

Table 2: Analytical parameters of UPLC-MS/MS quantitative methods; data for calibration curves, limit of detection (LOD), and limit of quantification (LOQ) values for four analyzed alkaloids. $y = Ax + B$, where y is the peak area, x is concentration of the alkaloids (μg/g), and R^2 is the correlation coefficient of the equation.

Analytes	Regression equations	R^2	Linear range (μg/g)	LOD (μg/g)	LOQ (μg/g)
Protopine	$y = -129.20 + 58.62x$	0.9992	88–2630	14.0	46.6
Berberine	$y = -607.10 + 133.00x$	0.9992	110–3316	47.8	159.6
Chelidonine	$y = -35.14 + 53.91x$	0.9996	122–3676	12.6	42.0
Sanguinarine	$y = -344.30 + 167.20x$	0.9997	106–3196	10.0	33.2

(chelidonine). These values are in good agreement with requirements for a developed method. The intra- and interday precision RSD values were less than 3.0% for all compounds, which showed good reproducibility of the method. The results are summarized in Table 3.

4. Conclusions

Despite the extensive research conducted on the phytochemical composition of the investigated species, several alkaloids were detected in this study for the first time. These were cryptopine in *Chelidonium majus*; N,N- dimethylhernovine in *Meconopsis cambrica*, *Berberis thunbergii*, *Mahonia aquifolium*, *Corydalis cava*, *Glaucium flavum*, and *Chelidonium majus*; methyl-hernovine in *Glaucium flavum*; columbamine in *Berberis thunbergii*; methyl-corypalmine, chelidonine, and sanguinarine in *Fumaria officinalis*; and sanguinarine in *Corydalis cava*. Environmental conditions are one of the possible causes of variation of alkaloidal composition of the tested plant materials, since the data were obtained from studies of the raw materials originating from Turkey and China. These differences may also result from

Table 3: Precision, repeatability, and stability of four alkaloids in *Ch. majus* L.

Analytes	Levels (μg/g)	Precision Intraday RSD (%)	Interday RSD (%)	Repeatability (RSD%)
Protopine	88	0.63	2.43	0.64
	1680.0	0.40	0.56	
	2620.0	0.62	0.28	
Berberine	140	0.62	0.43	0.58
	1800.0	0.97	1.80	
	3660	0.88	0.79	
Chelidonine	110	0.67	1.40	1.25
	1100.0	0.25	0.63	
	3300.0	0.63	0.99	
Sanguinarine	106	0.62	1.36	0.80
	1960.0	0.96	1.15	
	3180.0	0.36	0.84	

the analytical methods used, because extracts from *C. cava* and *F. officinalis* were not analyzed by UPLC-MS/MS method earlier.

Abbreviations

P: Protopine
B: Berberine
CH: Chelidonine
S: Sanguinarine
UPLC-MS/MS: Ultraperformance liquid chromatography-tandem mass spectrometry.

Conflicts of Interest

The authors declare no competing financial interests.

References

[1] R. Verpoorte, "Pharmacognosy in the new millenium: leadfinding and biotechnology," *Journal of Pharmacy and Pharmacology*, vol. 52, pp. 253–262, 2000.

[2] H. Ahsan, S. Reagan-Shaw, J. Breur, and N. Ahmad, "Sanguinarine induces apoptosis of human pancreatic carcinoma AsPC-1 nad BxPC-3 cells via modulations in Bcl-2 family proteins," *Cancer Letters*, vol. 249, pp. 198–208, 2007.

[3] M. C. Chang, C. P. Chan, Y. J. Wang et al., "Induction of necrosis and apoptosis to KB cancer cells by sanguinarine is associated with reactive oxygen species production and mitochondrial membrane depolarization," *Toxicology and Applied Pharmacology*, vol. 218, pp. 143–151, 2007.

[4] H. P. Kuo, T. C. Chuang, S. C. Tsai et al., "Berberine, an isoquinoline alkaloid, inhibits the metastatic potential of breast cancer cells via Akt pathway modulation," *Journal of Agricultural and Food Chemistry*, vol. 60, pp. 9649–9658, 2012.

[5] J. J. Park, S. M. Seo, E. J. Kim et al., "Berberine inhibits human colon cancer cell migration via AMP-activated protein kinase-mediated downregulation of integrin β 1 signaling," *Biochemistry Biophysics Research Communcations*, vol. 426, pp. 461–467, 2012.

[6] A. Kemény-Beke, J. Aradi, J. Damjanovich et al., "Apoptotic response of uveal melanoma cells upon treatment with chelidonine, sanguinarine and chelerythrine," *Cancer Letters*, vol. 237, pp. 67–75, 2006.

[7] S. K. Noureini and M. Wink, "Transcriptional down regulation of hTERT and senescence induction in HepG2 cells by chelidonine," *World Journal Gastroenterology*, vol. 15, pp. 3603–3610, 2009.

[8] V. Kaminsky, K. W. Lin, Y. Filyak, and R. Stoika, "Differential effect of sanguinarine, chelerythrine and chelidonine on DNA damage and cell viability in primary mouse spleen cells and mouse leukemic cells," *Cell Biology International*, vol. 32, pp. 271–277, 2008.

[9] S. A. Saeed, A. H. Gilani, R. U. Majoo, and B. H. Shah, "Anti-thrombotic and anti-inflammatory activities of protopine," *Pharmacology Research*, vol. 36, pp. 1–7, 1997.

[10] J. Vrba, E. Vrublova, M. Modriansky, and J. Ulrichova, "Protopine and allocryptopine increase mRNA levels of cytochromes P450 1A in human hepatocytes and HepG2 cells independently of AhR," *Toxicology Letters*, vol. 203, pp. 135–141, 2011.

[11] C. H. Chen, C. H. Liao, Y. L. Chang, J. H. Guh, S. L. Pan, and C. M. Teng, "Protopine, a novel microtubule-stabilizing agent, causes mitotic arrest and apoptotic cell death in human hormone-refractory prostate cancer cell lines," *Cancer Letters*, vol. 315, pp. 1–11, 2010.

[12] J. J. Lu, J. L. Bao, X. P. Chen, M. Huang, and Y. T. Wang, "Alkaloids isolated from natural herbs as the anticancer agents," *Evidence-Based Complementary and Alternative Medicine*, vol. 2012, Article ID 485042, 12 pages, 2012.

[13] Z. Habli, G. Toumieh, M. Fatfat, O. N. Rahal, and H. G. Muhtasib, "Emerging cytotoxic alkaloids in the battle against cancer: overview of molecular mechanisms," *Molecules*, vol. 22, pp. 1–22, 2017.

[14] Y. Gu, D. Qian, J. Duan et al., "Simultaneous determination of seven main alkaloids of *Chelidonium majus* L. by ultra-performance-LC with photodiode array detection," *Journal Separation Science*, vol. 33, pp. 1004–1009, 2010.

[15] M. G. Bogdanov and I. Svinyarov, "Ionic liquid-supported solid–liquid extraction of bioactive alkaloids. II. Kinetics, modeling and mechanism of glaucine extraction from *Glaucium flavum* Cr. (Papaveraceae)," *Separation Purify Technology*, vol. 103, pp. 279–232, 2013.

[16] A. Kardošová, A. Maloviková, V. Pätoprstý, G. Nosálová, and T. Matáková, "Structural characterization and antitussive activity of a glucuronoxylan from *Mahonia aquifolium* (Pursh) Nutt," *Carbohydrate Polymers*, vol. 47, pp. 27–33, 2002.

[17] G. Y. Zuo, F. Y. Meng, J. Han et al., "In vitro activity of plant extracts and alkaloids against clinical isolates of extended-spectrum β-lactamase (ESBL)-producing strains," *Molecules*, vol. 16, pp. 5453–5459, 2011.

[18] S. Sturm, C. Seger, and H. Stuppner, "Analysis of Central European *Corydalis* species by nonaqueous capillary electrophoresis-electrospray ion trap mass spectrometry," *Journal Chromatography*, vol. 1159, pp. 42–50, 2007.

[19] J. Slavik, J. Bochorakova, D. Kostalova, and V. Hrochova, "Alkaloids of *Mahonia aquifolium* (Pursh) Nutt. II," *Chemical Papers*, vol. 39, pp. 537–542, 1985.

[20] C. W. Kim, N. Takao, M. Ichimaru, and A. Kato, "On the alkaloid cell and contained alkaloids of *Dicentra spectabilis*

(Papaveraceae)," *Japanese Journal Pharmacognosy*, vol. 46, pp. 109–114, 1992.

[21] L. Rakotondramasy-Rabesiaka, J. L. Havet, C. Porte, and H. Fauduet, "Estimation of effective diffusion and transfer rate during the protopine extraction process from *Fumaria officinalis* L.," *Separation and Purification Technology*, vol. 76, pp. 126–131, 2010.

[22] J. Suchomelova, H. Bochorakova, H. Paulova, P. Musil, and E. Taborska, "HPLC quantification of seven quaternary benzo[c]phenanthridine alkaloids in six species of the family Papaveraceae," *Journal of Pharmaceutical and Biomedical Analysis*, vol. 44, pp. 283–287, 2007.

[23] J. Slavik and L. Slavikova, "Alkaloids of the Papaveraceae. LXVII. Alkaloids from *Corydalis cava* (L.). Collection of Czechoslovak," *Chemistry Communications*, vol. 44, pp. 2261–2274, 1979.

[24] A. Kardošová, A. Ebringerova, J. Alfoldia, G. Nosálová, T. Matáková, and V. Hrıbalova, "Structural features and biological activity of an acidic polysaccharide complex from *Mahonia aquifolium* (Pursh) Nutt," *Carbohydrate Polymers*, vol. 57, pp. 165–176, 2004.

[25] V. Brezová, D. Dvoranová, and D. Kostálová, "Oxygen activation by photoexcited protoberberinium alkaloids from *Mahonia aquifolium*," *Phytotherapy Research*, vol. 18, pp. 640–646, 2004.

[26] C. Seger, S. Sturm, E. Strasser, E. Ellmerer, and H. Stuppner, "1H and 13C NMR signal assignment of benzylisoquinoline alkaloids from *Fumaria officinalis* L. (Papaveraceae)," *Magnetic Resonance Chemistry*, vol. 42, pp. 882–886, 2004.

[27] B. Sener, "Turkish species of *Fumaria* L. and their alkaloids. VII. Alkaloids from *Fumaria officinalis* L. and *Fumaria cilicica* Hausskn," *Gazi Universitesi Eczacilik Fakultesi Dergisi*, vol. 2, pp. 45–49, 1985.

[28] Z. Novak, J. Chlebek, L. Opletal et al., "Corylucinine, a new alkaloid from *Corydalis cava* (Fumariaceae), and its cholinesterase activity," *Natural Products Communications*, vol. 7, pp. 859-860, 2012.

[29] G. Verzar-Petri and H. Minh, "Chromatographic separation of alkaloids from *Corydalis cava* L. (Fumariaceae)," *Scientia Pharmaceutica*, vol. 46, pp. 169–180, 1978.

[30] Y. Guo, J. Zeng, M. Tan, J. Huang, and X. Z. Y. Liu, "Contents of 4 alkaloids in leaves of *Macleaya microcarpa* (maxim) Fedde and *Macleaya cordata* (Willd.) R. Br," *Central South Pharmacy*, vol. 9, pp. 829–832, 2011.

[31] I. A. Israilov, F. M. Melikov, and D. A. Muravyeva, "Alkaloids of Dicentra," *Chemistry of Natural Compounds*, vol. 20, pp. 74–76, 1984.

Hindawi
Oxidative Medicine and Cellular Longevity
Volume 2017, Article ID 2694945, 16 pages
https://doi.org/10.1155/2017/2694945

Research Article

An Extract from the Plant *Deschampsia antarctica* Protects Fibroblasts from Senescence Induced by Hydrogen Peroxide

Ana Ortiz-Espín,[1] Esther Morel,[2] Ángeles Juarranz,[2] Antonio Guerrero,[3] Salvador González,[4,5] Ana Jiménez,[1] and Francisca Sevilla[1]

[1]*Department of Stress Biology and Plant Pathology, Centro de Edafología y Biología Aplicada del Segura, Consejo Superior de Investigaciones Científicas, Campus de Espinardo, 30100 Murcia, Spain*
[2]*Department of Biology, Faculty of Sciences, Universidad Autónoma de Madrid, 28049 Madrid, Spain*
[3]*IFC SA-Industrial Farmaceutica Cantabria, 28043 Madrid, Spain*
[4]*Department of Medicine and Medical Specialties, Universidad de Alcalá de Henares, 28805 Madrid, Spain*
[5]*Dermatology Service, Memorial Sloan-Kettering Cancer Center, New York, NY, USA*

Correspondence should be addressed to Francisca Sevilla; fsevilla@cebas.csic.es

Received 12 April 2017; Revised 30 June 2017; Accepted 5 July 2017; Published 15 August 2017

Academic Editor: Gabriele Saretzki

The Antarctic plant *Deschampsia antarctica* (DA) is able to survive in extreme conditions thanks to its special mechanism of protection against environmental aggressions. In this work, we investigated whether an aqueous extract of the plant (EDA) retains some of its defensive properties and is able to protect our skin against common external oxidants. We evaluated EDA over young human fibroblasts and exposed to H_2O_2, and we measured cell proliferation, viability, and senescence-associated β-galactosidase (SA-β-Gal). We also tested the expression of several senescence-associated proteins including sirtuin1, lamin A/C, the replicative protein PCNA, and the redox protein thioredoxin 2. We found that EDA promoted *per se* cell proliferation and viability and increased the expression of anti-senescence-related markers. Then, we selected a dose of H_2O_2 as an inductor of senescence in human fibroblasts, and we found that an EDA treatment 24 h prior H_2O_2 exposure increased fibroblast proliferation. EDA significantly inhibited the increase in SA-β-Gal levels induced by H_2O_2 and promoted the expression of sirtuin 1 and lamin A/C proteins. Altogether, these results suggest that EDA protects human fibroblasts from cellular senescence induced by H_2O_2, pointing to this compound as a potential therapeutic agent to treat or prevent skin senescence.

1. Introduction

Aging is a complex biological process that involves intrinsic genetic variations and external factors such as nutrition, diseases, or environmental conditions [1]. Hydrogen peroxide (H_2O_2) is an oxidant agent that induces a typical senescence called "stress-induced premature senescence" (SIPS) when applied exogenously *in vitro*. SIPS shares some features with natural or replicative senescence [2–4], including changes in the morphology of the cells, decreased cell proliferation, and DNA synthesis and increased SA-β-Gal levels [5, 6]. A previous work has shown that cellular senescence in human diploid fibroblasts is accompanied by a decrease in the expression of proliferating cell nuclear antigen (PCNA), a protein involved in replication and cell cycle [7, 8]. This effect on PCNA correlates with a decrease in cell proliferation as well as lower levels of several proteins involved in metabolism. Some of these are sirtuins (Sirt), which are nicotinamide adenine dinucleotide- (NAD^+-) dependent histone deacetylases. The Sirt family includes several members localized in different subcellular compartments: the nuclei (Sirt1, Sirt2, Sirt6, and Sirt7), cytoplasms (Sirt1 and Sirt2), and mitochondria (Sirt3, Sirt4, and Sirt5) [9, 10]. Stress downregulates Sirt1, promoting acetylation of p53 and the acquisition of a premature senescence-like phenotype [11–16]. Conversely, overexpression of

Sirt1 prevents cells from physiological alteration toward senescence [13].

Senescence also promotes changes in the architecture of the nucleus of mammalian cells. Lamins are nucleoskeletal proteins that define the structure of the nucleus. Some reports reveal that contents of lamin A/C (LmnA/C) show changes in expression along organism life [17, 18]. A reduction of LmnA/C has been observed in osteoblasts of old mice as compared to those of young mice [17].

During senescence, an increase of free radicals induces oxidative damage in almost every cell compartment [19]. Redox proteins such as thioredoxins (Trxs) reduce free radical-promoted damage in stress-induced premature senescence cells [20–22] through activation of the p16 and p53 tumor suppressor pathways [17, 22] or reducing indirectly the ROS levels [23]. Mammalian cells express two Trx isoforms, the cytosolic-nuclear Trx1 and the mitochondrial Trx2. Mitochondria is the main source of ROS in senescence, and Trx2 is one of the most important protein-regulating oxidative stress in this organelle [24].

Research of natural substances that can delay skin aging has been the object of increasing interest in the last few years [4, 25, 26]. In this regard, *Deschampsia antarctica* (DA) is an Antarctic plant able to live under high-solar irradiation, high-salinity and high-oxygen concentrations, low temperature, and extreme dryness. Some of the DA defensive properties have been reported *in vivo* in human cells, and an extract from the plant (EDA) prevents UV-induced human photoaging (patent US 8.357.407 B2). In order to get more information about the potential benefits of EDA over skin aging induced by external oxidants agents, we have evaluated the effect of different treatments of EDA on the senescence process of young fibroblasts from human foreskin induced by several H_2O_2 concentrations. Cell proliferation and morphological measurements together with quantification of the levels of PCNA as marker of DNA replication; the senescence markers β-galactosidase, Lamin A/C, and Sirt1; and the redox protein Trx2 revealed a protective effect of EDA, positioning it as a therapeutic candidate to counteract oxidation-dependent cell senescence induced by H_2O_2 exposure.

2. Materials and Methods

2.1. Reagents. Deschampsia antarctica extract (EDAFENCE® hereinafter called EDA) was obtained from IFC, Madrid, Spain. Briefly, dry green leaves, harvested from cultured *Deschampsia antarctica* plants in defined conditions, were milled and extracted by percolation with water at 40–60°C, during 4–6 hours. The extract was filtered through a 1 μm filter and lyophilized.

2.2. Cell Culture and Treatments. Senescent human foreskin fibroblasts (SHFF) were derived from primary human foreskin fibroblasts (HFF) by repeated passages. Stress-induced premature senescence fibroblasts (SIPSF) were obtained by exposure to H_2O_2. Primary young fibroblasts were considered of less than 20 population doublings (PD), presenescent between 21 and 29 PD, and senescent cultures at 30 PD or later. The cells were propagated in F-25 flasks. All experiments were done with young (13 PD), presenescent (26 PD), and senescent (45 PD) fibroblasts. The medium used was Dulbecco's modified Eagle's medium (DMEM) supplemented with 4.5 g/L glucose, 10% (*v*/*v*) fetal calf serum (FCS), 50 μg/mL penicillin, and 0.2 M L-glutamine. Cells were incubated at 37°C in an atmosphere containing 5% CO_2. When cells reached the confluency, they were subcultured using a solution containing 0.25% trypsin and 0.02% EDTA.

For the EDA treatment, this compound was dissolved in sterile water under agitation during 30 min at 25°C and sterilized by filtration through 0.22 μm syringe filters to a final concentration of 10 mg/mL. EDA treatments were done at 0.3 mg/mL, 0.5 mg/mL, and 1 mg/mL. HFF cultures were treated at different times: 24 h after seeding during 24 h (condition 1) and 48 h (condition 3) and 48 h after seeding during 24 h (condition 2), (Supplemental Figure S1 available online at https://doi.org/10.1155/2017/2694945). For H_2O_2-induced premature senescence, cells at 48 h after seeding were treated with different H_2O_2 concentrations (100 μM, 150 μM, and 200 μM) for different times (30 min, 1 h, and 2 h). In these assays, cells were incubated with 0.3, 0.5, and 1 mg/mL EDA during 24 h before H_2O_2 treatment (PRE-treatment), after H_2O_2 treatment (POST-treatment), and before and after the treatment (PRE-POST-treatment), (see Supplemental Figure S2). In all cases, the treatment with H_2O_2 was done only with basalt medium and H_2O_2. EDA was removed from the medium immediately before the H_2O_2 exposition.

2.3. Cell Viability and Proliferation Assays. Cell viability was measured by the MTT reduction assay and cell proliferation was assayed using the crystal violet staining. Cells were seeded in a 96-well plate at a density of 3.5×10^3cells/well. At the measure point, MTT was added at 0.5 mg/mL for 2 h at 37°C. The result formazan product was solubilized in DMSO under agitation during 30 min, and absorbance was measured at 570 nm and 690 nm (background). Crystal violet was prepared at 0.1% *w*/*v* in 2% ethanol. Previously, cells were fixed with Carnoy staining (methanol: acetic acid in 3 : 1 (*v*/*v* proportion)) during 5 min, and after being completely dried, they were incubated with the crystal violet solution during 30 min at 37°C. Cells were washed several times with water (until rinses were clear). Crystal violet was extracted from cells with 40% (*v*/*v*) methanol under agitation during 30 min and absorbance was measured at 570 nm.

2.4. SA Beta Galactosidase Level. The β-Gal level was determined as described elsewhere [27]. Briefly, subconfluent cultures were previously fixed for 5 min with 0.2% (*v*/*v*) glutaraldehyde and 2% (*v*/*v*) formaldehyde and afterwards rinsed with PBS. For the fluorescent assay, cells were incubated with a reaction solution containing 0.2 M citrate Na_2HPO_4 pH 5.0, 6.4 mM $MgCl_2$, 100 mM potassium hexacyanoferrate (II) trihydrate, 100 mM potassium hexacyanoferrate (III), 5 M NaCl, and 2 mM fluorescein di-β-galactopyranoside (FDG) solubilized in DMSO. Fixed fibroblasts were incubated with the reaction solution during 16–20 h at 37°C. Fluorescence was measured at 485/525 nm

excitation/emission wavelengths. For the colorimetric assay, FDG was substituted by 100 μM X-Gal (5-bromo-4-chloro-3-indolyl β-D-galactopyranoside). Positive cells were detected as blue stained, under a standard light microscopy. A total of 1000 cells were counted in five random fields on culture plates to determine the percentage of β-Gal-positive cells [27].

2.5. Western Blot Analysis. Subconfluent cultures were washed with PBS 1× and then lysed with RIPA buffer containing phosphatase cocktail 2 and protease inhibitor cocktail (Sigma, St Louis, MI, U.S.A.). The sample protein contents were adjusted to the same protein concentration measured by the BCA protein assay reagent (Pierce, Rockford, IL, U.S.A.), mixed with Laemmli sample buffer containing 50 mM DTT and boiled for 5 min. Afterwards, 80 μg of each sample was subjected to electrophoretic separation in 6–12% SDS-PAGE. Gels were then transferred to a nitrocellulose membrane (0.2 μm pore, Millipore, Bedford, MA, U.S.A.) for 10 minutes using the Trans-Blot Turbo Transfer System (Bio-Rad, California, USA). Membranes were stained with Ponceau S staining solution (0.1% (*w*/*v*) Ponceau S in 5% (*v*/*v*) acetic acid) to control the loading, and after bleaching, membranes were blocked with 1% BSA in Tris-buffered saline (TBS: 25 mM Tris-HCl pH 7.5, 150 mM NaCl). The membranes were incubated in TBS containing 0.1% Tween-20 and 1% BSA (TBST) and the following specific antibodies: goat polyclonal Actin-C (1 : 1000), mouse monoclonal PCNA (1 : 3000), goat polyclonal Trx2 (1 : 1000), goat polyclonal Sirt1 (1 : 1000), and goat polyclonal LmnA/C (1 : 1000). As secondary antibodies, we used HRP monoclonal antibody anti-mouse Ig G (1 : 6000) and HRP polyclonal anti-goat IgG (1:1000). Membranes were incubated with primary antibodies overnight at 4°C, and after being washed with TBST, secondary antibody was used to incubate the membranes 1 h at room temperature. Detection of bands was performed using ECL Plus Western blotting detection system (GE Healthcare, Hertfordshire, U.K.). To quantify the bands we applied Quantity One software-based analysis (Bio-Rad). All antibodies used were from Santa Cruz Biotechnology.

2.6. Microscopic Observations and Statistical Analysis. Microscopic observations and photographs were performed in a Nikon Mod. Diaphot-TMD photomicroscope equipped with a HBO 100 W mercury lamp and the corresponding filter sets for fluorescence microscopy: green (545 nm, exciting filter BP 545). Data were expressed as mean ± S.E. The statistical significance was determined using the analysis of variance (ANOVA) showed by Duncan post hoc test ($p < 0.05$) using SPSS software (IBM^R SPSS^R Statistics 19).

3. Results

3.1. EDA Affects Cell Proliferation and Viability of HFF Cells. To test whether EDA affected the proliferation of HFF cells (13 PD), we incubated cultures after 24 h and/or 48 h from seeding with different concentrations of EDA (0, 0.3, 0.5, and 1 mg/mL), as it is shown in Supplemental Figure S1. In all cases, we evaluated the different parameters after 72 h postseeding. In condition 1, only 0.5 mg/mL EDA increased cell proliferation whereas in condition 3, 0.3 mg/mL and 0.5 mg/mL increased this parameter. Both EDA concentrations also increased the survival rate in conditions 1 and 3, and 0.5 mg/mL increased it also in condition 2. Higher concentrations of EDA (1 mg/mL) decreased survival in conditions 2 and 3 but increased in condition 1 (Figures 1(a) and 1(b)).

We also evaluated cell proliferation indirectly by measuring the levels of PCNA, an important marker of cell replication. We found that in conditions 1 and 3, 0.3 and 0.5 mg/mL EDA induced a significant increase in the PCNA level compared to that in the control conditions. Nevertheless, higher EDA concentrations (1 mg/mL) decreased PCNA levels in conditions 1 and 2 but increased it in condition 3 (Figure 1(c)).

These results indicate that cell proliferation, survival rate, and PCNA levels are in agreement with the fact that cell proliferation of HFF cells increased with an EDA treatment of 0.3 and 0.5 mg/mL in both conditions 1 and 3.

3.2. EDA Treatment Promotes Expression of Both Sirt1 and LmnC and Decreases SA-β-Gal. We assessed the effect of EDA on the levels of several senescence markers in HFF cells (13 PD). In this regard, the process of senescence is characterized by an increase of SA-β-Gal-positive cells and by changes in the expression of known senescence markers such as Sirt1 and LmnA/C.

The addition of EDA to HFF caused a decrease in the SA-β-Gal level. In condition 1, any of the EDA concentrations decreased the SA-β-Gal level; however, all EDA concentrations were able to decrease SA-β-Gal in conditions 2 and 3 (Figure 2(a)). We next tested whether EDA treatments were able to induce expression of Sirt1, a marker of metabolism status and senescence. Western blot showed only an increase in Sirt1 protein content at 0.3 mg/mL EDA in condition 1 (Figures 2(b) and 2(c)). On the other hand, the nucleoskeleton protein LmnA/C increased at EDA doses of 1 mg/mL in condition 1 but increased at all EDA concentrations tested in conditions 2 and 3 (Figure 2(d)).

These results showed that different EDA treatments induced a decrease in markers of basal senescence including higher levels of LmnA/C and Sirt1 and a decrease in the SA-β-Gal level (Figure 2).

3.3. H_2O_2 Decreases Cell Proliferation and Survival. In order to establish a condition of extrinsic senescence, we evaluated the effect of different H_2O_2 concentrations over cell proliferation, viability, and associated senescence markers described in the previous section. Cell cultures (13 PD) were treated 48 h after seeding (50% of confluency) with different doses of H_2O_2 (100 and 200 μM) for different times (30 min, 1 h, and 2 h). We performed the analysis at 24 h, 48 h, and 72 h after H_2O_2 exposure. A decrease in cell proliferation was observed at both H_2O_2 concentrations applied for 1 h and 2 h treatments. This effect was noticeable 24 h after H_2O_2 recovery, becoming more pronounced at 72 h. Data obtained from the survival rate were in agreement with these results

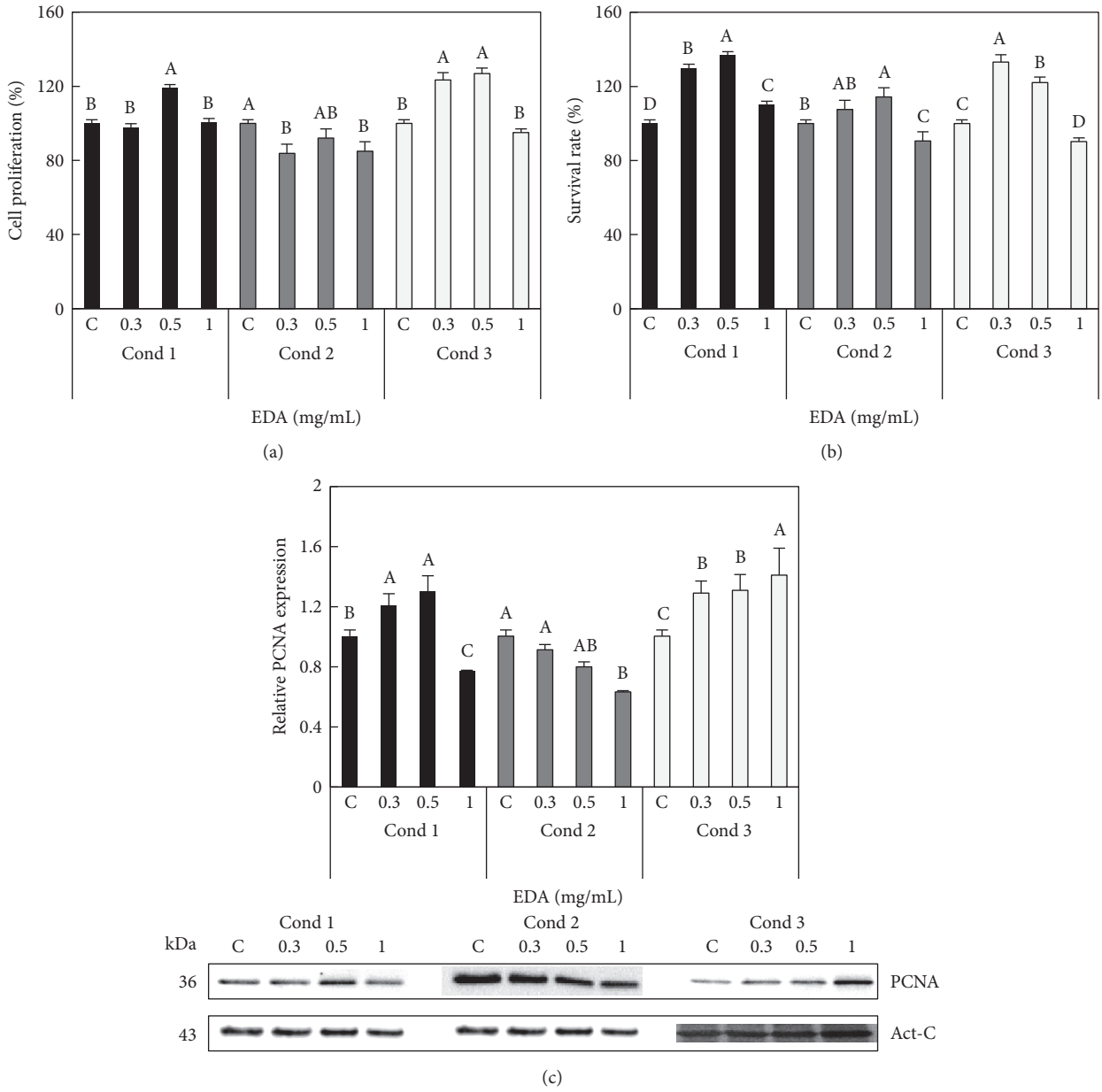

Figure 1: Effect of EDA in cell proliferation and viability of HFF cells. (a) Cell proliferation and (b) survival rate of control (C, untreated EDA cells) and EDA-treated cells with 0.3, 0.5, and 1 mg/mL. (c) Densitogram (upper panel) and Western blot (lower panel) of PCNA in control and EDA-treated cells. Act-C is used as loading control. The time of EDA treatment was 24 h after seeding during 24 h (Cond 1), 48 h after seeding during 24 h (Cond 2), and 24 h after seeding during 48 h (Cond 3). See more details in Supplemental Figure S1. Each bar represents the mean ± S.E. of three replicates from three independent experiments, and samples that do not have a common letter are significantly different in each condition by Duncan's test at $P < 0.05$.

(Figures 3(a), 3(b), and 3(c)). As expected, PCNA levels decreased significantly compared to those of control (C13), but only in cells treated with 200 μM H_2O_2 for 2 h and after 24 h of H_2O_2 recovery (Figure 3(d)).

In conclusion, these results indicate that a range of 100–200 μM H_2O_2 applied during 1-2 h decreased cell proliferation and viability in human fibroblasts in a sustained manner from 24 h to 72 h of recovery from the H_2O_2 treatment.

3.4. H_2O_2 Increases the Expression of Senescence-Related Proteins. We next analyzed the effect of H_2O_2 on the onset of the extrinsic senescence in HFF. Different H_2O_2 doses were used and we measured the SA-β-Gal level by colorimetric and fluorescence assays. Hydrogen peroxide induced an increase in the percentage of positive SA-β-Gal cells (blue cells) at every dose assayed, particularly at the highest one (200 μM H_2O_2) (Figure 4(a)), but we were able to detect this increase only 48 h after H_2O_2 recovery. As an alternative measurement, we quantified SA-β-Gal using the fluorescence reagent FDG. After 24 h of H_2O_2 recovery, (see Material and Methods) all hydrogen peroxide concentrations assayed showed an

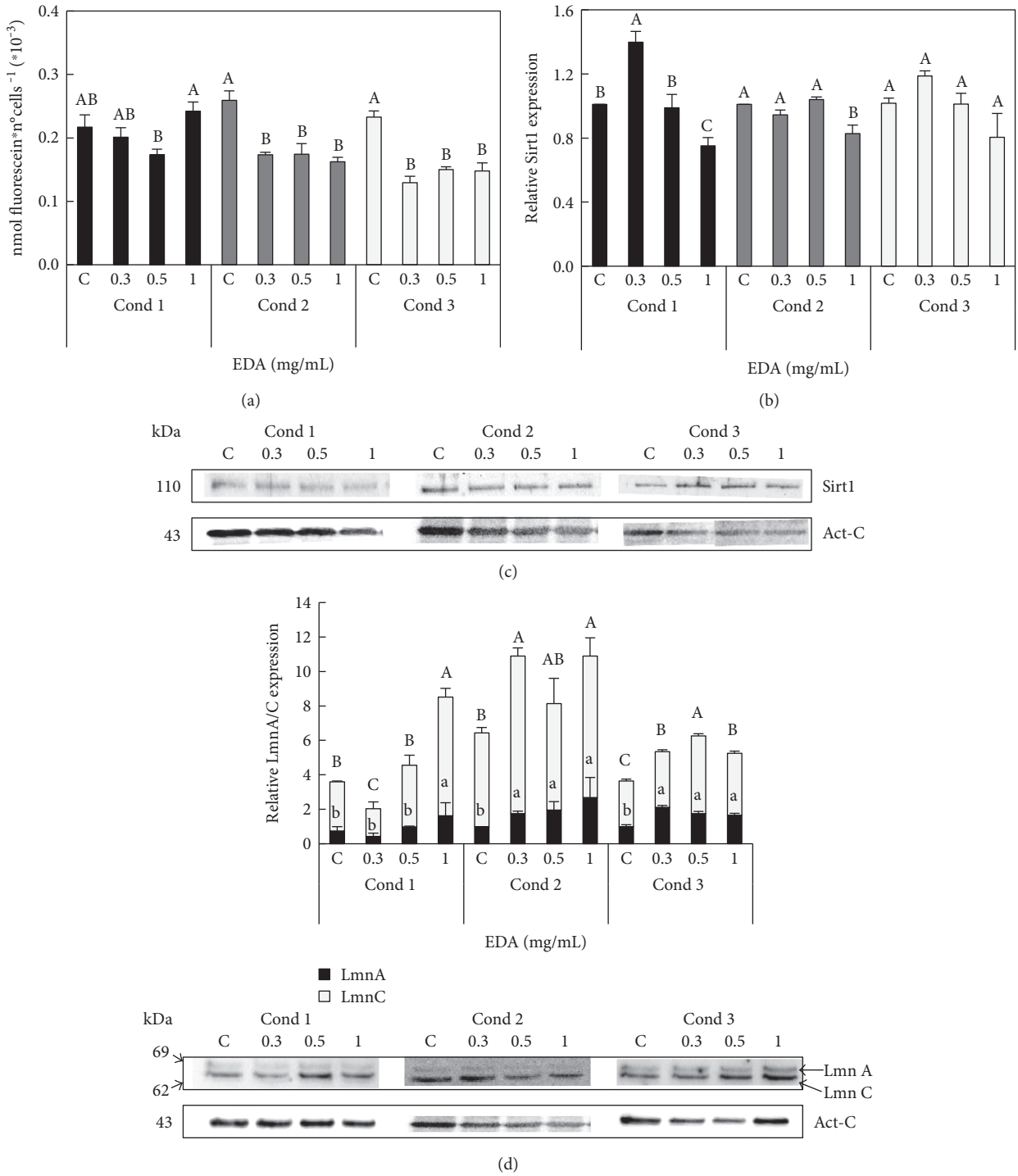

Figure 2: Effect of EDA in SA-β-Gal levels and protein contents of Sirt1 and Lmn A/C of HFF cells. (a) SA-β-Gal levels were measured as nmol of fluorescein by number of cells in control (C, untreated EDA cells) and EDA-treated cells with 0.3, 0.5, and 1 mg/mL. (b) Densitogram of Sirt1 in control and EDA-treated cells. (c) Western blot of Sirt1 in control and EDA-treated cells. (d) Densitogram (upper panel) and Western blot for LmnA/C (lower panel) in control and EDA-treated cells. Capital letters indicate statistical comparative analysis among LmnA data and lowercase letters among LmnC. Act-C is used as loading control. The time of EDA treatment was 24 h after seeding during 24 h (Cond 1), 48 h after seeding during 24 h (Cond 2), and 24 h after seeding during 48 h (Cond 3). See more details in Supplemental Figure S1. Each bar represents the mean ± S.E. of three replicates from three independent experiments, and samples that do not have a common letter are significantly different in each condition by Duncan's test at $P < 0.05$.

increase in SA-β-Gal levels (Figure 4(b)). The sensitivity of this method affords us to detect SA-β-Gal in hydrogen peroxide cultures, 24 h before, than with the colorimetric method. However, the differences in SA-β-Gal levels between H_2O_2 treatments were more evident 48 h after recovery as it is shown in the colorimetric assay.

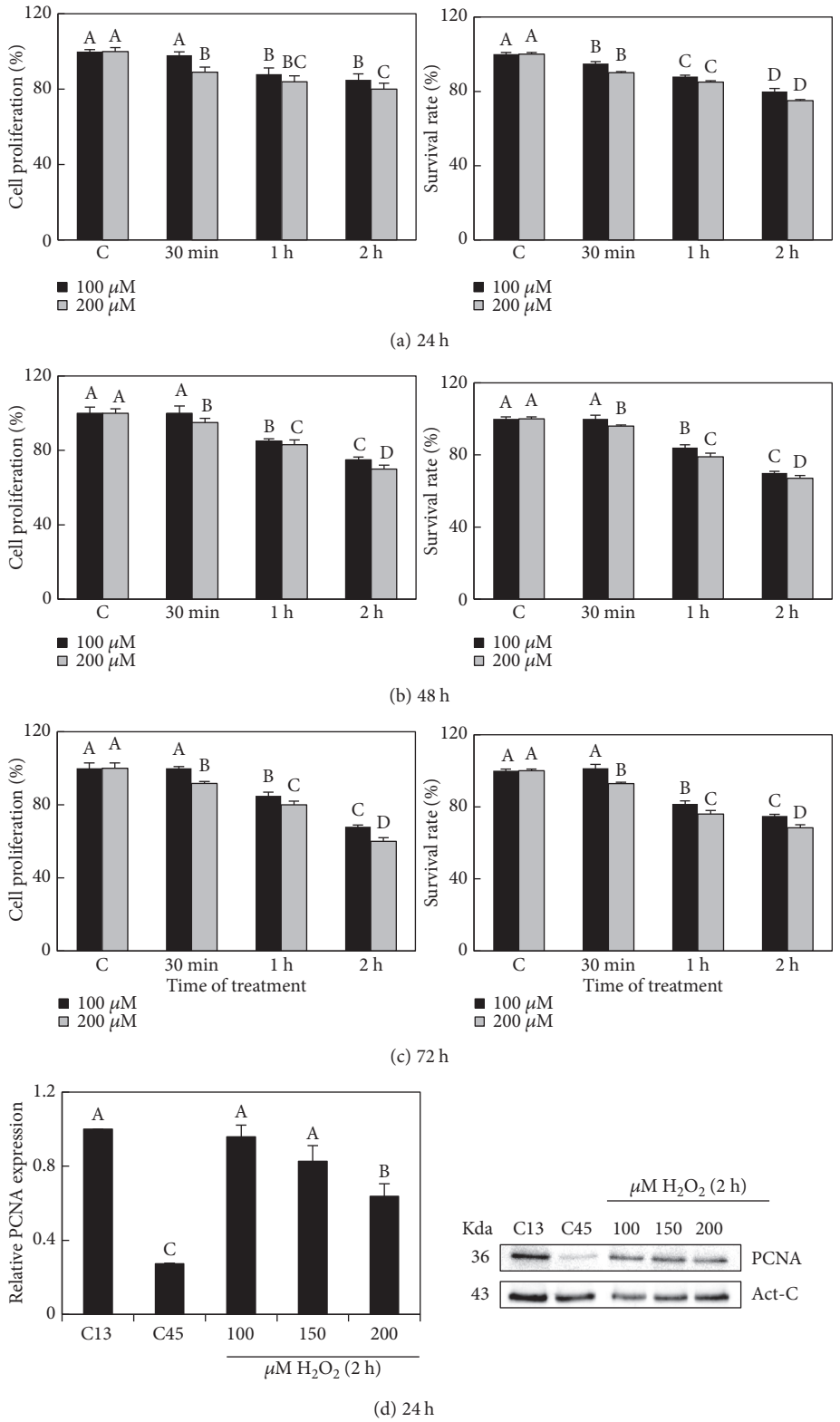

Figure 3: Effect of H_2O_2 in cell proliferation and survival rate of HFF cells. Cell proliferation and survival rate of control (H_2O_2-unexposed cells) and cells exposed to 100 and 200 μM H_2O_2 during 30 min, 1 h, and 2 h. Measures were done at 24 h (a), 48 h (b), and 72 h (c) after H_2O_2 recovery. (d) Densitogram (left panel) and Western blot (right panel) of PCNA in controls (C13, cells of 13 PD (HFF) and C45, cells of 45 PD (SHFF)), and cells exposed to 100, 150, and 200 μM H_2O_2 during 2 h and after 24 h of recovery. Capital letters indicate statistical comparative analysis among data from 100 μM H_2O_2 treatment and lowercase letters among the 200 μM H_2O_2 treatment. Each bar represents the mean ± S.E. of three replicates from three independent experiments, and samples that do not have a common letter are significantly different by Duncan's test at $P < 0.05$.

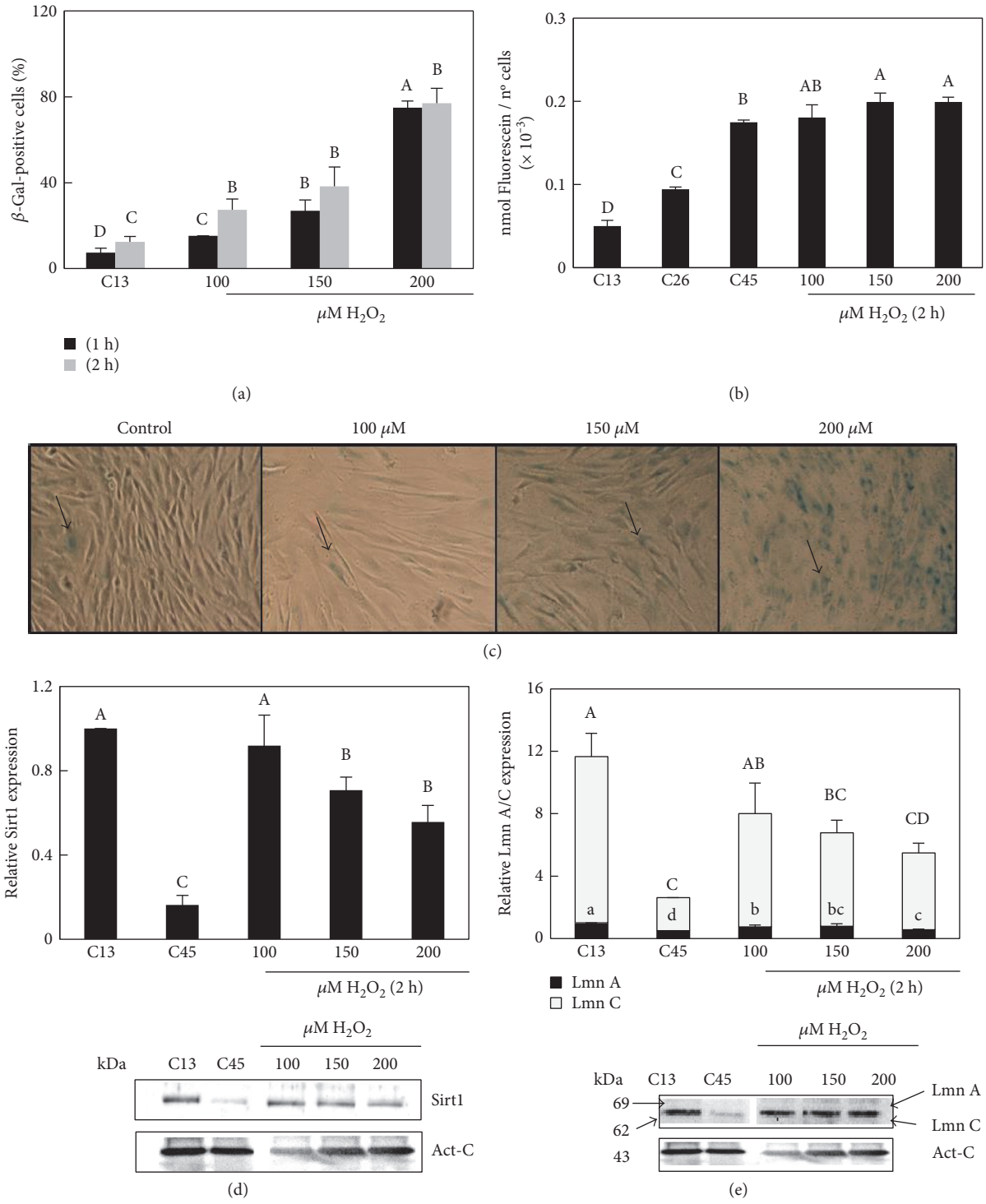

Figure 4: Effect of H_2O_2 treatment in the SA-β-Gal level and protein content of Sirt1 and LmnA/C of HFF cells. (a) The SA-β-Gal level measured as a number of blue cells in control (C13, H_2O_2-unexposed cells) and cells exposed to 100, 150, and 200 μM H_2O_2 during 1 and 2 h and after 24 h of H_2O_2 recovery. Capital letters indicate statistical comparative analysis among data from 1 h H_2O_2 treatment and lowercase letters among 2 h H_2O_2 treatment (b) The β-Gal level measured as nmol of fluorescein per number of cells in controls (H_2O_2-unexposed cells, C13: 13 PD; C26: 26 PD; and C45: 45 PD) and cells exposed to 100, 150, and 200 μM H_2O_2 during 2 h and after 24 h of recovery. (c) Cells stained with the chromogenic substrate 5-bromo-4-chloro-3-indolyl-beta-d-galactopyranoside (X-gal) prior to 100, 150, and 200 μM H_2O_2 exposition and after 24 h of H_2O_2 recovery. (d, e) Densitogram (upper panel) and Western blot for Sirt1 and LmnA/C (lower panel) in controls (H_2O_2-unexposed cells: C13, C45) and H_2O_2-exposed cells during 2 h and after 24 h H_2O_2 recovery. Panel LmnA/C; capital letters indicate statistical comparative analysis among LmnA data and lowercase letters among LmnC. Act-C is used as loading control. Each bar represents the mean ± S.E. of three replicates from three independent experiments, and samples that do not have a common letter are significantly different by Duncan's test at $P < 0.05$.

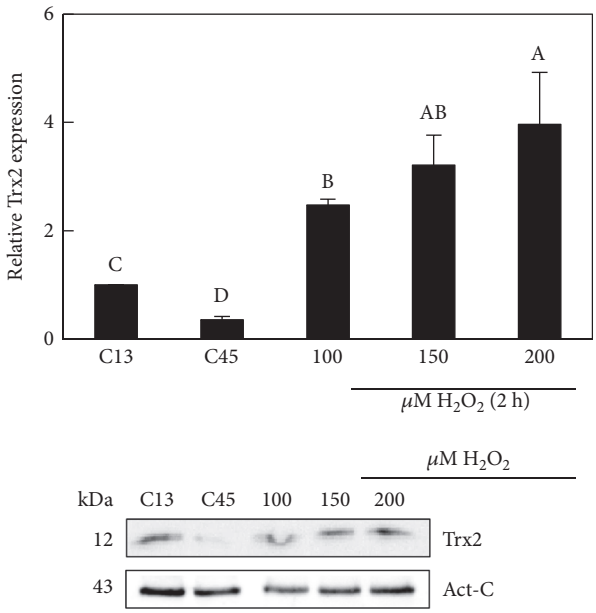

Figure 5: Effect of H_2O_2 in protein contents of Trx2 of HFF cells. Densitogram (upper panel) and Western blot (lower panel) of Trx2 in control (unexposed H_2O_2 cells: C13, C45) and H_2O_2-exposed cells during 2 h and after 24 h H_2O_2 recovery. Act-C is used as loading control. Each bar represents the mean ± S.E. of three replicates from three independent experiments, and samples that do not have a common letter are significantly different by Duncan's test at $P < 0.05$.

We next tested whether H_2O_2 exposure modulated expression of Sirt1 in HFF cells. We found that 150 and 200 μM H_2O_2 decreased Sirt1 protein content compared to control cells from 13 PD (C13, Figure 4(d)). Regarding lamins, we found that cell cultures exposed to 150 and 200 μM of hydrogen peroxide decreased around two fold levels of LmnA/C compared to those of the HFF control (Figure 4(e)).

In summary, our results are consistent with H_2O_2 inducing a senescent phenotype and they allowed us to determine an optimal dose and timing (200 μM for 2 h).

3.5. A Treatment of H_2O_2 Induces Trx2 Expression. Trx2 is an important mitochondrial redox protein involved in different processes including apoptosis, cell cycle, and ROS response. Parallel to the previous assays, we also tested the Trx2 protein content in HFF (13 PD, C13), SHFF (45 PD, C45), and H_2O_2-exposed HFF cultures (SIPSF), (Figure 5). The results showed a decrease of Trx2 in SHFF although its level increased significantly ($P < 0.05$) after the exposition of HFF to 100, 150, and 200 μM H_2O_2 for 2 h compared to unexposed HFF cells.

3.6. EDA Prevents Loss of Cell Viability in H_2O_2-Exposed Cells. To assess the ability of EDA to protect against oxidative senescence-related damage or to repair its deleterious effects, we assessed different concentrations of EDA (0, 0.3, 0.5, and 1 mg/mL) and different incubation times in HFF, measuring proliferation and survival rate. HFF cells were treated with different concentrations of EDA prior to H_2O_2 exposure (PRE-condition) and/or after H_2O_2 exposition (PRE-POST condition and POST-condition, resp.). The evaluation of the different parameters was carried out 24 h after recovery from the H_2O_2 treatment (see supplemental Figure S2). As it can be seen in Figures 6(a) and 6(b), an EDA treatment (0.3, 0.5, and 1 mg/mL) prior H_2O_2 exposure and prior and after H_2O_2 exposure (PRE-POST-treatment) increased both cell proliferation and survival rate, even though there are over values found in control conditions (C) (approximately 10–20% increase).

We also found that the levels of PCNA correlated well with the data on survival and proliferation. We noted that PRE-treatment of 0.3 mg/mL EDA increased PCNA levels of SIPSF cells compared with those of control H_2O_2-exposed cells. Besides, the PRE-POST treatment increased PCNA levels in all EDA doses (0.3, 0.5, and 1 mg/mL). By contrast, the addition of EDA (0.3, 0.5 mg/mL) only after H_2O_2 treatment neither induced changes in cell proliferation nor improved their survival rate (Figure 6(b)). Moreover, the higher EDA doses (1 mg/mL) decreased cell proliferation, survival rate, and PCNA protein content (Figure 6).

3.7. EDA Modulates the Expression of Senescence Proteins in H_2O_2-Exposed Cells. Senescence causes profound changes in cell morphology. Hence, we tested whether the morphological changes promoted by H_2O_2 could be prevented or reverted by the EDA treatments. Morphological observations after crystal violet staining indicated that control SIPSF cells (C + H_2O_2) presented a more evident polyhedral morphology and were larger compared to that of control HFF cells (C13), which showed the characteristic spindle shape (Figure 7(a)). The morphology of cells treated with 0.3 mg/mL EDA prior H_2O_2 exposure was similar to H_2O_2-unexposed cells (control C13). However, treatments at higher doses (0.5 and 1 mg/mL EDA) did not cause substantial changes compared to those of control SIPSF cells (Figure 7(a)).

Also, PRE-treatment with 0.3 and 0.5 mg/mL EDA prior to H_2O_2 exposition significantly decreased H_2O_2-induced SA-β-Gal ($P < 0.05$) at 24 h and 48 h after H_2O_2 recovery (Figure 7(b)). Furthermore, EDA POST-treatment decreased SA-β-Gal ($P < 0.05$), but only at 0.3 mg/mL EDA doses. Noteworthy, PRE-POST-treatment did not decrease SA-β-Gal levels more than PRE-treatment and POST-treatment conditions separately.

Regarding Sirt1, we observed significantly decreased levels in H_2O_2-exposed cells, compared to those in the control group. However, EDA treatments increased Sirt1 expression (Figure 8(a)). Specifically, the application of 0.3 mg/mL EDA prior H_2O_2 exposition increased Sirt1 expression whereas 0.5 and 1 mg/mL increased Sirt1 similarly in POST and PRE-POST conditions.

In case of LmnA/C, as it can be observed in Figure 8(b), both the PRE-treatment and POST-treatment of 0.3 mg/mL EDA induced an increase in LmnC levels, but not LmnA, which remained stable in every treatment comparing with SIPSF cells (C + H_2O_2). Strikingly, PRE-POST-treatment with EDA had no effects in protein LmnA/C contents.

These results indicate that different EDA doses have different effects on the onset of senescence markers in SIPSF

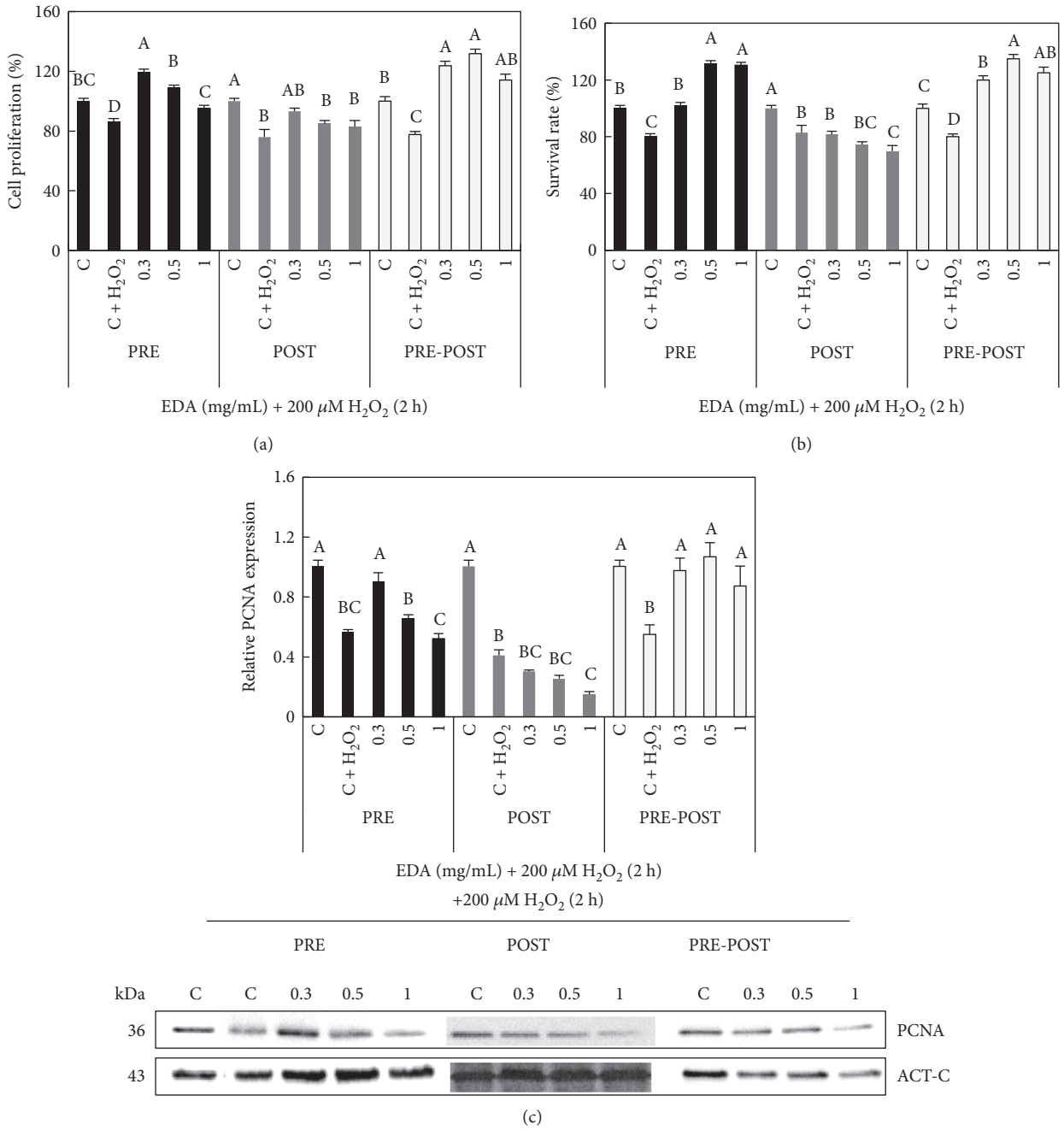

Figure 6: Effect of EDA in cell proliferation and viability of SIPSF cells. (a) Cell proliferation and (b) survival rate of control (C, unexposed HFF cells, neither EDA nor H_2O_2), control 200 μM H_2O_2-exposed cells (C + H_2O_2), and H_2O_2-exposed cells treated with 0.3, 0.5, and 1 mg/mL EDA. (c) Densitogram (upper panel) and Western blot (lower panel) of PCNA in control (C, unexposed HFF cells, neither EDA nor H_2O_2), control 200 μM H_2O_2-exposed cells (C + H_2O_2), and H_2O_2-exposed cells treated with 0.3, 0.5, and 1 mg/mL EDA. The time of EDA treatment was 24 h before H_2O_2 exposition (PRE), just after H_2O_2 exposition (POST), and after and before H_2O_2 exposition (PRE-POST). Each bar represents the mean ± S.E. of three replicates from three independent experiments, and samples that do not have a common letter are significantly different in each condition (PRE, POST, and PRE-POST) by Duncan's test at $P < 0.05$.

cells. The morphology, SA-β-Gal, and contents of Sirt1 and LmnA/C suggested that treatment with 0.3 mg/mL EDA had a protective effect against H_2O_2 stress.

3.8. EDA Decreases the Expression of Trx2 in H_2O_2-Exposed Cells. Finally, we investigated the effect of EDA treatment over unexposed *versus* H_2O_2-exposed cells in the conditions previously described (see Supplemental Figure S2). We checked that 0.5 and 1 mg/mL EDA decreased Trx2 contents in HFF cells in condition 1 but increased in condition 2 (Figure 9(a)). Levels of Trx2 were higher than those of the control in EDA-treated cells with 0.3 mg/mL in condition 2. In condition 3, only EDA treatment of 0.5 mg/mL increased levels of Trx2.

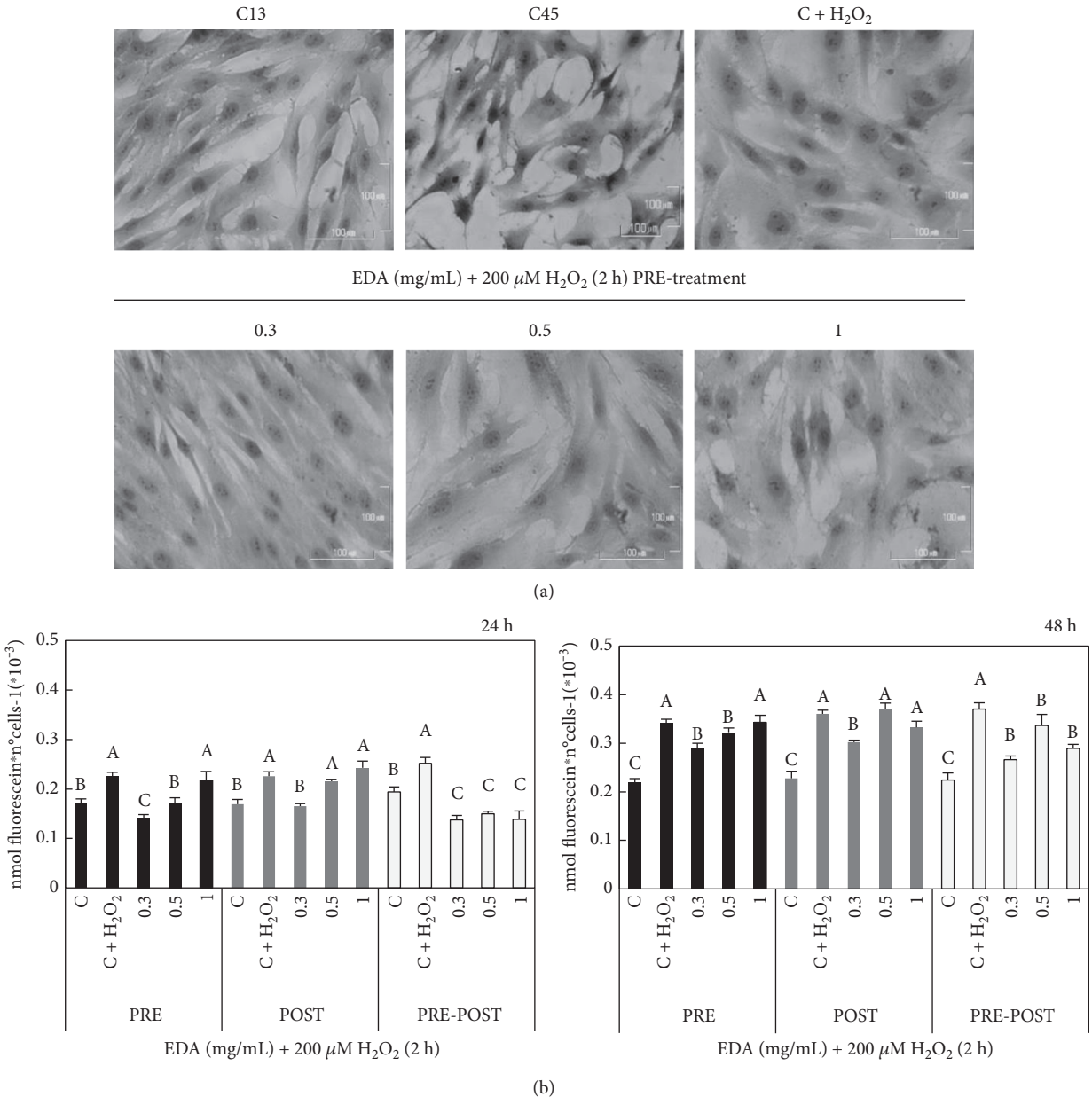

Figure 7: Effect of EDA in cellular morphology and SA-β-Gal of SIPSF cells. (a) SA-β-Gal was measured as nmol of fluorescein per number of cells in control (C, unexposed HFF cells), control 200 μM H_2O_2-exposed cells (C + H_2O_2), and H_2O_2-exposed cells treated with 0.3, 0.5, and 1 mg/mL EDA measured at 24 h and 48 h after H_2O_2 exposition. (b) Cellular morphology in control cells (C13, cells from 13 PD; C45, cells from 45 PD; and C + H_2O_2) and H_2O_2-exposed cells treated with 0.3, 0.5, and 1 mg/mL EDA previous H_2O_2 exposure and 24 h after H_2O_2 recovery (lower line). The time of EDA treatment was 24 h before H_2O_2 exposition (PRE), just after H_2O_2 exposition (POST), and after and before H_2O_2 exposition (PRE-POST). Each bar represents the mean ± S.E. of three replicates from three independent experiments, and samples that do not have a common letter are significantly different in each condition (PRE, POST, and PRE-POST) by Duncan's test at $P < 0.05$.

Besides, we observed that exposition to 200 μM H_2O_2 increased Trx2 expression in HFF cells. PRE- and POST-treatment with 0.3, 0.5, and 1 mg/ml EDA significantly decreased ($P < 0.05$) Trx2 protein content compared to that of H_2O_2-exposed cells, whereas PRE-POST-treatment had no effects (Figure 9(b)). These experiments suggest that the protective effect of EDA may be unrelated to the role of Trx2 in the curbing ROS generation and/or their deleterious effects.

4. Discussion

Skin aging is a complex process influenced by intrinsic and extrinsic factors. Intrinsic factors such as genetic and metabolic aspects confer inevitable physiological changes over time. In contrast, extrinsic agents such as UV light exposure, extreme temperatures, pollution, or diet, among others, can accelerate the intrinsic senescence process [4, 28, 29]. During senescence, an increase in production of cellular reactive

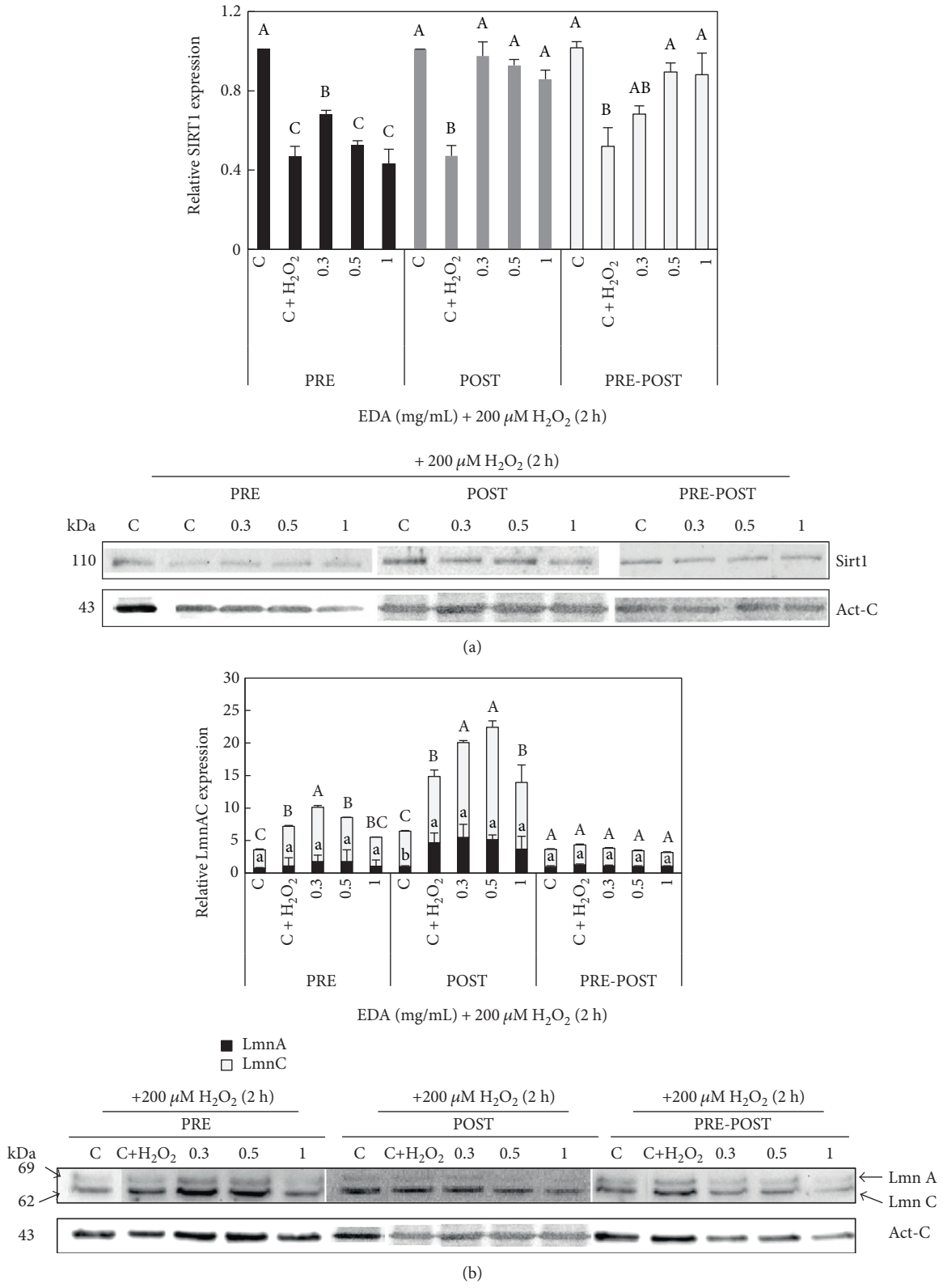

Figure 8: Effect of EDA in protein levels of Sirt1 and LmnA/C of SIPSF cells. (a) Densitogram (upper panel) and Western blot (lower panel) of Sirt1 and (b) LmnA/C in control (C, unexposed HFF cells), control 200 μM H_2O_2-exposed cells (C + H_2O_2), and H_2O_2-exposed cells treated with 0.3, 0.5, and 1 mg/mL EDA. The time of EDA treatment was 24 h before H_2O_2 exposition (PRE), just after H_2O_2 exposition (POST), and after and before H_2O_2 exposition (PRE-POST). Capital letters indicate statistical comparative analysis among LmnA data and lowercase letters among LmnC. Each bar represents the mean ± S.E. of three replicates from three independent experiments, and samples that do not have a common letter are significantly different in each condition (PRE, POST, and PRE-POST) by Duncan's test at $P < 0.05$.

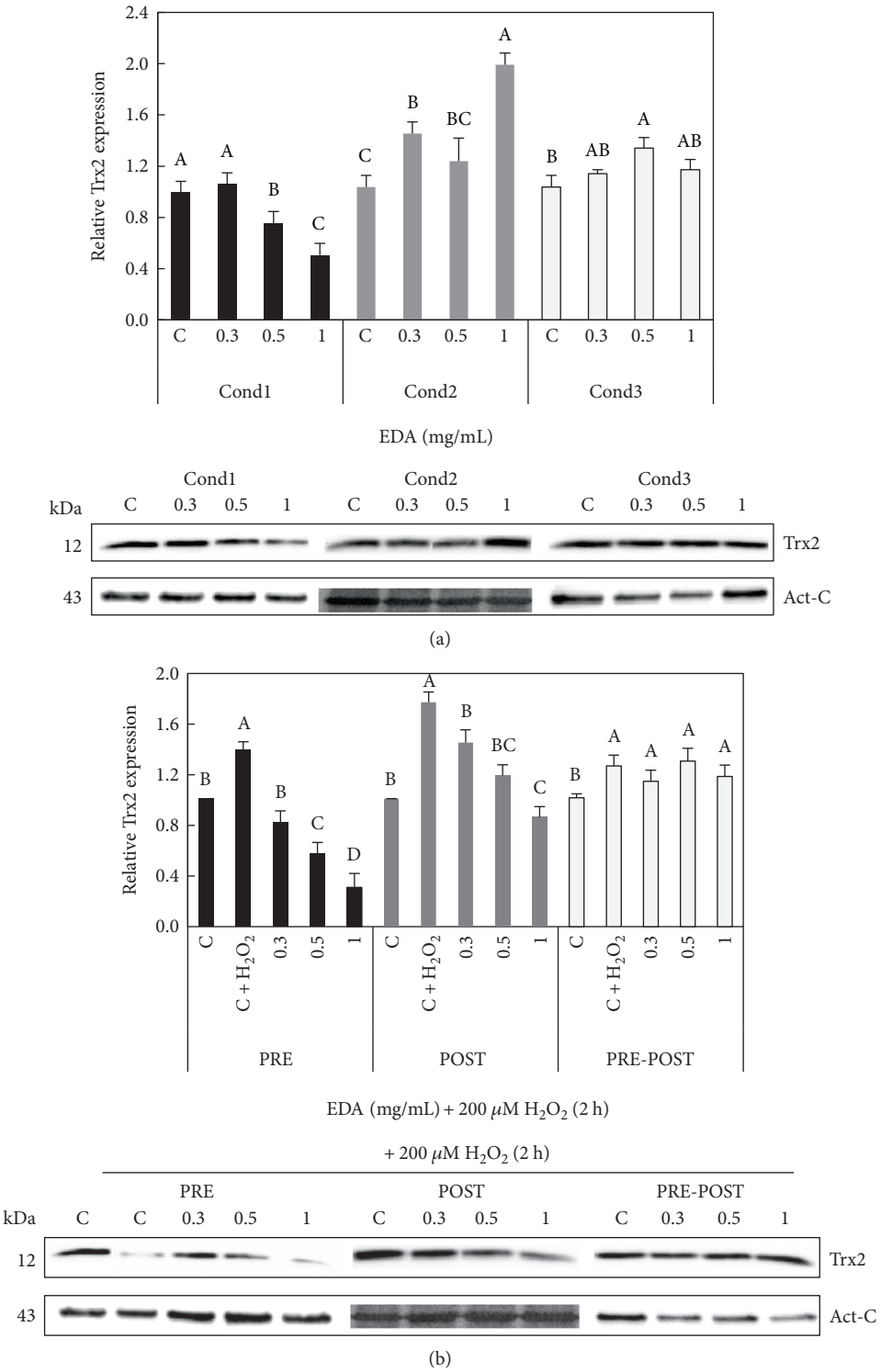

Figure 9: Effect of EDA over contents of Trx2 of HFF and SIPSF cells. (a) Densitogram (upper panel) and Western blot (lower panel) of Trx2 in HFF cells treated with different EDA doses. The time of EDA treatment was 24 h after seeding during 24 h (Cond1), 48 h after seeding during 24 h (Cond2), and 24 h after seeding during 48 h (Cond3). (b) Densitogram (upper panel) and Western blot (lower panel) of Trx2 in control (C, unexposed HFF cells), control 200 μM H_2O_2-exposed cells (C + H_2O_2), and H_2O_2-exposed cells treated with 0.3, 0.5, and 1 mg/mL EDA. The time of EDA treatment was 24 h before H_2O_2 exposition (PRE), just after H_2O_2 exposition (POST), and after and before H_2O_2 exposition (PRE-POST). Each bar represents the mean ± S.E. of three replicates from three independent experiments, and samples that do not have a common letter are significantly different in each condition (Cond (a) or PRE, POST, and PRE-POST (b)) by Duncan's test at $P < 0.05$.

oxygen species (ROS) results in deleterious damages in different cell components. Antioxidants provide defense against ROS, and depletion in the levels of these compounds has been found in senescence cells *in vitro* as well as *in vivo* [30, 31]. In this context, the search for products and mainly natural products that can reduce oxidative stress and, hence, senescence induced by stressors is being object of increased interest in recent years.

Many natural products are endowed with regenerative properties as well as antioxidant activity. In the past, some of them have been identified in several products, such as, a secretion of the mollusk *Cryptomphalus aspersa* (SCA) [32], extracts from fern leaves [33], curcumin [34], green tea [35], or resveratrol [36]. In this study, we have tested the antisenescence effects of an extract from the Antarctic plant *Deschampsia antarctica* (EDA), an extremophile plant endowed with a high antioxidant capacity and with tested resistance to oxidant stressors such as UV radiation [37]. To carry out this work, we selected human foreskin fibroblasts as a model due to their importance in skin regeneration [4, 26], and as a trigger of stress-induced senescence, we used H_2O_2, which is known to be a ROS generator of premature aging [38, 39].

Premature senescence shares some characteristics with replicative or chronologic senescence, such as typical cell morphology, decreased cell proliferation up to irreversible growth arrest or increased SA-β-Gal levels. Morphological changes involved in senescence are a consequence of the cytoskeleton reorganization [4, 26]. *In vitro*, SHFF are much larger, displaying round and flat appearance compared to HFF. Moreover, H_2O_2-exposed cells were also similar to SHFF, whereas EDA PRE-treatment prevented the morphological changes associated to senescence. Indeed, EDA PRE-treatment of H_2O_2-exposed HFF cells maintained similar morphological characteristics (spindle shape and smaller size) to that of untreated HFF cells. This effect is consistent with that of other proven natural-origin antioxidants [4].

As previously indicated, senescence involves a decrease in cell proliferation until growth arrest. In this regard, PCNA is a marker of cell proliferation that decreases its expression with age [40]. Some antioxidants such as genistein increase PCNA contents, preserving cutaneous proliferation [7]. Likewise, other antioxidant agents, for example, SCA, resveratrol, caffeic acid, or ascorbic acid, have been described to increase cell proliferation, and this effect seems to be related to the repair ability of each compound [26, 32, 41, 42]. Here, we demonstrate that EDA promotes a slight increase in HFF proliferation and viability, which indicates the proliferative effect of this compound.

The effects of H_2O_2 over cell proliferation as inductor of oxidative damage have been broadly studied in several cell types [28, 43–45]. We report that EDA PRE-treatment prevents the antiproliferative effect of H_2O_2, moreover, increasing cell proliferation over control non-H_2O_2-exposed cells. This behavior was similar to that found in other antioxidant compounds [20, 33, 46]. In fact, EDA extracts are rich in phenolic substances including flavonoids such as apigenin and luteolin, suggesting that the protective role of EDA may be related to its antioxidant capability. Nevertheless, this role would need further studies. Additional mechanisms may include an effect on the cellular levels of DNA-modifying enzymes, for example, Sirt1. Sirt1 is a nicotinamide adenine dinucleotide- (NAD^+-) dependent deacetylase and ADP-ribosyltransferase that is involved in mitochondrial biogenesis and DNA modification. Importantly, transgenic mice for Sirt1 display a significantly longer life span and delayed onset of senescence, including improved physical parameters [47]. At a molecular level, Sirt1 promotes cell proliferation and its expression levels decreased with cellular senescence [48, 49]. Furthermore, deacetylation of FOXO, p53, p73, Ku70, and Smad7 proteins by Sirt1 induced tolerance to oxidative stress and inhibited apoptosis [50, 51]. Different doses of EDA negated the inhibition of Sirt1 expression caused by H_2O_2, which partly explains the positive effect of EDA protecting against senescence via increased resistance to oxidative stress [52]. In this regard, EDA was also effective in preventing other markers of stress-induced senescence, for example, increased SA-β-Gal, which is a commonly used marker of cell senescence [53, 54].

It has been showed that a significant negative correlation exists between the percentage of senescent cells and the percentage of proliferating cells during human disc tissue degeneration [55]. However, this relationship is not always so; in some cases, an excessive mitogenic stimulation may induce senescence [56]. These reports underline that EDA decreases senescence markers, but this fact is not completely parallel to an increase in cell proliferation.

We find that the increase of Trx2 after the exposition of HFF to H_2O_2 is counteracted by the EDA treatment, indicating that EDA could promote protection against H_2O_2 premature-induced senescence decreasing the levels of oxidative stress. Recent studies have shown that Trx2 overexpression *in vitro* can protect mammalian cells against t-butyl hydroperoxide and etoposide-induced apoptosis, as well as increasing the mitochondrial membrane potential [57, 58]. In addition, human cardiomyocytes deficient in Trx2 display increased cellular ROS and apoptosis [23]. On the other hand, overexpression of either *Trx1* or *Trx2* has been shown to influence life span in experimental models [24, 59]. The increase in Trx1, Trx2, and thioredoxin reductase proteins has been proposed as a compensatory response to counteract increased oxidative stress during the senescence process [60].

EDA also prevents the stress-induced decrease in proteins that control the nuclear architecture, for example, lamins A and C. These proteins are key players in cellular senescence, as illustrated by their genetic depletion, which causes early onset of senescence, comprising a group of rare genetic diseases collectively referred to as laminopathies. In natural senescence, LmnA seems to remain constant over time whereas LmnC decreases significantly [17, 18], although this could be cell-type dependent, since other studies report a concomitant decrease of both isoforms [17]. In our experiments, H_2O_2 decreased LmnC and LmnA, and this decrease was counteracted by the PRE-treatment with EDA, which is consistent with an antisenescence effect of EDA in H_2O_2-exposed HFF cells.

In conclusion, our data proves the positive effect of an extract from *Deschampsia antarctica* to counteract H_2O_2 stress-induced premature senescence in human diploid foreskin fibroblasts suggesting its potential as a therapeutic agent for treating skin aging.

Abbreviations

SA-β-Gal: Senescence-associated beta-galactosidase
DMEM: Dulbecco's modified Eagle's medium
EDA: Extract from Deschampsia antárctica
EDTA: Ethylenediaminetetraacetic acid
FDG: Fluorescein di-β-galactopyranoside
HFF: Human foreskin fibroblasts
LmnA/C: Lamin A/C
MTT: 3-(4,5-Dimethylthiazol-2-yl)-2,5-diphenyltetrazolium bromide
PCNA: Proliferating cell nuclear antigen
PD: Population doubling
SHFF: Senescence human foreskin fibroblasts
SIPS: Stress-induced premature senescence
SIPSF: Stress-induced premature senescence fibroblasts
Sirt: Sirtuin.

Conflicts of Interest

The authors declare that there are no conflicts of interest regarding the publication of this paper.

Acknowledgments

This work was supported by the "Industrial Farmaceutica Cantabria" (IFC company, OTT: 20159760), Spanish Ministry of Economy and Competitiveness (MICINN, Ref. BFU2014-52452-P cofinanced by FEDER) and Seneca Foundation from Murcia, Spain (Excellence Group: 19876/GERM/15). Salvador González plays a consultant role for IFC that partially supported this research work. Esther Morel and Ángeles Juarranz were supported by a Grant PI15/00974, from the Instituto de Salud Carlos III, MINECO and FEDER Funds. The authors thank Dr F. Pallardó (University of Valencia) for the kind gift of the Trx2 antibody.

References

[1] N. Getoff, "Anti-aging and aging factors in life. The role of free radicals," *Radiation Physics and Chemistry*, vol. 76, no. 10, pp. 1577–1586, 2007.

[2] M. J. Choi, B. K. Kim, K. Y. Park, T. Yokozawa, Y. O. Song, and E. J. Cho, "Anti-aging effects of cyanidin under a stress-induced premature senescence cellular system," *Biological and Pharmaceutical Bulletin*, vol. 33, no. 3, pp. 421–426, 2010.

[3] O. Toussaint, V. Royer, M. Salmon, and J. Remacle, "Stress-induced premature senescence and tissue ageing," *Biochemical Pharmacology*, vol. 64, no. 5-6, pp. 1007–1009, 2002.

[4] J. Espada, M. Matabuena, N. Salazar et al., "*Cryptomphalus aspersa* mollusc eggs extract promotes migration and prevents cutaneous ageing in keratinocytes and dermal fibroblasts *in vitro*," *International Journal of Cosmetic Science*, vol. 37, no. 1, pp. 41–55, 2015.

[5] F. I. Wolf, A. Torsello, V. Covacci et al., "Oxidative DNA damage as a marker of aging in WI-38 human fibroblasts," *Experimental Gerontology*, vol. 37, no. 5, pp. 647–656, 2002.

[6] O. Toussaint, E. E. Medrano, and T. v. Zglinicki, "Cellular and molecular mechanisms of stress-induced premature senescence (SIPS) of human diploid fibroblasts and melanocytes," *Experimental Gerontology*, vol. 35, no. 8, pp. 927–945, 2000.

[7] J. O. Moore, Y. Wang, W. G. Stebbins et al., "Photoprotective effect of isoflavone genistein on ultraviolet B-induced pyrimidine dimer formation and PCNA expression in human reconstituted skin and its implications in dermatology and prevention of cutaneous carcinogenesis," *Carcinogenesis*, vol. 27, no. 8, pp. 1627–1635, 2006.

[8] J. L. Pablos, P. E. Carreira, L. Serrano, P. D. Castillo, and J. J. Gomez-Reino, "Apoptosis and proliferation of fibroblasts during postnatal skin development and scleroderma in the Ttght-skin mouse," *Journal of Histochemistry & Cytochemistry*, vol. 45, no. 5, pp. 711–719, 1997.

[9] L. Guarente, "Sirtuins in aging and disease," *Cold Spring Harbor Symposia on Quantitative Biology*, vol. 72, pp. 483–488, 2007.

[10] D. Camejo, A. Ortiz-Espín, J. J. Lázaro et al., "Functional and structural changes in plant mitochondrial PrxII F caused by NO," *Journal of Proteomics*, vol. 119, pp. 112–125, 2015.

[11] I. A. Calvo, J. Ayte, and E. Hidalgo, "Reversible thiol oxidation in the H_2O_2-dependent activation of the transcription factor Pap1," *Journal of Cell Science*, vol. 126, no. 10, pp. 2279–2284, 2013.

[12] K. W. Chung, Y. J. Choi, M. H. Park et al., "Molecular insights into SIRT1 protection against UVB-induced skin fibroblast senescence by suppression of oxidative stress and p53 acetylation," *The Journals of Gerontology Series A: Biological Sciences and Medical Sciences*, vol. 70, no. 8, pp. 959–968, 2015.

[13] S. García-Santamarina, S. Boronat, I. A. Calvo et al., "Is oxidized thioredoxin a major trigger for cysteine oxidation? Clues from a redox proteomics approach," *Antioxidants & Redox Signaling*, vol. 18, no. 13, pp. 1549–1556, 2013.

[14] J. Chen, S. Xavier, E. Moskowitz-Kassai et al., "Cathepsin cleavage of sirtuin 1 in endothelial progenitor cells mediates stress-induced premature senescence," *The American Journal of Pathology*, vol. 180, no. 3, pp. 973–983, 2012.

[15] D. Knoefler, M. Thamsen, M. Koniczek, N. J. Niemuth, A.-K. Diederich, and U. Jakob, "Quantitative *in vivo* redox sensors uncover oxidative stress as an early event in life," *Molecular Cell*, vol. 47, no. 5, pp. 767–776, 2012.

[16] M. Abo and E. Weerapana, "A caged electrophilic probe for global analysis of cysteine reactivity in living cells," *Journal of the American Chemical Society*, vol. 137, no. 22, pp. 7087–7090, 2015.

[17] G. Duque and D. Rivas, "Age-related changes in lamin A/C expression in the osteoarticular system: Laminopathies as a potential new aging mechanism," *Mechanisms of Ageing and Development*, vol. 127, no. 4, pp. 378–383, 2006.

[18] G. Viteri, Y. W. Chung, and E. R. Stadtman, "Effect of progerin on the accumulation of oxidized proteins in fibroblasts from Hutchinson Gilford progeria patients," *Mechanisms of Ageing and Development*, vol. 131, no. 1, pp. 2–8, 2010.

[19] J. Viña, C. Borras, K. M. Abdelaziz, R. Garcia-Valles, and M. C. Gomez-Cabrera, "The free radical theory of aging revisited: the cell signaling disruption theory of aging," *Antioxidants & Redox Signaling*, vol. 19, no. 8, pp. 779–787, 2013.

[20] K. A. Kang, K. H. Lee, R. Zhang et al., "Caffeic acid protects hydrogen peroxide induced cell damage in WI-38 human lung fibroblast cells," *Biological and Pharmaceutical Bulletin*, vol. 29, no. 9, pp. 1820–1824, 2006.

[21] Z.-Q. Ou, T. Rades, and A. McDowell, "Anti-ageing effects of *Sonchus oleraceus* l. (pūhā) leaf extracts on H_2O_2-induced cell senescence," *Molecules*, vol. 20, no. 3, pp. 4548–4564, 2015.

[22] J. J. Young, A. Patel, and P. Rai, "Suppression of thioredoxin-1 induces premature senescence in normal human fibroblasts," *Biochemical and Biophysical Research Communications*, vol. 392, no. 3, pp. 363–368, 2010.

[23] Q. Huang, H. J. Zhou, H. Zhang et al., "Thioredoxin-2 inhibits mitochondrial reactive oxygen species generation and apoptosis stress kinase-1 activity to maintain cardiac function," *Circulation*, vol. 131, no. 12, pp. 1082–1097, 2015.

[24] M. J. Svensson and J. Larsson, "Thioredoxin-2 affects lifespan and oxidative stress in Drosophila," *Hereditas*, vol. 144, no. 1, pp. 25–32, 2007.

[25] M. Sitar, S. Aydin, and U. Cakatay, "Human serum albumin and its relation with oxidative stress," *Clinical Laboratory*, vol. 59, no. 9-10, pp. 945–952, 2013.

[26] M. C. Iglesias-de la Cruz, F. Sanz-Rodríguez, A. Zamarrón et al., "A secretion of the mollusc *Cryptomphalus aspersa* promotes proliferation, migration and survival of keratinocytes and dermal fibroblasts *in vitro*," *International Journal of Cosmetic Science*, vol. 34, no. 2, pp. 183–189, 2012.

[27] F. Debacq-Chainiaux, J. D. Erusalimsky, J. Campisi, and O. Toussaint, "Protocols to detect senescence-associated beta-galactosidase (SA-βgal) activity, a biomarker of senescent cells in culture and in vivo," *Nature Protocols*, vol. 4, no. 12, pp. 1798–1806, 2009.

[28] S. Zdanov, J. Remacle, and O. Toussaint, "Establishment of H_2O_2-induced premature senescence in human fibroblasts concomitant with increased cellular production of H_2O_2," *Annals of the New York Academy of Sciences*, vol. 1067, no. 1, pp. 210–216, 2006.

[29] M. Sørensen, H. Autrup, P. Møller et al., "Linking exposure to environmental pollutants with biological effects," *Mutation Research/Reviews in Mutation Research*, vol. 544, no. 2-3, pp. 255–271, 2003.

[30] Y. Tanuja, S. Mishra, S. Das, S. Aggarwal, and V. Rani, "Antcedants and natural prevention of environmental toxicants induced accelerated aging of skin," *Environmental Toxicology and Pharmacology*, vol. 39, no. 1, pp. 384–391, 2015.

[31] P. Sen, S. Mukherjee, G. Bhaumik et al., "Enhancement of catalase activity by repetitive low-grade H_2O_2 exposures protects fibroblasts from subsequent stress-induced apoptosis," *Mutation Research/Fundamental and Molecular Mechanisms of Mutagenesis*, vol. 529, no. 1-2, pp. 87–94, 2003.

[32] A. Brieva, N. Philips, R. Tejedor et al., "Molecular basis for the regenerative properties of a secretion of the mollusk *Cryptomphalus aspersa*," *Skin Pharmacology and Physiology*, vol. 21, no. 1, pp. 15–22, 2008.

[33] R. Capote, J. L. Alonso-Lebrero, F. García, A. Brieva, J. P. Pivel, and S. González, "*Polypodium leucotomos* extract inhibits trans-urocanic acid photoisomerization and photodecomposition," *Journal of Photochemistry and Photobiology B: Biology*, vol. 82, no. 3, pp. 173–179, 2006.

[34] Y. Sun, X. Hu, G. Hu, C. Xu, and H. Jiang, "Curcumin attenuates hydrogen peroxide-induced premature senescence *via* the activation of sirt1 in human umbilical vein endothelial cells," *Biological and Pharmaceutical Bulletin*, vol. 38, no. 8, pp. 1134–1141, 2015.

[35] P. Farris, "Idebenone, green tea, and Coffeeberry® extract: new and innovative antioxidants," *Dermatologic Therapy*, vol. 20, no. 5, pp. 322–329, 2007.

[36] K. B. Harikumar and B. B. Aggarwal, "Resveratrol: a multitargeted agent for age-associated chronic diseases," *Cell Cycle*, vol. 7, no. 8, pp. 1020–1035, 2014.

[37] E. Pérez-Torres, A. García, J. Dinamarca et al., "The role of photochemical quenching and antioxidants in photoprotection of *Deschampsia antarctica*," *Functional Plant Biology*, vol. 31, no. 7, p. 731, 2004.

[38] J. Duan, J. Duan, Z. Zhang, and T. Tong, "Irreversible cellular senescence induced by prolonged exposure to H_2O_2 involves DNA-damage-and-repair genes and telomere shortening," *The International Journal of Biochemistry & Cell Biology*, vol. 37, no. 7, pp. 1407–1420, 2005.

[39] C. Frippiat, Q. M. Chen, S. Zdanov, J. P. Magalhaes, J. Remacle, and O. Toussaint, "Subcytotoxic H_2O_2 stress triggers a release of transforming growth factor-1, which induces biomarkers of cellular senescence of human diploid fibroblasts," *Journal of Biological Chemistry*, vol. 276, no. 4, pp. 2531–2537, 2000.

[40] A. Y. Leung, J. C. Leung, L. Y. Chan et al., "Proliferating cell nuclear antigen (PCNA) as a proliferative marker during embryonic and adult zebrafish hematopoiesis," *Histochemistry and Cell Biology*, vol. 124, no. 2, pp. 105–111, 2005.

[41] E. Ledo, M. E. Heras de las, and A. Ledo, "Treatment of acute radiodermatitis with *Cryptomphalus aspersa* secretion," *Radioproteccion (Madrid)*, vol. 23, no. VII, pp. 34–38, 1999.

[42] İ. Gülçin, "Antioxidant activity of caffeic acid (3,4-dihydroxycinnamic acid)," *Toxicology*, vol. 217, no. 2-3, pp. 213–220, 2006.

[43] R. d. Wit, A. Capello, J. Boonstra, A. J. Verkleij, and J. A. Post, "Hydrogen peroxide inhibits epidermal growth factor receptor internalization in human fibroblasts," *Free Radical Biology and Medicine*, vol. 28, no. 1, pp. 28–38, 2000.

[44] S. Nobrega-Pereira, P. J. Fernandez-Marcos, T. Brioche et al., "G6PD protects from oxidative damage and improves healthspan in mice," *Nature Communications*, vol. 7, 2016.

[45] K. B. Choo, L. Tai, K. S. Hymavathee et al., "Oxidative stress-induced premature senescence in Wharton's jelly-derived mesenchymal stem cells," *International Journal of Medical Sciences*, vol. 11, no. 11, pp. 1201–1207, 2014.

[46] M. Taniguchi, N. Arai, K. Kohno, S. Ushio, and S. Fukuda, "Anti-oxidative and anti-aging activities of 2-O-α-glucopyranosyl-L-ascorbic acid on human dermal fibroblasts," *European Journal of Pharmacology*, vol. 674, no. 2-3, pp. 126–131, 2012.

[47] K. Oettl and R. E. Stauber, "Physiological and pathological changes in the redox state of human serum albumin critically influence its binding properties," *British Journal of Pharmacology*, vol. 151, no. 5, pp. 580–590, 2007.

[48] J. Huang, Q. Gan, L. Han et al., "SIRT1 overexpression antagonizes cellular senescence with activated ERK/S6k1 signaling in human diploid fibroblasts," *PloS One*, vol. 3, no. 3, article e1710, 2008.

[49] L. R. Saunders and E. Verdin, "Sirtuins: critical regulators at the crossroads between cancer and aging," *Oncogene*, vol. 26, no. 37, pp. 5489–5504, 2007.

[50] H.-L. Cheng, R. Mostoslavsky, S.i. Saito et al., "Developmental defects and p53 hyperacetylation in Sir2 homolog (SIRT1)-deficient mice," *Proceedings of the National Academy*

of Sciences of the United States of America, vol. 100, no. 19, pp. 10794–10799, 2003.

[51] J. N. Feige and J. Auwerx, "Transcriptional targets of sirtuins in the coordination of mammalian physiology," *Current Opinion in Cell Biology*, vol. 20, no. 3, pp. 303–309, 2008.

[52] L. Guarente, "Sirtuins, aging, and metabolism," *Cold Spring Harbor Symposia on Quantitative Biology*, vol. 76, pp. 81–90, 2011.

[53] N. Yang and M. Hu, "The limitations and validities of senescence associated-β-galactosidase activity as an aging marker for human foreskin fibroblast Hs68 cells," *Experimental Gerontology*, vol. 40, no. 10, pp. 813–819, 2005.

[54] Y. Zhou, Y. Dong, Q.-G. Xu et al., "Mussel oligopeptides protect human fibroblasts from hydrogen peroxide (H_2O_2)-induced premature senescence," *Archives of Gerontology and Geriatrics*, vol. 58, no. 2, pp. 293–299, 2014.

[55] H. E. Gruber, J. A. Ingram, D. E. Davis, and E. N. Hanley Jr., "Increased cell senescence is associated with decreased cell proliferation *in vivo* in the degenerating human annulus," *The Spine Journal*, vol. 9, no. 3, pp. 210–215, 2009.

[56] N. F. Mathon, D. S. Malcolm, M. C. Harrisingh, L. Cheng, and A. C. Lloyd, "Lack of replicative senescence in normal rodent glia," *Science*, vol. 291, no. 5505, pp. 872–875, 2001.

[57] S. J. Wei, A. Botero, K. Hirota et al., "Thioredoxin nuclear translocation and interaction with redox factor-1 activates the activator protein-1 transcription factor in response to ionizing radiation," *Cancer Research*, vol. 60, no. 23, pp. 6688–6695, 2000.

[58] K. Hirota, M. Murata, Y. Sachi et al., "Distinct roles of thioredoxin in the cytoplasm and in the nucleus: a two-step mechanism of redox regulation of transcription factor NF-κB," *Journal of Biological Chemistry*, vol. 274, no. 39, pp. 27891–27897, 1999.

[59] V. I. Perez, L. A. Cortez, C. M. Lew et al., "Thioredoxin 1 overexpression extends mainly the earlier part of life span in mice," *The Journals of Gerontology Series A: Biological Sciences and Medical Sciences*, vol. 66A, no. 12, pp. 1286–1299, 2011.

[60] L. L. Ji, D. Dillon, and E. Wu, "Alteration of antioxidant enzymes with aging in rat skeletal muscle and liver," *American Journal of Physiology-Regulatory, Integrative and Comparative Physiology*, vol. 258, no. 4, pp. R918–R923, 1990.

Hindawi
Oxidative Medicine and Cellular Longevity
Volume 2017, Article ID 4674918, 8 pages
https://doi.org/10.1155/2017/4674918

Research Article

Quercetin Reverses Rat Liver Preneoplastic Lesions Induced by Chemical Carcinogenesis

Gabriela Carrasco-Torres,[1] Hugo Christian Monroy-Ramírez,[2] Arturo Axayacatl Martínez-Guerra,[1] Rafael Baltiérrez-Hoyos,[3] María de los Ángeles Romero-Tlalolini,[3] Saúl Villa-Treviño,[1] Xariss Sánchez-Chino,[4] and Verónica Rocío Vásquez-Garzón[1,3]

[1]*Departamento de Biología Celular, Centro de Investigación y de Estudios Avanzados del Instituto Politécnico Nacional, Ciudad de México, Mexico*
[2]*Departamento de Farmacología, Facultad de Medicina Mexicali, Universidad Autónoma de Baja California, Baja California, Mixicali, BC, Mexico*
[3]*CONACYT, Facultad de Medicina y Cirugía, Universidad Autónoma Benito Juárez de Oaxaca, Oaxaca de Juárez, OAX, Mexico*
[4]*Dirección de Investigación y Desarrollo Tecnológico, Universidad Politécnica Mesoamericana, Tenosique, TAB, Mexico*

Correspondence should be addressed to Verónica Rocío Vásquez-Garzón; vrvasquezga@conacyt.mx

Received 11 March 2017; Accepted 16 April 2017; Published 27 June 2017

Academic Editor: Consolato M. Sergi

Quercetin is a flavonoid widely studied as a chemopreventive agent in different types of cancer. Previously, we reported that quercetin has a chemopreventive effect on the liver-induced preneoplastic lesions in rats. Here, we evaluated if quercetin was able not only to prevent but also to reverse rat liver preneoplastic lesions. We used the modified resistant hepatocyte model (MRHM) to evaluate this possibility. Treatment with quercetin was used 15 days after the induction of preneoplastic lesions. We found that quercetin reverses the number of preneoplastic lesions and their areas. Our results showed that quercetin downregulates the expression of EGFR and modulates this signaling pathway in spite of the activated status of EGFR as detected by the upregulation of this receptor, with respect to that observed in control rats. Besides, quercetin affects the phosphorylation status of Src-1, STAT5, and Sp-1. The better status of the liver after the treatment with quercetin could also be confirmed by the recovery in the expression of IGF-1. In conclusion, we suggest that quercetin reversed preneoplastic lesions by EGFR modulation and the activation state of Src, STAT5, and Sp1, so as the basal IGF-1.

1. Introduction

Hepatocellular carcinoma (HCC) is one of the most common and deadly cancers worldwide [1]. HCC, as another type of cancer, is established by a multistep and multifactorial process; there, we can distinguish three stages, the initiation, the promotion, and the progression. Different risk factors stimulate the progression of the malignancy, and when it is detected, actual treatments are not efficient. Some of these factors are the infection with hepatitis B or C virus, heavy alcohol intake, nonalcoholic steatohepatitis, and exposure to toxic substances such as aflatoxin B or vinyl chloride, among others. Even if the relation is not clear, the diet has been also shown to play an important role in the development of HCC [2, 3].

Antioxidants in the diet, such as flavonoids contained in several fruits and vegetables, have a beneficial effect on liver tumors in animal models and induce apoptosis in cancer cell lines [2, 4, 5]. Quercetin, a flavonoid widely studied as a chemopreventive agent in different types of cancer, is considered an excellent antioxidant with a proapoptotic effect and able to inhibit the growth of different cancer cell lines [6]. It has been proved that quercetin is able to inhibit the metabolic activity and cell death by apoptosis in HCC cell lines like HepG2, HuH7, and Hep3B2 [7]. It also induces a decrease in oxidative stress and a significant decrease of antioxidant

activity in the liver of rats treated with N-nitrosodiethylamine as a cancer inducer [5]. We have also previously reported that quercetin has a chemopreventive effect on the liver of rats when this is used previously to the use of the MRHM to induce HCC. Quercetin reduces the number of cells initiated to cancer through decreasing lipoperoxidation, activating caspases 3 and 9, and promoting the enzymatic and nonenzymatic antioxidant defense system during the initiation of hepatocarcinogenesis [8, 9]. While the use of chemoprotective substances would have a major impact on the incidence of HCC, it is also necessary to discover substances that contribute to reverse the injuries, since this type of cancer is usually detected in late stages.

The MRHM is a well-characterized model useful for the analysis and quantitation of different stages of HCC. On this model, N-diethylnitrosamine (DEN) in single doses is applied as an initiator agent. Later, 2-acetylaminofluorene (2-AAF) and partial hepatectomy act in promoting the development of initiated cells and their progression to altered hepatic foci [10, 11]. Moreover, the detection of gamma-glutamyl transpeptidase (GGT) is a useful tool, which has been used in detecting HCC-related lesions. GGT is not present in hepatocytes of adult rats, but it is detected in altered hepatic foci induced by carcinogens, in most animal models, from the initial lesions caused by carcinogens until the tumor formation [9].

It has been proposed that quercetin can influence the activation of epidermal growth factor receptor (EGFR) through the overexpression of some ligands like amphiregulin [12] and also has been shown that quercetin, at a dose of 10 μM, decreases the phosphorylation of EGFR in prostate cancer cells (PC3), producing a diminished expression of target proteins like vimentin, N-cadherin, and cyclin D1 [13]. Quercetin has been also proven to affect other signaling pathways in different cancers or cell lines, like JAK/STAT in cholangiocarcinoma cells [14] or phosphoinositide 3-kinase (PI3K) and mitogen-activated protein (MAP) kinases in B16F10 melanoma cells [15]. In view of the mentioned effects of quercetin on different molecular pathways, we evaluated EGFR signaling pathways as a possible participating mechanism of quercetin to reverse rat liver preneoplastic lesions.

Here, we show that quercetin reverses liver preneoplastic lesions in the MRHM, influences the expression of EGFR, and modulates other related signaling pathways through the induction of the phosphorylation of Src-1, STAT5, and Sp-1. And finally, quercetin induces the recovery in the expression of IGF-1B, which reflects a recuperation of a better status of the liver.

2. Materials and Methods

2.1. Materials. Primary antibodies used were EGFR-t (C2C3, GeneTex), EGFR-p (S.684.2, Thermo), Src (36D10, Cell Signaling), Src-p (GTX24816, Genetex), STAT5 (9310, Cell Signaling), STAT5-p (9359, Cell Signaling), Sp1 (GTX110593, Genetex), Sp1-p (phosphor Thr739, Genetex), IGF1 (sc-9013, Santa Cruz Biotechnology), and β-actin (mouse monoclonal, CINVESTAV). Secondary antibodies used were goat anti-rabbit HRP (catalog number 62-6120, Invitrogen) or goat anti-mouse HRP (catalog number A9044, Sigma), WesternSure Chemiluminescent Western blotting reagent, and the Li-COR C-DiGit Blot Scanner (LI-COR Biosciences, Finland).

2.2. Animals and Treatments. Three groups of seven Fischer 344 male rats were used to perform this study. All the experiments were done according to the guidelines of the Institutional Committee for Animal Care and Use. Male rats, with 180 to 200 g of weight, were provided by the Unit of Production and Experimentation on Animals of Laboratory (UPEAL), at CINVESTAV, Mexico City, Mexico. All the rats were maintained under controlled temperature conditions with 12 hours light/dark cycles. Access to food and water was given ad libitum. Two groups of rats were subject to the MRHM, and an additional group was used as a control. In this last group, only the vehicles were administrated and were named the nontreated group (NT).

In the two groups where the MRHM was used, an intraperitoneal single dose of 200 mg/kg of diethylnitrosamine (DEN) was administered in order to initiate a carcinogenic process. After this, three consecutive intragastric doses of 20 mg/kg of the promoter agent 2-acetylaminofluorene (2-AAF) were administrated in days seven, eight, and nine of the experimentation. Finally, ten days after initiation, a proliferative stimulus was induced through a partial hepatectomy including the 75% of the liver. From day fifteen until the sacrifice, quercetin in doses of 10 mg/kg was administrated every two days in one of the groups (FT + Q group). In the second group, only the vehicle for quercetin, carboxymethylcellulose (CMC) at 0.5%, was given (FT). The animals of the three groups were sacrificed at day thirty after DEN administration (Figure 1).

After sacrifice, livers were removed and each one was sectioned in two parts. One of them was frozen, cryosections of 20 μ of thickness were obtained, and slices were kept frozen until the GGT detection was performed. The other part was cryopreserved with liquid nitrogen for further protein analysis.

2.3. Histochemistry for Gamma-Glutamyl Transpeptidase (GGT). Slices of 20 μ thickness on slides with gelatine were fixed in ethanol at −20°C for 10 minutes. Then, a Tris buffer solution (pH 7, containing gamma glutamyl-4-methoxy-2 naphthylamide (GMNA), glycyl-glycine, and fast blue) was added. Slices were incubated. After the incubation, the red color produced by a 100 mM solution of copper sulfate ($CuSO_4$) made the enzymatic activity evident (all the chemicals were from Sigma Chemicals Co., St. Louis, MO). Using a polychromatic camera coupled to an OLYMPUS SZ045 microscope, images of the stained liver were captured.

2.4. Western Blot. From each rat of the three groups, total protein was obtained from a frozen liver sample of 100 mg of tissue. Tissues were mechanically homogenized in 1 ml of cold RIPA buffer supplemented with the protease inhibitors PhosSTOP and Complete (Roche Life Science, both). Extracts were centrifuged at 3500 rpm, at 4°C for 15 min. The supernatant was transferred to a new tube and centrifuged at

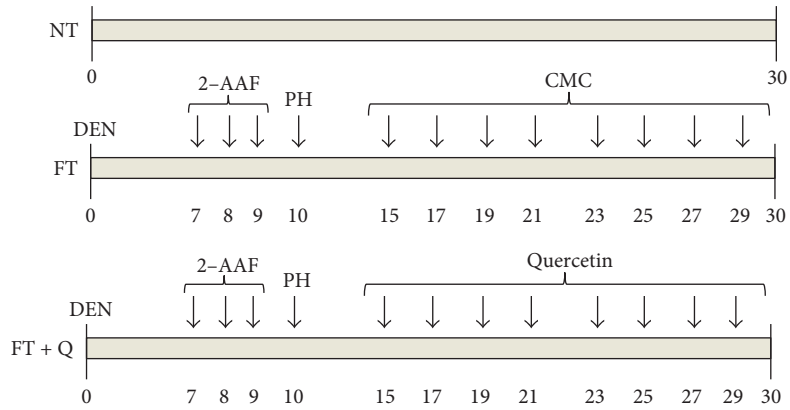

Figure 1: Groups of treatment. The rats were sacrificed 30 days after initiating the carcinogenesis treatment. NT, rats without treatment and just received the quercetin vehicle. FT, rats treated with MRHM and received the quercetin vehicle. FT + Q, rats treated with MRHM and received the quercetin. $n = 7$ rats per group.

12,000 ×g at 4°C for 10 min. The supernatant was recovered again, and the total protein was quantified by the modified method of Bradford. Proteins were boiled 5 min in Laemmli buffer 2x and immediately placed on ice. 60 μg of each sample were separated by SDS-PAGE in concentrated acrylamide gels between 6% and 15% (according to the protein in analysis). Later, proteins were transferred to polyvinylidene fluoride (PVDF) membranes. Nonspecific binding was blocked with TBS-T containing 10% of nonfat dry milk at room temperature for 2 h. Membranes were then incubated at 4°C overnight, with their corresponding primary antibodies. Primary antibodies were EGFR-t, EGFR-p, Src, Src-p, STAT5, STAT5-p, Sp1, Sp1-p, IGF1, and β-actin. After three washes, membranes were incubated with secondary antibodies goat anti-rabbit HRP and goat anti-mouse HRP at room temperature for 2 h. The membranes were newly washed, by three times, and the proteins of interest were visualized and analyzed using the WesternSure Chemiluminescent Western blotting reagent and the C-DiGit Blot Scanner (Li-COR. both).

2.5. Statistical Analysis. The number of GGT-positive foci and their area were quantified by using the analysis software AnalySIS Soft Imaging System GmbH. The intensity of the bands obtained in Western blot analysis was quantified with the software included in the C-DiGit Blot Scanner. The data were collected and statistically analyzed to generate the corresponding graphs, all this using the GraphPad Prism 4 software. The data were expressed as the mean ± SE.

3. Results

3.1. The Quercetin Reverses the Number and Area of Foci Related to Preneoplastic Lesions. We use the modified resistant hepatocyte model (MRHM), in order to induce preneoplastic lesions in the liver of rats (FT group) and to evaluate the capacity of quercetin for reversing the lesions (FT + Q group). Briefly, lesions were induced with a single dose of DEN administrated to rats, whose characteristics have been previously described, to initiate the carcinogenic process. Seven days after DEN administration, the rats were treated during four days with the promoter agent 2-AAF, and a partial hepatectomy was done 10 days after DEN administration. From the fifteenth to the thirtieth day, one dose of quercetin (Q) was administrated to the rats in the FT + Q group every two days or only to the vehicle in the CMC group. All the rats, in the experimental and control groups, were sacrificed thirty days after the initiation (Figure 1). The expression pattern of the tumor marker GGT was analyzed to evaluate the effect of quercetin in chemoprevention of preneoplastic lesions. Gamma-glutamyl transpeptidase (GGT) is an enzymatic protein highly expressed in most models of hepatic cancer and is consider an early tumor marker on them. The activity of this enzyme was evaluated on liver slices, and the number of foci and their areas were determined. As it was expected, the activity of this enzyme could be detected in the liver of rats in the FT group (Figure 2(a), FT) but not in those of the control group without any treatment (Figure 2(a), NT). The FT and FT + Q groups present preneoplastic lesions as shown by GGT enzyme-positive staining, but preneoplastic lesions did not have a particular assigned distribution; they were in random distribution throughout the lobes. The observed difference was in the number and area of the lesions; the FT group was the one with more and with the most positive mark for GGT (Figure 2(a)). In general, on haematoxylin and eosin staining (data not shown), hepatocytes were observed altered, intensely basophilic, and translucent with vesicular nuclei and with prominent nucleoli, as expected. The treatment with quercetin, after the induction of premalignant lesions, produced a reduction in the number of foci positive for GGT (Figure 2(a), FT + Q). The quantitation of the number of foci positive for GGT indicates that there was a reduction of 58% in the number of preneoplastic lesions (Figure 2(b)). A reduction of the area in 81% of the preneoplastic lesions was observed; this decrease in number and area of preneoplastic lesions was statistically significant (Figure 2(c)). This result indicates that quercetin not only prevents the development of lesions as previously reported but also reverses them.

3.2. Diminished Expression of EGFR Was Observed When Premalignant Lesions Were Reversed by Quercetin. Because

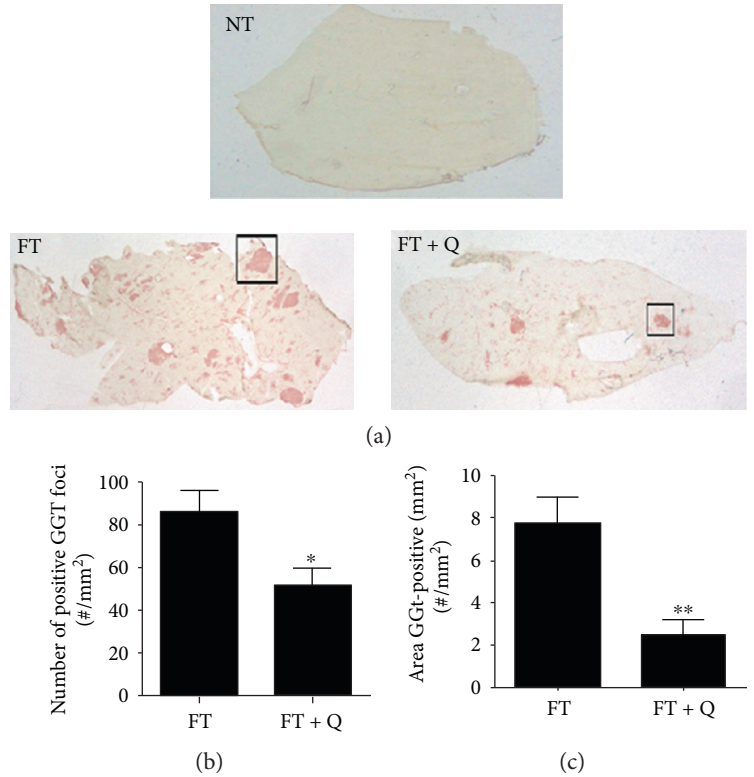

Figure 2: Effect of quercetin on GGT tumor-marker activity. (a) Preneoplastic lesions were detected by GGT activity (red area). (b) Number/mm^2 of GGT-positive liver lesions. (c) Total GGT-positive area. A 2 mg/kg dose of quercetin showed reversion of preneoplastic lesions. $^{**}p < 0.01$ and $^{*}p < 0.05$

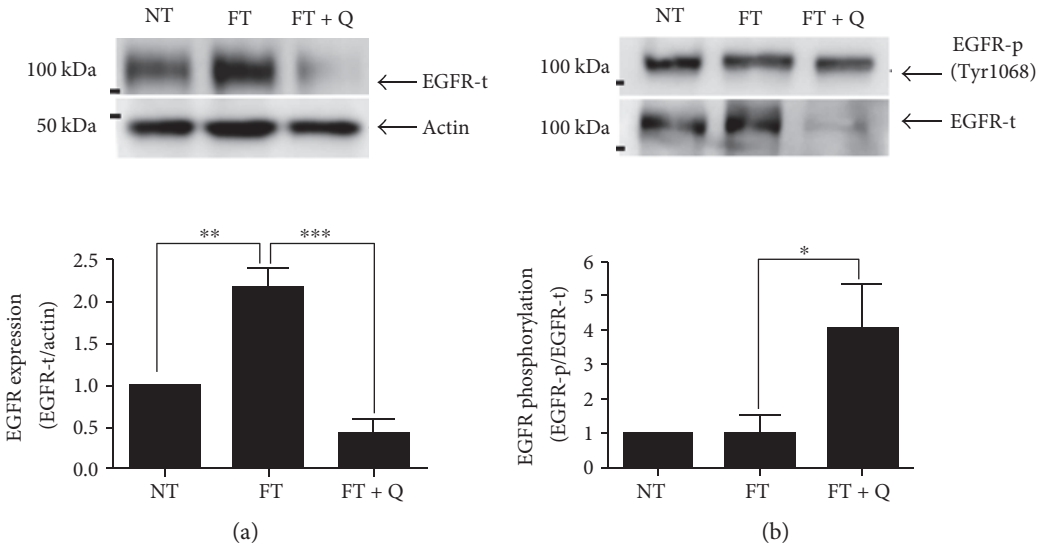

Figure 3: Expression of EGFR during quercetin treatment. (a) Western blot of EGFR expression. (b) Western blot of EGFR-p expression. A representative image and the analyses of seven independent events are shown. $^{***}p < 0.001$, $^{**}p < 0.01$ and $^{*}p < 0.05$.

some signaling pathways are activated by quercetin through the EGFR protein, we analyze if EGFR participates in the observed effect of the quercetin reversion of preneoplastic lesions. The analysis by Western blot indicates that the total EGFR was 2.2 times overexpressed with respect to control values in the liver tissue of rats when preneoplasic lesions were induced (Figure 3(a), FT), but this was diminished to half of control values when quercetin was used to reverse the lesions. (Figure 3(a), FT + Q). To know the activation status of EGFR, the phosphorylated form of this receptor was evaluated by Western blot (Figure 3(b)). The activation of EGFR as shown by the ratio of phosphorylated EGFR versus total EGFR in the liver of rats with preneoplastic lesions was similar to that observed in the liver of rats without lesions

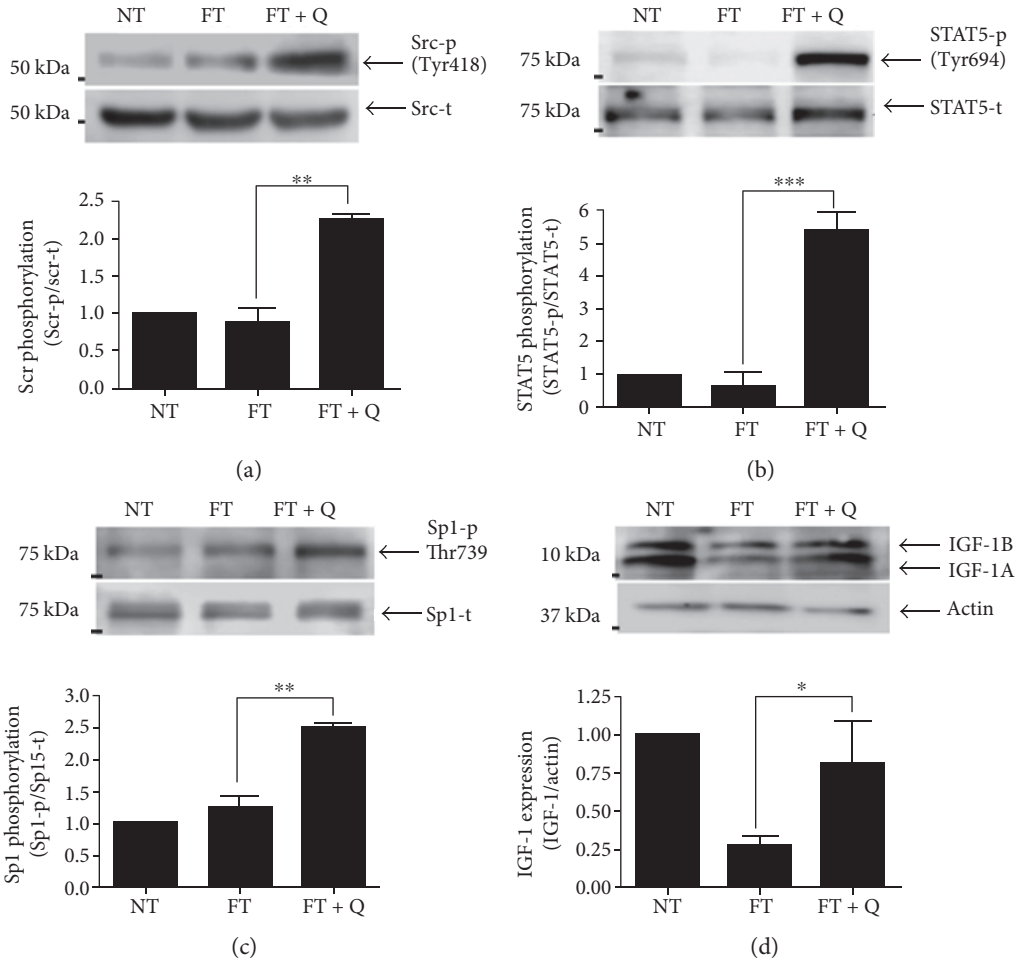

Figure 4: Signaling pathway activation through EGFR phosphorylation. (a) Western blot of phospho-Src. (b) Western blot of phospho-STAT5. (c) Western blot of phospho-Sp1. (d) Western blot of IGF-1A and IGF-1B. A representative image and the analyses of seven independent events are shown. $^{***}p < 0.001$, $^{**}p < 0.01$ and $^{*}p < 0.05$.

(Figure 3(b), FT and NT); this ratio increases 3.0 times showing the activation of EGFR when the treatment with quercetin was used (Figure 3(b), FT + Q).

3.3. The Reversion of Premalignant Lesions by Quercetin Corresponds with the Activation of the STAT5 Signaling Pathway. The phosphorylation of EGFR induces the expression of several molecules through the activation of some signaling pathways; Src is one protein activated by EGFR, and it was increased in livers where quercetin was used to revert the preneoplastic lesions. The increase in the activation was 2.3 times more in the FT + Q group than in the FT group, which is statistically significant as could be observed by densitometric analysis. The activation of Src (Src-t) was similar in both the NT and FT groups (Figure 4(a)). In summary, the activity of Src was increased during the reversion of lesions, when quercetin was used.

The evaluation of some signaling pathways activated by EGFR allowed us to observe an increase in the activation status of STAT5. STAT5 was phosphorylated in a similar way in the liver from rats in the NT and FT groups. But an important increase in the activation of STAT5 (STAT5-p) was observed in the group where the preneoplastic lesions were diminished by the treatment with quercetin (4.4 times more than that in the NT group). The higher activation status of STAT5 in the FT + Q group, with respect to that observed in the FT group, was also statistically significant (Figure 4(b)). So, we could think that quercetin induces the phosphorylation of STAT5, increasing its activity.

The activation of Sp1 along with STAT5 has been previously reported. Then, the activation status of Sp1 was also evaluated in the liver of rats in the study. The analysis of the group where the treatment with quercetin was used to revert preneoplastic lesion revealed an increase in the activation of Sp1which was quantified by densitometry. The increase observed was more than 1.4 times with respect to that in the FT group (Figure 4(c)). There was no significant difference in the activation status of Sp1 between the NT group and FT group. In such manner, Sp1 is activated along with STAT5 when quercetin is used.

The target gene IGF-1 that is an indicator of the functional status of the liver was also evaluated. As we expected, the induction of preneoplastic lesions by using the MRHM resulted in a 74% decrease of IGF-1 expression (Figure 4(d),

FT). When we analyzed its expression in the liver of rats in the FT + Q group, the expression of IGF was recuperated, from 26% to 83% of control values (Figure 4(d), FT + Q group). This last result is a reflection of the functional status of the liver in the three groups.

4. Discussion

The ability of quercetin to reverse preneoplastic lesions in the liver was tested in the MRHM. This model has been used by us [9] and other authors in order to observe the three different stages associated with the development of HCC: initiation, promotion, and progression [11, 16, 17]. The evaluation of the presence of preneoplastic lesions was done through the activity of the GGT. This enzyme has been analyzed in the different stages, and it is expressed all along from the initiation to progression in models of chemical carcinogenesis and led to the identification of preneoplastic cells [18, 19]. The GGT enzyme is a focal marker commonly used and also considered as a tumor marker. We found that the administration of quercetin reverse the preneoplastic lesions in this model, which was evident by the lower number of altered hepatic foci (positive for GGT) but the major effect was seen in the decrease of the area. In the FT and FT + Q groups, we observed lesions with GGT staining; however, it is evident that in the FT group, multiple lesions were observed and the FT + Q group showed a drastic effect on GGT decline. In the quantification of GGT, 0.01 mm^2 was a low-end measure to discard stains not associated with preneoplastic lesions (ductile cells) with a preferential circular shape. Several reports indicate that quercetin has diverse antitumor activities in different cancers or precancerous lesions. And its activity occurs through the regulation of different signaling pathways like β-catenin/Tcf or AMP-activated protein kinase (AMPK) in colon cancer cells [20, 21], NF-κB and AP-1/JNK in human hepatoma cells [22], or EGFR/PI3K/Akt pathway in prostate cancer [13] and EGFR in liver cells [12]. The signaling pathways are maintained overexpressed during the progression of cancer. So if quercetin is able to regulate several pathways during the progression, it was expected to cause a reversible effect over the lesions.

We observed a clear decrease in the number of altered hepatic foci and their area, which coincides with the diminished expression of EGFR and then a lower quantity of phosphorylated EGFR. But due to the increase in the ratio of phosphorylated EGFR, we evaluated the activation of Src and we found that phosphorylated Src was higher in the tissues treated with quercetin. This last result agrees with previous reports which indicate that the transactivation of EGFR can occur through GPCR ligands and some cytokines. These can induce phosphorylation of EGFR in the absence of a ligand and, as a consequence, the activation of Src or Janus tyrosine kinase 1 (Jak1) [23]. In addition, Src can activate different STATs. STATs could be activated by JAK kinases, growth factor receptors (EGFR), or Src family members [24]. Here, we showed that STAT5 is phosphorylated in the liver of rats treated with quercetin to reverse the preneoplastic lesions. The activation of STAT5 by Src has been previously reported [24]. Even more, in rat hepatocytes in primary culture, it has been proved that EGF induces the activation of STAT5 apparently through a Src-dependent mechanism [25]. Moreover, Src induces the expression of proteins, like MMP2, through the ERK/Sp1 pathway [26]. And a signaling interaction between STAT5 and Sp1 has also been proved, mainly in the expression of cyclin D2 [27]. Here, we found that Sp1 is more active in the liver of rats treated with quercetin. It is important to highlight that Src, STAT5, and Sp1 were more phosphorylated in the liver of rats when treated with quercetin. But there were no significant differences in the phosphorylation of Src, STAT5, and Sp1, between the groups with induced preneoplastic lesions and controls. Therefore, we can deduce that the reversion of preneoplastic lesions by quercetin occurs by a direct effect on signaling pathways responsible for the development of lesions, like EGFR, and additionally to the activation of signaling pathways whose molecules are considered as a tumor suppressor, like STAT5 [28]. The STAT5 activity as a tumor suppressor is attributed mainly to the control of reactive oxygen species through the expression of PUMA, BIM, and NOX4 [28]. We also analyzed the expression of IGF-1, and it was diminished in the liver of rats with preneoplastic lesions. This was expected since, previously, it has been showed that diminished expression of IGF-1 is related to the progression of different liver diseases [29]. Specifically, in HCC, serum levels of IGF-1 are diminished and it has been associated with poor prognosis [30, 31], but the patients with the highest levels of IGF previously to antiangiogenic treatment are associated with a better disease control rate [31]. Our results showed that the treatment with quercetin recuperates IGF-1 almost to control values. Even if the level did not reach that in the control group, this increase in the expression of IGF-1 coincided with the lower number and area of the neoplastic lesions. This allowed us to conclude that this last reflects a better control of the preneoplastic lesions in the liver of rats treated with quercetin.

5. Conclusions

In conclusion, we showed that besides the known effect of quercetin as a protective agent, quercetin treatment is also useful to reverse preneoplastic lesions. This effect is observed not only on the decreased proliferation, but we also cannot discard the possibility that tumor-initiating cells were removed. Therefore, the expression of EGFR as well as the modulation of its activation state participates in the decrease of the preneoplastic lesions. Also, the activation state of Src, STAT5, and Sp1 as the basal IGF-1 restoration participates on the decrease in the number and size of preneoplastic lesions caused by quercetin.

Abbreviations

HCC: Hepatocellular carcinoma
MRHM: Modified resistant hepatocyte model
DEN: N-Diethylnitrosamine
2-AAF: 2-Acetylaminofluorene
GGT: Gamma-glutamyl transpeptidase

EGFR: Epidermal growth factor receptor
PI3K: Phosphoinositide 3-kinase
MAP: Mitogen-activated protein
NT: Nontreated group
Jak1: Janus tyrosine kinase 1.

Conflicts of Interest

The authors declare that there is no conflict of interest.

Acknowledgments

This work was supported by a grant contribution from CONACYT and Project 178558 and by the SVT grant from CINVESTAV and project Cátedra CONACYT 2014-2499. The authors thank Samia Fattel Fazenda for the technical support.

References

[1] J. Ferlay, I. Soerjomataram, R. Dikshit et al., "Cancer incidence and mortality worldwide: sources, methods and major patterns in GLOBOCAN 2012," *International Journal of Cancer*, vol. 136, no. 5, pp. E359–E386, 2015.

[2] H. B. El-Serag and K. L. Rudolph, "Hepatocellular carcinoma: epidemiology and molecular carcinogenesis," *Gastroenterology*, vol. 132, no. 7, pp. 2557–2576, 2007.

[3] C. Y. Liao, C. C. Lee, C. C. Tsai et al., "Novel investigations of flavonoids as chemopreventive agents for hepatocellular carcinoma," *BioMed Research International*, vol. 2015, Article ID 840542, 26 pages, 2015.

[4] J. H. Jeong, J. Y. An, Y. T. Kwon, J. G. Rhee, and Y. J. Lee, "Effects of low dose quercetin: cancer cell-specific inhibition of cell cycle progression," *Journal of Cellular Biochemistry*, vol. 106, no. 1, pp. 73–82, 2009.

[5] A. M. Seufi, S. S. Ibrahim, T. K. Elmaghraby, and E. E. Hafez, "Preventive effect of the flavonoid, quercetin, on hepatic cancer in rats via oxidant/antioxidant activity: molecular and histological evidences," *Journal of Experimental & Clinical Cancer Research*, vol. 28, no. 1, p. 80, 2009.

[6] L. Gibellini, M. Pinti, M. Nasi et al., "Quercetin and cancer chemoprevention," *Evidence-Based Complementary and Alternative Medicine*, vol. 2011, Article ID 591356, 15 pages, 2011.

[7] A. F. Brito, M. Ribeiro, A. M. Abrantes et al., "New approach for treatment of primary liver tumors: the role of quercetin," *Nutrition and Cancer*, vol. 68, no. 2, pp. 250–266, 2016.

[8] V. R. Vasquez-Garzon, J. Arellanes-Robledo, R. García-Román, D. I. Aparicio-Rautista, and S. Villa-Treviño, "Inhibition of reactive oxygen species and pre-neoplastic lesions by quercetin through an antioxidant defense mechanism," *Free Radical Research*, vol. 43, no. 2, pp. 128–137, 2009.

[9] V. R. Vasquez-Garzon, J. R. Macias-Pérez, M. N. Jiménez-García, V. Villegas, S. Fattel-Fazenta, and S. Villa-Treviño, "The chemopreventive capacity of quercetin to induce programmed cell death in hepatocarcinogenesis," *Toxicologic Pathology*, vol. 41, no. 6, pp. 857–865, 2013.

[10] A. Marche-Cova, S. Fattel-Fazenda, A. Rojas-Ochoa, E. Arce-Popoca, and S. Villa-Treviño, "Follow-up of GST-P during hepatocarcinogenesis with DEN-2AAF in F344 rats," *Archives of Medical Research*, vol. 26, Spec No, pp. S169–S173, 1995.

[11] H. C. Pitot, Y. P. Dragan, J. Teeguarden, S. Hsia, and H. Campbell, "Quantitation of multistage carcinogenesis in rat liver," *Toxicologic Pathology*, vol. 24, no. 1, pp. 119–128, 1996.

[12] M. J. Cuevas, J. Tieppo, N. P. Marroni, M. J. Tuñón, and J. González-Gallego, "Suppression of amphiregulin/epidermal growth factor receptor signals contributes to the protective effects of quercetin in cirrhotic rats," *The Journal of Nutrition*, vol. 141, no. 7, pp. 1299–1305, 2011.

[13] A. B. Firdous, G. Sharmila, S. Balakrishnan et al., "Quercetin, a natural dietary flavonoid, acts as a chemopreventive agent against prostate cancer in an in vivo model by inhibiting the EGFR signaling pathway," *Food & Function*, vol. 5, no. 10, pp. 2632–2645, 2014.

[14] L. Senggunprai, V. Kukongviriyapan, A. Prawan, and U. Kukongviriyapan, "Quercetin and EGCG exhibit chemopreventive effects in cholangiocarcinoma cells via suppression of JAK/STAT signaling pathway," *Phytotherapy Research*, vol. 28, no. 6, pp. 841–848, 2014.

[15] R. A. Rafiq, A. Quadri, L. A. Nazir, K. Peerzada, B. A. Ganai, and S. A. Tasduq, "A potent inhibitor of phosphoinositide 3-kinase (PI3K) and mitogen activated protein (MAP) kinase signalling, quercetin (3, 3′, 4′, 5, 7-pentahydroxyflavone) promotes cell death in ultraviolet (UV)-B-irradiated B16F10 melanoma cells," *PLoS One*, vol. 10, no. 7, article e0131253, 2015.

[16] E. Farber, "The multistep nature of cancer development," *Cancer Research*, vol. 44, no. 10, pp. 4217–4223, 1984.

[17] P. A. Oliveira, A. Colaço, R. Chaves et al., "Chemical carcinogenesis," *Anais da Academia Brasileira de Ciências*, vol. 79, no. 4, pp. 593–616, 2007.

[18] Y. P. Dragan and H. C. Pitot, "The role of the stages of initiation and promotion in phenotypic diversity during hepatocarcinogenesis in the rat," *Carcinogenesis*, vol. 13, no. 5, pp. 739–750, 1992.

[19] M. H. Hanigan, "Gamma-glutamyl transpeptidase, a glutathionase: its expression and function in carcinogenesis," *Chemico-Biological Interactions*, vol. 111-112, pp. 333–342, 1998.

[20] H. J. Kim, S. K. Kim, B. S. Kim et al., "Apoptotic effect of quercetin on HT-29 colon cancer cells via the AMPK signaling pathway," *Journal of Agricultural and Food Chemistry*, vol. 58, no. 15, pp. 8643–8650, 2010.

[21] C. H. Park, J. Y. Chang, E. R. Hahm, S. Park, H. K. Kim, and C. H. Yang, "Quercetin, a potent inhibitor against beta-catenin/Tcf signaling in SW480 colon cancer cells," *Biochemical and Biophysical Research Communications*, vol. 328, no. 1, pp. 227–234, 2005.

[22] A. B. Granado-Serrano, M. A. Martín, L. Bravo, L. Goya, and S. Ramos, "Quercetin modulates NF-kappa B and AP-1/JNK pathways to induce cell death in human hepatoma cells," *Nutrition and Cancer*, vol. 62, no. 3, pp. 390–401, 2010.

[23] C. Berasain, M. Ujue Latasa, R. Urtasun et al., "Epidermal growth factor receptor (EGFR) crosstalks in liver cancer," *Cancers (Basel)*, vol. 3, no. 2, pp. 2444–2461, 2011.

[24] C. M. Silva, "Role of STATs as downstream signal transducers in Src family kinase-mediated tumorigenesis," *Oncogene*, vol. 23, no. 48, pp. 8017–8023, 2004.

[25] T. K. Guren, J. Ødegård, H. Abrahamsen et al., "EGF receptor-mediated, c-Src-dependent, activation of Stat5b is downregulated in mitogenically responsive hepatocytes," *Journal of Cellular Physiology*, vol. 196, no. 1, pp. 113–123, 2003.

[26] A. Patel, H. Sabbineni, A. Clarke, and P. R. Somanath, "Novel roles of Src in cancer cell epithelial-to-mesenchymal transition, vascular permeability, microinvasion and metastasis," *Life Sciences*, vol. 157, pp. 52–61, 2016.

[27] A. Martino, J. H. Holmes 4th, J. D. Lord, J. J. Moon, and B. H. Nelson, "Stat5 and Sp1 regulate transcription of the cyclin D2 gene in response to IL-2," *Journal of Immunology*, vol. 166, no. 3, pp. 1723–1729, 2001.

[28] J. H. Yu, B. M. Zhu, G. Riedlinger, K. Kang, and L. Hennighausen, "The liver-specific tumor suppressor STAT5 controls expression of the reactive oxygen species-generating enzyme NOX4 and the proapoptotic proteins PUMA and BIM in mice," *Hepatology*, vol. 56, no. 6, pp. 2375–2386, 2012.

[29] A. Kasprzak and A. Adamek, "The insulin-like growth factor (IGF) signaling axis and hepatitis C virus-associated carcinogenesis (review)," *International Journal of Oncology*, vol. 41, no. 6, pp. 1919–1931, 2012.

[30] T. M. Hung, C. M. Ho, Y. C. Liu et al., "Up-regulation of microRNA-190b plays a role for decreased IGF-1 that induces insulin resistance in human hepatocellular carcinoma," *PLoS One*, vol. 9, no. 2, article e89446, 2014.

[31] Y. Y. Shao, C. C. Huang, S. D. Lin, C. H. Hsu, and A. L. Cheng, "Serum insulin-like growth factor-1 levels predict outcomes of patients with advanced hepatocellular carcinoma receiving antiangiogenic therapy," *Clinical Cancer Research*, vol. 18, no. 14, pp. 3992–3997, 2012.

Hindawi
Oxidative Medicine and Cellular Longevity
Volume 2017, Article ID 1767198, 12 pages
https://doi.org/10.1155/2017/1767198

Research Article

Apple Flavonoids Suppress Carcinogen-Induced DNA Damage in Normal Human Bronchial Epithelial Cells

Vazhappilly Cijo George[1] and H. P. Vasantha Rupasinghe[1,2]

[1]*Department of Plant, Food, and Environmental Sciences, Faculty of Agriculture, Dalhousie University, Truro, NS, Canada*
[2]*Department of Pathology, Faculty of Medicine, Dalhousie University, Halifax, NS, Canada*

Correspondence should be addressed to H. P. Vasantha Rupasinghe; vrupasinghe@dal.ca

Received 4 January 2017; Accepted 2 May 2017; Published 18 June 2017

Academic Editor: Debasish Roy

Scope. Human neoplastic transformation due to DNA damage poses an increasing global healthcare concern. Maintaining genomic integrity is crucial for avoiding tumor initiation and progression. The present study aimed to investigate the efficacy of an apple flavonoid fraction (AF4) against various carcinogen-induced toxicity in normal human bronchial epithelial cells and its mechanism of DNA damage response and repair processes. *Methods and Results*. AF4-pretreated cells were exposed to nicotine-derived nitrosamine ketones (NNK), NNK acetate (NNK-Ae), methotrexate (MTX), and cisplatin to validate cytotoxicity, total reactive oxygen species, intracellular antioxidants, DNA fragmentation, and DNA tail damage. Furthermore, phosphorylated histone (γ-H2AX) and proteins involved in DNA damage (ATM/ATR, Chk1, Chk2, and p53) and repair (DNA-PKcs and Ku80) mechanisms were evaluated by immunofluorescence and western blotting, respectively. The results revealed that AF4-pretreated cells showed lower cytotoxicity, total ROS generation, and DNA fragmentation along with consequent inhibition of DNA tail moment. An increased level of γ-H2AX and DNA damage proteins was observed in carcinogen-treated cells and that was significantly ($p \leq 0.05$) inhibited in AF4-pretreated cells, in an ATR-dependent manner. AF4 pretreatment also facilitated the phosphorylation of DNA-PKcs and thus initiation of repair mechanisms. *Conclusion*. Apple flavonoids can protect in vitro oxidative DNA damage and facilitate repair mechanisms.

1. Introduction

Mammalian genomic DNA is susceptible to various environmental, cytotoxic, or genotoxic agents that sense DNA damage and activate signaling cascades for effective repair mechanisms. Under a normal circumstance with a specific type of DNA lesion, DNA damage is commonly repaired through nonhomologous end joining (NHEJ)/homologous recombination (HR) mechanisms [1, 2]. Alkylating agents, platinum drugs, antimetabolites, topoisomerase inhibitors and ionizing radiations, nitrosoureas, aziridine compounds, alkyl sulphonates, and triazine compounds are some of the electrophiles that covalently transfer alkyl-groups onto the DNA bases, disrupting the DNA helix and induces DNA breaks [3]. DNA double-strand breaks (DSBs) are the most lethal lesions that can result in mutations, chromosomal aberrations, and cell death [4, 5]. Extensive DNA damage and defects in repair systems can lead to poor genomic stability and initiate cardiovascular disease and cancer [2, 6]. Hence, maintaining genomic integrity possess global healthcare challenge and should be well addressed.

An increased level of oxidative stress often causes excessive reactive oxygen species (ROS) generation, which breaks the equilibrium of metabolic process of normal cells and initiates DSBs [7]. As a result, the cells activate DNA damage response (DDR) mechanisms and initiate various enzymes that modify the DNA and nuclear damage. Recruitment of phosphatidylinositol-3-kinase (PI3K) family members to the site of DNA damage is the first step of DDR mechanisms, and the phosphorylation of ataxia telangiectasia-mutated (ATM) or ATM-Rad3-related (ATR) kinases are often followed in DDR process [8]. The phosphorylation of ATM/ATR regulates downstream targets including cell cycle check point kinases (Chk2/Chk1), tumor suppressor p53,

and phosphorylated histone γ-H2AX foci, commonly known as a marker for DSBs [9]. γ-H2AX foci serve as a platform for the assembly and recruitment of other DNA repair factors, including mediators of DNA damage check point 1 (MDC1) to initiate DDR mechanisms [10]. DNA-dependent protein kinases (DNA-PK), composed of Ku70/80 heterodimer and a catalytic subunit (DNA-PKcs), serve as the pinnacle protein that cooperates with ATR/ATM to phosphorylate other proteins involved in the DNA damage [11, 12]. Upon phosphorylation in serine and threonine residues (T2609, T3950, and S2056), DNA-PK initiates NHEJ repair mechanisms which are found to be very common in mammalian cells [4]. DNA-PK also gets autophosphorylated and expressed differentially in normal and malignant human tissues with relatively little variation in level [13]. However, there are many other proteins involved in this complex mechanisms and their roles are still inconclusive.

Development of effective nutraceuticals from natural resources has been major research endeavors over the past decade. While several reports are available to show the protective effects of various plant flavonoids and extracts against different genotoxicity [14], to the best of our knowledge, there are no specific studies available to show the mechanism of action of apple flavonoids to exert protection against DNA damage in normal human cells. Our previous studies have shown that an apple peel flavonoid fraction (AF4) possess antioxidant, neuroprotective, anti-inflammatory, and anticancer activities in various in vitro and in vivo models [15–17]. Moreover, AF4 is highly rich with flavonoids and phenolic acids such as quercetin glycosides, cyanidin 3-galactoside, epicatechin, phloridzin, and chlorogenic acid [17]. In light of these findings, we hypothesized that AF4 could possibly render protection against DNA damage induced by various chemicals or environmental agents, whose primary target is inevitably airway epithelial cells in the lung. To test this hypothesis, we investigated the effects of AF4 on normal human bronchial epithelial cells (BEAS-2B) challenged with known carcinogenic chemical agents such as 4-(methylnitrosamino)-1-(3-pyridyl-d4)-1-butanone (NNK), 4-[(acetoxymethyl) nitrosamino]-1-(3-pyridyl)-1-butanone (NNK acetate; NNK-Ae), methotrexate (MTX), and cisplatin. We also analyzed the signaling proteins involved in DNA damage pathways since understanding the DNA repair mechanisms has important implication in developing a potent therapeutic agent.

2. Material and Methods

2.1. Chemicals, Kits, and Antibodies. Bronchial Epithelial Cell Growth Medium (BEGM) for BEAS-2B cells was purchased from Lonza (Walkersville, MD, USA). COMET SCGE assay kit was purchased from ENZO (New York, NY, USA). Cellular DNA fragmentation ELISA kit was purchased from Roche Diagnostics (Berlin, Germany). For immunofluorescence studies, anti-H2AX primary antibody (S139) was obtained from Millipore (Etobicoke, ON, Canada) and secondary antibody Alexa Flour 594 donkey anti-mouse from Life Tech (Carlsbad, CA, USA). Bicinchoninic acid (BCA) protein assay kit was purchased from Thermo Scientific (Chelmsford, MA, USA). The total antioxidant capacity (TAC) kit was purchased from Biovision (Milpitas, CA, USA). Antibodies for DNA-PK, p-ATM, p-ATR, p-Chk1, p-Chk2, p-H2AX, p-P53, Ku80, SOD1, catalase, GPX1, and beta-actin were purchased from Cell Signaling Technology (Danvers, MA, USA). p-DNA-PKcs antibody was purchased from Abcam (Toronto, ON, Canada). DNA-PK inhibitor [NU7026; (2-(morpholin-4-yl)-benzo[h]chomen-4-one)] was purchased from Sigma-Aldrich (Oakville, ON, Canada). NNK and NNK-Ae were purchased from Toronto Research Chemicals (Toronto, ON, Canada). Cisplatin, MTX, and NP-40 were purchased from Sigma-Aldrich (Oakville, ON, Canada). Apple flavonoid fraction (AF4) was isolated from apple peels as described previously [14]. Stock solutions were prepared in 100% dimethyl sulfoxide (DMSO), and the final concentrations never exceeded 0.5% (*v*/*v*) in culture treatment medium.

2.2. Cell Culture. Normal human bronchial epithelial cells (BEAS-2B) were purchased from American Tissue Type Culture Collection (ATCC; CRL-9609) and were cultured in BEGM media at 37°C in a humidified incubator with 5% CO_2. Cells were cultured on polystyrene T75 (75 cm^2) culture flasks, precoated with a mixture of 0.01 mg/mL fibronectin, 0.03 mg/mL bovine collagen type I, and 0.01 mg/mL bovine serum albumin dissolved in BEBM (basal) medium for overnight. Cells were grown to ~70% confluence during all experimental conditions and were used from early passages (<10) and within exponential growth phase.

2.3. Cell Viability by MTS Assay. Cell Titer 96™ aqueous cell viability assay (MTS) [18] was used to perform the viability of BEAS-2B cells under different treatment conditions. In order to find out the sublethal dose for AF4, a dose-dependent preliminary assay for various concentrations of AF4 was performed for 24 h. Similarly, the dose-response effect for various carcinogens (NNK, NNK-Ae, cisplatin, and MTX) was also standardized using this assay. For cytoprotection analysis, 1×10^4 cells were plated on a 96-well plate with media of 150 μL/well. After 24 h, cells were either pretreated with AF4 (50 μg/mL) prior to different carcinogen treatments (200 μM NNK; 100 μM NNK-A; 10 μM cisplatin; and 200 μM MTX) or alone with carcinogens for additional 24 h. Fifteen microliters of MTS reagent (with PMS) was then added to each well and incubated further 3 h at dark. Absorbance was recorded at 490 nm using a microplate reader (Infinite® 200 PRO, TECAN, Switzerland). DMSO control cells which are devoid of any treatments and cells containing only culture medium and MTS reagent served as the blank for each experiment.

2.4. Measurement of Intracellular ROS. The ROS level was measured in BEAS-2B cells after treatments as described previously [19]. 2′,7′-Dichlorofluorescin diacetate (DCFH-DA) is readily taken up by cells and is subsequently hydrolyzed to DCFH, which can be oxidized to measurable fluorescent product dichlorofluorescein (DCF). AF4-pretreated cells (for 1 h) were exposed to 3 h of carcinogens or alone in different experimental groups. Cells with only DMSO media

served as the vehicle control. After treatments, DCFH-DA was added to the cell culture plates at a final concentration of 5 μM followed by 40 min incubation at dark. The fluorescence degradation was then measured at an excitation wavelength of 490 nm and an emission wavelength of 510 nm by using Infinite 200 PRO, TECAN, Switzerland. The results were expressed as relative total ROS level with respect to DMSO control.

2.5. Total Antioxidant Capacity (TAC). A colorimetric-based method was used to measure intracellular TAC, according to the manufacturer's instructions with slight modification. Briefly, the total cell lysate was prepared after treatments in NP-40 lysis buffer (5 M NaCl, 1 M Tris, 10% NP-40). Each sample was added with 100 μL of freshly prepared Cu^{2+} working solution and incubated for 1.5 h at dark. The reduction (Cu^{2+} to Cu^{+}) reaction was then measured at 570 nm by using Infinite 200 PRO, TECAN, Switzerland. Trolox was used as the standard to quantify the TAC of the tested samples, and the results were expressed in Trolox equivalence.

2.6. γ-H2AX Immunofluorescence Assay. Immunofluorescence method [20] was used to measure the DNA damage at histone level by quantifying γ-H2AX foci in BEAS-2B cells. Briefly, 2×10^5 cells were seeded on a coated cover slip placed in a 6-well plate with 24 h incubation. For experimental setup, the cells were then treated with AF4 alone for 1 h or prior to each carcinogen treatment for 3 h (same treatment conditions were maintained for all following experiments). DMSO media served as a control for each test sample. After treatments, cells were washed thoroughly with PBS and fixed in 3.7% formaldehyde for 20 min at dark. The cells were then permeabilized with 0.5% Triton X-100 in PBS for 15 min on a rocker at room temperature followed by blocking with 4% BSA for 20 min. The cells were incubated with primary antibody (1 : 250) for 1 h at room temperature, washed three times with PBS, and then incubated with secondary antibody (1 : 500) for 45 min. After washing the cells three times in PBS, coverslips were carefully transferred into slides and mounted by using wet-mounting medium, Vectashield® containing DAPI and sealed with nail polish. The fluorescent images were then captured by using a microscopy (ZEISS, X-Cite series 120 PC) at 100x magnification.

2.7. DNA Fragmentation Analysis. DNA fragmentation in BEAS-2B cells was measured by cellular DNA fragmentation ELISA kit [21] as per the supplier's instructions. In short, BEAS-2B cells were labeled with 10 μM bromodeoxyuridine (BrdU) at 1×10^5 cells/mL density. Hundred microliters of BrdU-labelled cells in culture medium were treated as per above-mentioned conditions. The cells were then lysed with lysis buffer, and apoptotic DNA fragments in supernatants were collected for each sample after centrifugation at 270*g* for 10 min. Hundred microliters of the sample was then transferred to precoated anti-DNA 96-well, flat-bottom microplates with incubation for 90 min at 25°C. The DNA was then denatured by microwave irradiation (500 W for 5 min) followed by the addition of 100 μL anti-BrdU-POD conjugate solution with additional 90 min of incubation. The plates were washed by three times with wash buffer (1x), and 100 μL of substrate (TMB) solution was then added for color development. Twenty-five microliters of stop solution was added after 5 min, and the plates were read at 450 nm using a microplate reader (Infinite 200 PRO, TECAN, Switzerland).

2.8. Comet Assay. The comet assay was performed to measure the DNA tail moment as per kit instructions with minor modifications. After treatments, 1×10^5 cells were combined with molten LMA (low melting agarose) at a ratio of 1 : 10 (*v*/*v*) and 75 μL of each sample was pipetted on to a comet slide and incubated in dark at 4°C for 20 min. The slides were then immersed in cold lysis buffer at 4°C for 45 min followed by alkaline treatment (300 mM NaOH, 1 mM EDTA, pH > 13) for additional 45 min in dark. The slides were washed with TBE buffer (1x) for 5 min and subjected to horizontal electrophoresis conditions (1 V/cm for 10 min). The slides were air-dried after dipping in 70% ethanol for 5 min, stained with CYGREEN® dye (1 : 1000), and examined under epifluorescence microscopy (ZEISS, X-Cite series 120 PC; Toronto, ON, Canada) with 40x magnification (excitation/emission 489/515 nm). The comets were scored by commercially available software, OpenComet (http://www.cometbio.org), and a minimum of 50 cells was quantified by measuring percentage DNA tail moment.

2.9. Western Blotting. The cells were harvested after the treatments and were lysed using 1 × SDS lysis buffer (1 mM Tris–HCl [pH 6.8], 2% *w*/*v* SDS, 10% glycerol) under reduced conditions on the ice. Total protein concentration in each sample was measured by using BCA protein assay kit. A total of 25 μg of protein samples were loaded on 4–12% SDS-PAGE gel and electro-transferred to a nitrocellulose membrane. The membrane was then blocked with 5% nonfat milk solution, probed with specific primary antibodies (1 : 1000) for overnight incubation, washed and reprobed with respective secondary antibodies (1 : 2000) for 45 min, and then developed by enhanced chemiluminescence (ECL) method using Chemidoc MP (Bio-Rad, Mississauga, ON, Canada). Protein expression of each band was normalized with respective actin level, and relative protein expression was quantified with respect to untreated control bands for each experiment.

2.10. Statistical Analysis. All the experiments were performed in triplicates ($n = 3$) and for at least three independent times and analyzed by two-tailed Student's *t*-test by using GraphPad Prism software (GraphPad Software Inc., San Diego, CA, USA). Data were presented as mean ± standard deviation (SD), and p values ≤ 0.05 were considered as significant between experimental groups.

3. Results

3.1. Cell Viability and Cytoprotective Effects of AF4. In order to realize the sublethal dosage for AF4, preliminary dose-responsive effects on the viability of BEAS-2B cells were studied using MTS assay. A dose-responsive decline in cell viability was observed in BEAS-2B cells with increasing concentrations of AF4, especially at 100 and 200 μg/mL

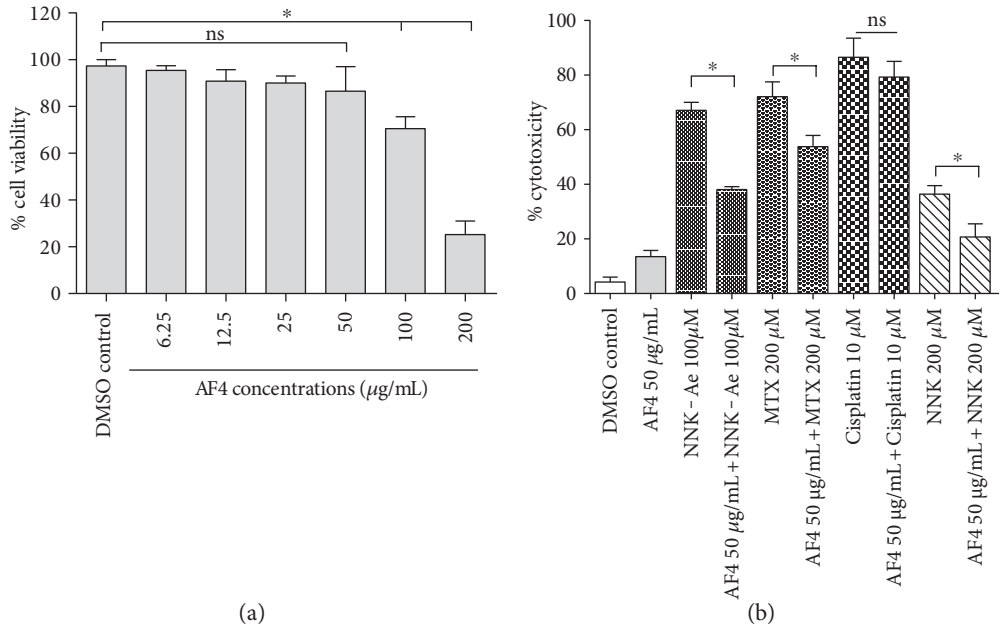

Figure 1: (a) Dose-dependent effect of AF4 on BEAS-2B cells after 24 h of treatment. (b) Cytoprotective effects of AF4 against various carcinogens challenged after 24 h of treatment. Experimental values presented as mean ± SD of $n = 3$ independent experiments. $*$ indicated statistical difference at $P \leq 0.05$. ns: nonsignificant.

(Figure 1(a)). However, over ≥80% cell viability was observed up to 50 μg/mL concentrations of AF4 and hence taken for evaluating protective effects in further experiments. Our previous studies have also shown that 50 μg/mL of AF4 did not alter cell viabilities of three primary normal cells treated for 24 and 48 h [17]. DMSO control in all experiments showed ≤5% cytotoxicity. After 24 h of treatments with each carcinogen, we observed a higher cytotoxicity (>50%) for 10 μM of cisplatin, 200 μM of MTX, and 100 μM of NNK-Ae (Figure 1(b)). Cisplatin exhibited a very high cytotoxicity (>80%) among the carcinogens studied. However, NNK did not show higher cytotoxicity for BEAS-2B cells (<50%). Likewise, for studying cytoprotective effects of AF4, we initially treated BEAS-2B cells with AF4 (50 μg/mL) prior to each carcinogen exposure. AF4 pretreatment showed significant ($p \leq 0.05$) reduction in cytotoxic level for NNK-Ae, MTX, and NNK exposed cells when compared to their treatments alone. In contrast, AF4 pretreatment did not show any significant reduction in cytotoxicity for cisplatin-treated cells and found to be morphologically distinct with rounded-shape or detached cells (data not shown).

3.2. ROS Mitigating and Antioxidant Potentials of AF4. Excessive ROS is one of the primary factors that can initiate DNA damage in healthy cells [22]. ROS level was studied either with AF4 alone or with carcinogen-treated BEAS-2B cells, and the data is shown in Figure 2(a). All the carcinogen-treated cells showed an almost two-fold increase in relative to total ROS (DMSO control) levels when compared to AF4-treated cells. Pretreatment with AF4 prior to each carcinogen exposure significantly ($p \leq 0.05$) reduced ROS levels in these cells. Interestingly, in all the AF4 preexposed cells, we observed similar levels of ROS despite each carcinogen tested in the study.

Antioxidants are well-known for their capacity to mitigate ROS generation, especially under oxidative stress, which is considered as the primary event in many diseases [23]. We assessed the antioxidant enzymes [superoxide dismutase (SOD), glutathione peroxidase (GPX), and catalase] (Figure 2(b)) and TAC (Figure 2(c)) in BEAS-2B cells after treated with either AF4 alone or with carcinogens. Preexposure of AF4 showed an increased SOD1 expression in NNK-Ae or MTX-treated samples when compared to their controls. However, both catalase and GPX levels remained almost the same in all the tested groups. TAC in AF4 preexposed groups showed greater antioxidant capacity than carcinogens alone. The findings indicate that AF4 has enhanced intracellular antioxidant potential.

3.3. AF4 Inhibits DNA-Histone Protein Damage. γ-H2AX immunofluorescence assay was used to analyze the DNA damage at histone level after each treatment conditions, and the results are shown in Figure 3(a). DAPI was used to stain the nucleus (blue color) colocalized with γ-H2AX foci, which appeared as red color when observed under fluorescence microscope. Cisplatin-, NNK-Ae-, or MTX-treated groups exhibited severe damage at histone level (S 139) when compared to DMSO control cells. Treatment with AF4 did not cause any increase in histone damage level when compared to DMSO control cells. Quantification of data (Figure 3(b)) showed that pretreatment with AF4 significantly ($p \leq 0.05$) inhibited γ-H2AX damage (foci/nucleus) level caused by NNK-Ae or MTX exposure. The DNA damage caused by cisplatin could not able to reduce by preexposure to AF4. As observed in other assays, cisplatin showed the

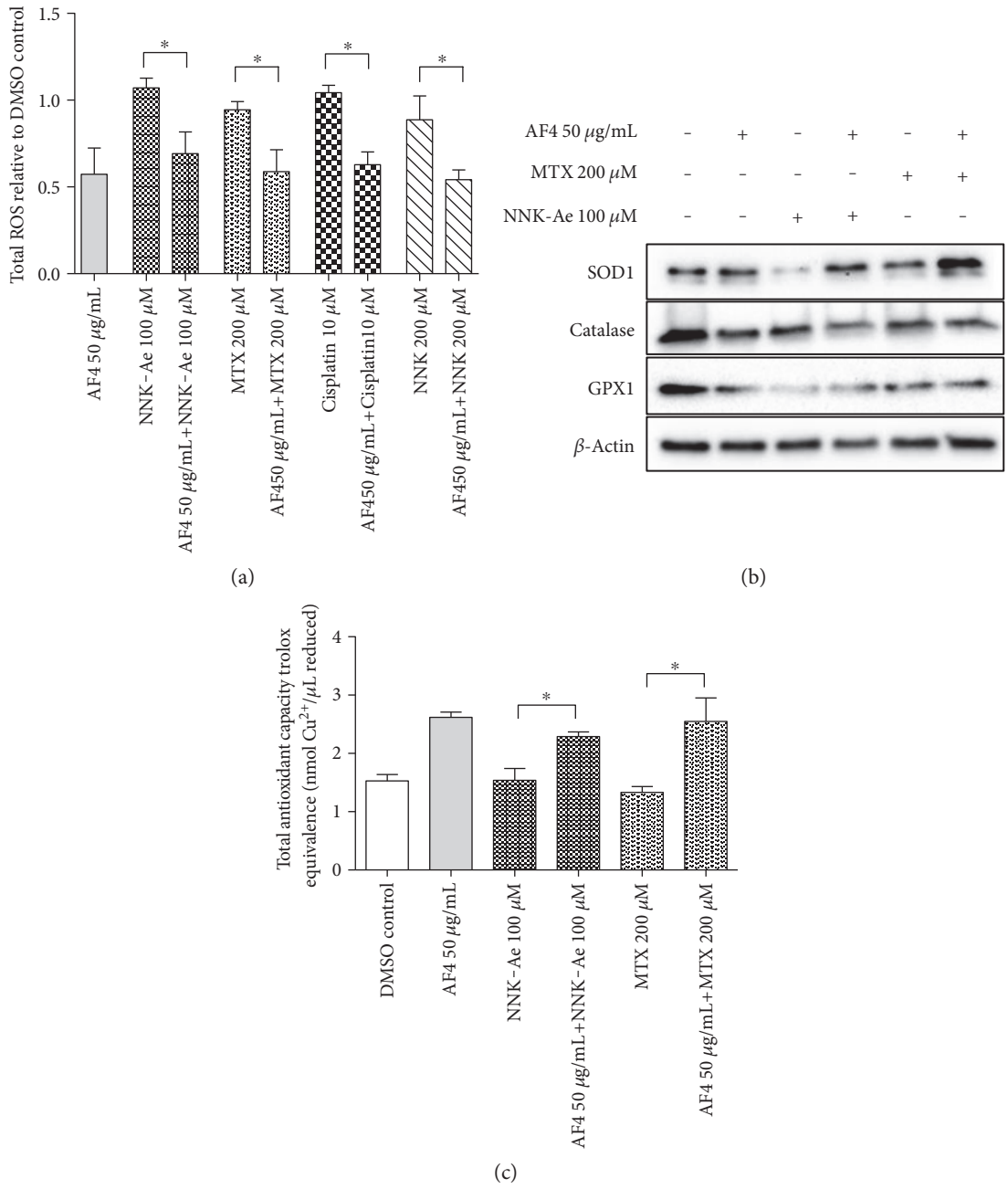

Figure 2: (a) The relative amount of ROS assessed on BEAS-2B cells after exposed to either carcinogen alone or with pretreatment of AF4. (b) Effects of AF4 on intracellular antioxidant enzymes (SOD1, catalase, and GPX1) along with carcinogen-treated groups as shown by western blotting. Beta-actin is used as in internal control to demonstrate equal protein in all tested samples. (c) TAC of BEAS-2B cells after various treatments was measured by a colorimetric kit-based method and showed in Trolox equivalence. Experimental values presented as mean ± SD of $n = 3$ independent experiments. $*$ indicated statistical difference at $P \leq 0.05$.

highest damage among all carcinogens tested. Cisplatin and NNK were therefore avoided from all the remaining studies since they are found to be either too toxic or less toxic, respectively, as observed from the γ-H2AX assay.

3.4. AF4 Protects DNA Fragmentation in BEAS-2B Cells. DNA fragmentation was considered as an early event that initiates the phosphorylation of H2AX histone proteins at Serine 139 position [24]. To investigate whether AF4 protects severe toxic effects of NNK-Ae or MTX at DNA level, we used an ELISA method and the fragmentation levels are shown in Figure 4. OD at 450 nm corresponds to the DNA fragmentation levels in BEAS-2B cells. The treatment with NNK-Ae and MTX enhanced the DNA fragmentation levels when compared to DMSO control. We do observe some DNA fragmentation in AF4-treated cells but was found to be nonsignificant with respect to DMSO control. Pretreatment with AF4 significantly ($p \leq 0.05$) reduced DNA fragmentation in both NNK-Ae- and MTX-treated groups and protect DNA integrity in these cells.

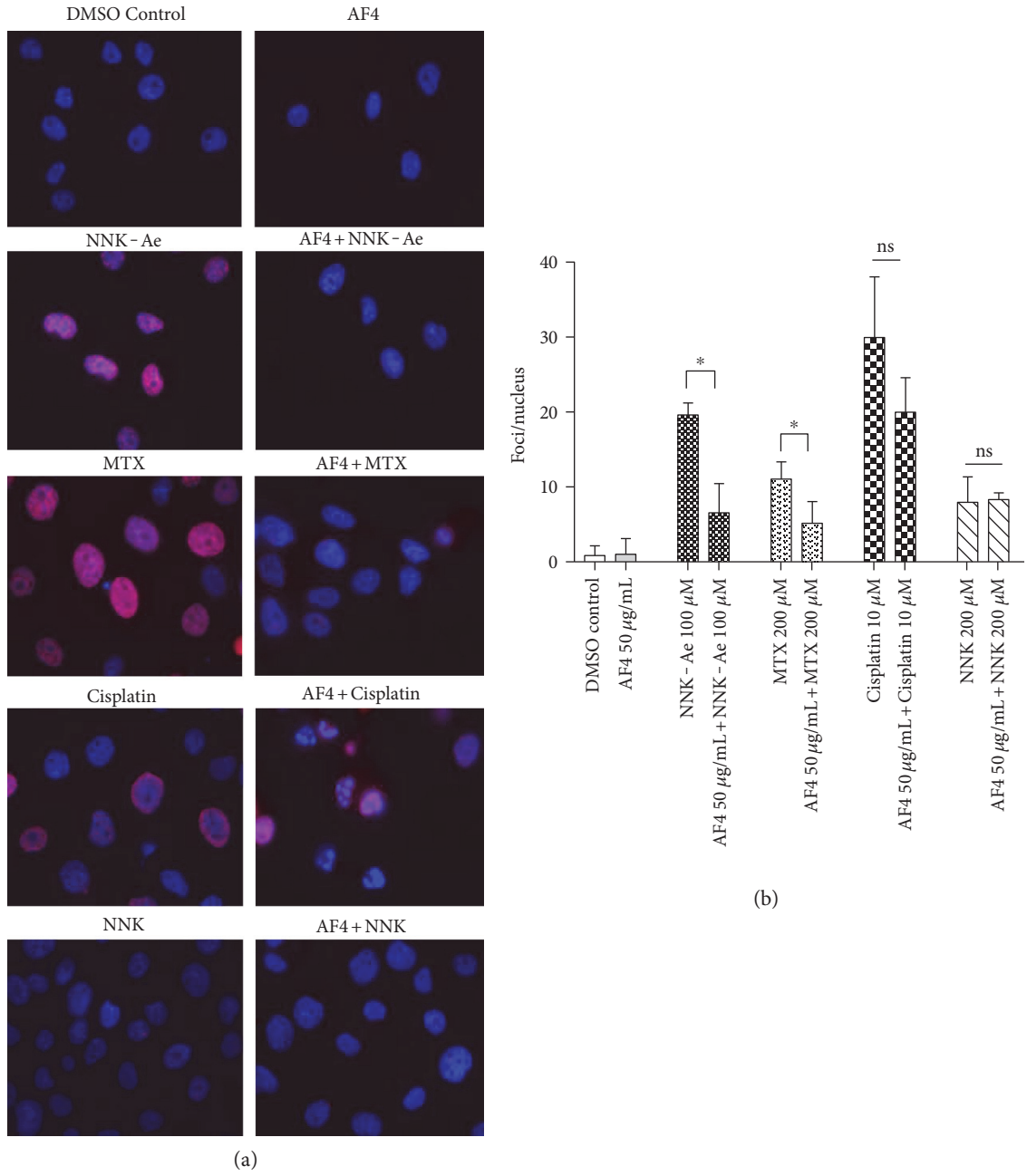

Figure 3: (a) BEAS-2B cells were exposed to either carcinogens alone or in combination with pretreatment of AF4 followed by immunofluorescence staining with γ-H2AX antibody and were captured by epifluorescence microscopy at 100x magnification. Nuclei were stained as blue and γ-H2AX foci (S 139) appeared as red. The image shown represents cells from three independent experiments. (b) Quantification of focus/nucleus ratio was calculated for each sample from at least 50 cells. $*$ indicated statistical difference at $P \leq 0.05$.

3.5. Preexposure to AF4 Reduces DNA Tail Damage. Comet assay was used to measure the DNA strand breaks in an individual eukaryotic cell and got multiple applications such as monitoring environmental contamination with genotoxins, human biomonitoring and molecular epidemiology, DNA damage, and repair studies [25]. After the treatments, DNA tail damage was evaluated as the migration of DNA from the nucleus and the data was quantified and depicted in Figures 5(a) and 5(b). Untreated cells (DMSO control) and AF4-treated cells retained their cellular integrity, and their percentage tail damage were <15%. Similar results were also observed for untreated PC12 neuronal cells [26]. BEAS-2B cells treated with either NNK-Ae or MTX showed a higher percentage of DNA damaged tails (97.4% and 68.0%, respectively), and AF4 pretreatment significantly ($p \leq 0.05$) reduced the length of percentage tail damage, as quantified from at least 50 comet cells. NNK-Ae-treated cells showed the highest DNA tail damage compared to MTX treatment at identical concentration and time.

3.6. AF4 Inhibits DDR Signaling and Facilitate Repair Mechanisms. We further investigated the mechanism of

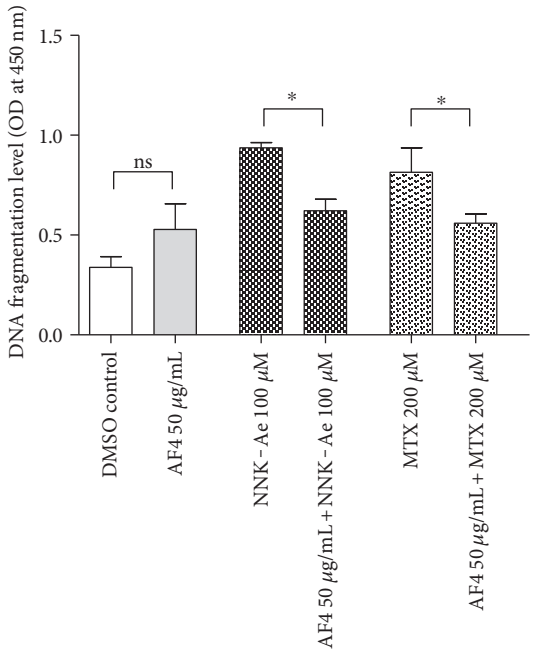

Figure 4: DNA fragmentation level in BEAS-2B cells after exposed to either carcinogen alone or in combination with pretreatment of AF4. OD at 450 nm corresponds to the amount of DNA fragments. Data expressed as mean ± SD of $n = 3$. * indicated statistical difference at $P \leq 0.05$.

action of AF4 to render protection against NNK-Ae- and MTX-induced toxicity in BEAS-2B cells by analyzing signaling proteins involved in DDR process. The phosphorylation levels of ATM, ATR, and DNA-PK were studied using western blotting (Figure 6). Cell cycle check point kinases Chk1 and Chk2 and tumor suppressor protein p53 were also analyzed and quantified (Figure 6). ATM/ATR mutations are the primary causes for DNA damage, and they act upstream of p53 sensors and sense DDR functions to the cells [9]. Treatment with NNK-Ae and MTX augmented DDR signaling and ATR phosphorylation (serine 428) in BEAS-2B cells with respect to control cells. However, we did not observe any phosphorylation of ATM protein at identical dosages and time. Expression of DNA-PK level was found to be the same with untreated control or carcinogen-treated cells. Interestingly, pretreatment with AF4 downregulated DNA-PK protein with respect to control cells. Effector proteins like Chk1, Chk2, and p53 were found to be phosphorylated in NNK-Ae-treated cells. In contrast, MTX treatment did not induce these signaling proteins. Pretreatment with AF4 showed significant ($p \leq 0.05$) reduction in the phosphorylation of ATR, Chk1, and p-53 levels in NNK-Ae-treated cells. We also observed a significant inhibition of γ-H2AX protein in AF4-pretreated cells prior to NNK-Ae treatment. Overall, our data showed that pretreatment with AF4 significantly attenuates DDR proteins especially challenged against NNK-Ae genotoxicity.

Further, to investigate whether AF4 facilitates DNA repair mechanisms in vitro, we also tested for proteins such as p-DNA-PKcs and KU80 with AF4-pretreated cells prior to NNK-Ae treatment (Figure 7(a)). Interestingly, AF4 reduced DNA-PK level either when treated alone or in combination with NNK-Ae but activates p-DNA-PKcs at the T2609 position. The phosphorylation level of DNA-PKcs was found to be comparatively higher in AF4-pretreated cells than in NNK-Ae-treated cells, indicating its DNA repairing potential. Further to confirm this, we have used NU7026 that inhibits DNA-PK protein expression [27]. Treatment with NU7026 on BEAS-2B cells for 20 μM (30 min) almost eliminated DNA-PK protein in these cells (Figure 7(b)). An autophosphorylated DNA-PKcs protein was observed in untreated cells, and treatment with inhibitor reduces the DNA-PKcs level even in AF4-pretreated cells. This preliminary result further confirms that AF4 pretreatment will facilitate the cells to phosphorylate DNA-PKcs which is essential in NHEJ repair mechanism.

4. Discussion

Aberrant mutations in the genome of an organism caused by increased exposure to a carcinogen often lead to a condition called genomic instability. Even low-dose chemicals or environmental exposure can induce DNA damage especially when there is a failure in proper DNA repair mechanism [28]. Due to the excessive ROS, a disturbance in natural antioxidant defense system is expected with damage to all biomolecules, including nucleic acids. Antioxidant-rich diet and nutraceutical supplements can be a good therapeutic strategy to overcome oxidative nucleic acid damage [29]. Hence, in this study, we have evaluated the apple flavonoids, which are a rich source of antioxidants [17, 30, 31] against various carcinogen-induced DNA damage in BEAS-2B cells. We also aimed to study the underlying mechanism of AF4's effects in DDR and repair process followed by DNA damage.

Our previous studies have demonstrated the selective cytotoxicity of AF4 to induce cell death in cancer cells without altering physiological functions of normal cells, including primary human hepatocytes (NHEPS), primary rat hepatocytes (RTCP-10), and primary lung cells (WI-38) [17]. To expand this knowledge, we have analyzed the impact of different doses of AF4 on the viability of BEAS-2B cells and observed that 50 μg/mL maintains cellular integrity with more than 80% viability even after 24 h treatment. However, higher doses were found to reduce the viability considerably and also reported by others [32], suggesting the hormetic effects of dietary flavonoids [14, 33]. Hence, we have chosen 50 μg/mL for evaluating the protective effects of AF4 in BEAS-2B cells. NNK, NNK-Ae, MTX, and cisplatin were used to induce DNA damage in BEAS-2B cells since we and others have observed that these carcinogens can significantly reduce cell viabilities of normal cells by enhancing ROS levels and cell death mechanisms [34, 35]. Pretreatment of AF4 significantly reduced toxic effects of these carcinogens but not for cisplatin treatment. This could be because of an increased intracellular antioxidant enzyme (SOD and small molecules or proteins, as observed in AF4-pretreated groups, which could possibly play a role in scavenging these ROS and helped the cells to mitigate the oxidative stress. Flavonoids are well-known for their ROS scavenging potentials

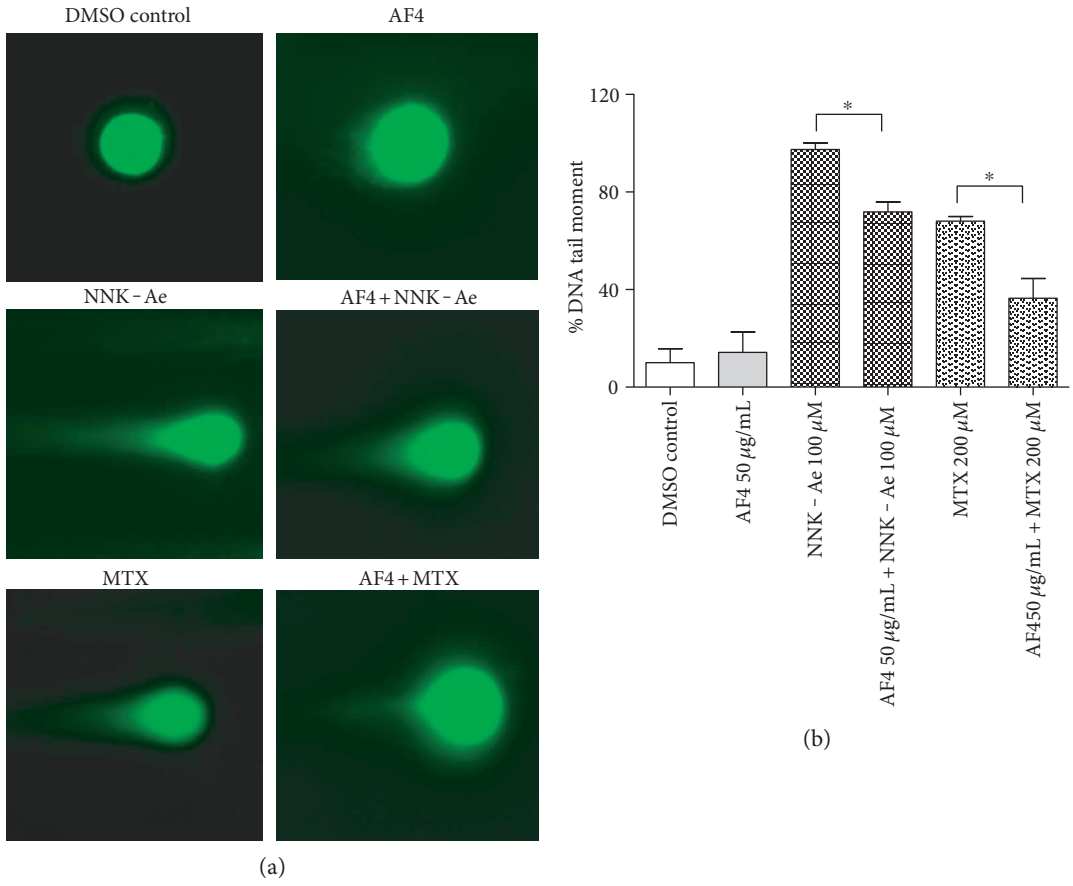

Figure 5: (a) DNA tail damage in BEAS-2B cells exposed to either carcinogen alone or in combination with pretreatment of AF4, as assessed by comet assay. (b) Quantification of DNA tail damage using OpenComet freeware. At least 50 comets for each sample were analyzed and examined with a fluorescence microscopy under 40x. Experimental values presented as mean ± SD of $n = 3$ independent experiments. ∗ indicated statistical difference at $P \leq 0.05$.

[14, 36], and similar effects for apples were reported by many investigators [15, 16, 31].

Histone posttranslational modifications are one of the earliest events in DSBs and are often characterized by remodeling of chromatin organization [37]. The carcinogens used in this study were observed to modulate posttranslational mechanisms of histone proteins even at 3 h of exposure. This observed toxicity could possibly due to the interstrand crosslink-induced DSBs that are produced at replication forks and are largely responsible for observed γ-H2AX foci in carcinogen-treated cells [38]. Each focus assumed to represent a single DSB [39]. However, pretreatment with AF4 inhibited the reorganization of histone variants that regulates DNA methylation. This could account for the similarities in protective effects of both at histone and DNA fragmentation, which appeared to be sensitive tools for analyzing DNA lesions. DNA fragmentation is considered as the hallmark of cell death mechanisms and an irreversible event that commits the normal cell to die [20]. AF4 was found to protect this phenomenon in BEAS-2B cells against NNK-Ae and MTX toxicity. Flavonoids are known to exhibit these protective potentials against various genotoxicity as evident from various studies [14, 29, 40, 41]. The fragmentation level observed in untreated cells could be because of the normal mechanism of the body to dispose large fragments of DNA from dying cells, which may be critical in maintaining normal tissue homeostasis [42].

Consequently, quantitative analysis was carried out by using comet assay to understand the extent of DNA damage caused by carcinogenic factors. Increased comet tails indicated the induction of DSBs through excision followed by resynthesis and ligation of fragments. A significant inhibition of DNA tail damage was recorded in AF4-pretreated cells when compared to carcinogen treatments, further, substantiate the potential of AF4 to render DNA protection in BEAS-2B cells. Taken together, we speculate that these protective effects are mainly due to either AF4's antioxidant properties or its ability to stimulate DNA repair enzymes. Polyphenols such as luteolin, quercetin, and rosmarinic acid have shown similar effects to protect DNA damage against oxidative stress in neuronal cells [14, 26]. A recent study has also shown that sesaminol, a lignin from sesame seeds with increasing activities of catalase and SOD, protects BEAS-2B cells against DNA damage caused from cigarette smoke extract [43]. All these studies confirm that plant polyphenols with antioxidant activity could counteract the toxic effects of carcinogens and may help to maintain genomic stability.

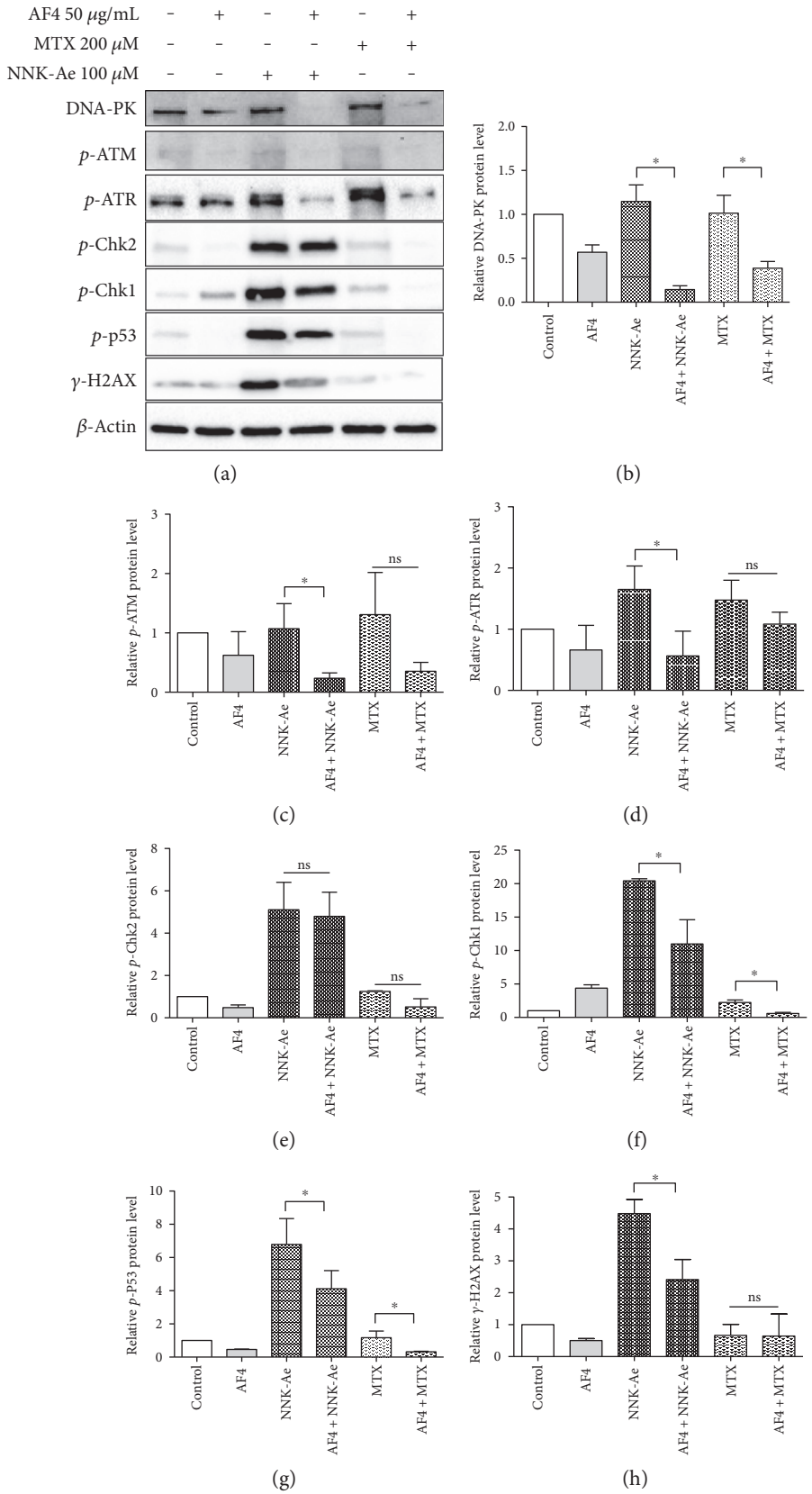

Figure 6: (a) Effects of AF4 on various DDR signaling proteins exposed to NNK-Ae or MTX as assessed by western blotting. (b), (c), (d), (e), (f), (g), and (h) The relative amount of each protein expression levels (DNA-PK, p-ATR, p-ATM, p-Chk2, p-Chk1, p-P53, and γ-H2AX) with respect to beta-actin loading control, quantified from at least 3 independent experiments. $*$ indicated statistical difference at $P \leq 0.05$ with mean $\pm$ SD. ns: nonsignificant.

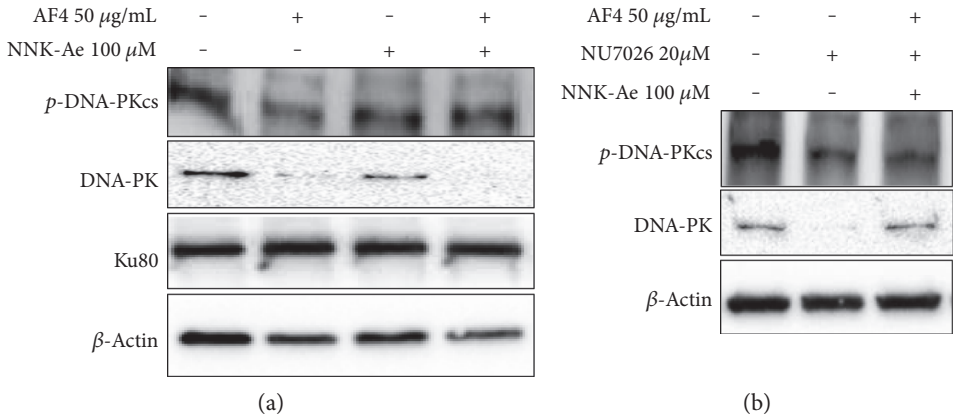

Figure 7: (a) Effects of AF4 on DNA repairing proteins (DNA-PK, p-DNA-PKcs, and KU80) challenged with NNK-Ae alone or in combination. (b) Inhibitory effect of NU7620 (20 μM for 30 mins) against DNA-PK expression on BEAS-2B cells treated alone or with a combination of AF4 and NNK-Ae.

In order to test our hypothesis, we further investigated the molecular mechanism of DSBs induced by NNK-Ae or MTX, since it is crucial to identify therapeutic targets during drug discovery process. The recruitment of DDR factors to DSBs was analyzed by immunoprobing against different proteins (ATM, ATR, DNA-PK, Chk1, Chk2, and p53). ATM/ATR mutation plays a key role in surveillance of genomic integrity along with signal transducers [38]. ATM-Chk2 or ATR-Chk1 are the two common pathways that get activated during DSBs and ultimately triggers p53 [44]. Our data showed that NNK-Ae induces DSBs through the phosphorylation of ATR and not ATM in BEAS-2B cells. ATR is the major kinase activated during a replication stress and plays a key role in "S" phase cell cycle arrest [11]. Effector proteins such as Chk1, Chk2, and p53 also became activated by NNK-Ae treatment. However, MTX did not induce these proteins in BEAS-2B cells. We speculate that lower dosage and exposure time for MTX may be ideal for inducing early events in DSBs but may not be sufficient to activate a cascade of effector proteins. Moreover, MTX is also known to have therapeutic applications when used at lower doses [45]. We have also observed the phosphorylation of DNA-PK at T2609 loci which is the most common target for its activation [46]. ATM/ATR often thought to coregulate DNA-PK expression in DSBs, but their choice of involvement still remains inconclusive [4, 11, 46].

Consistent with our immunofluorescence data, exposure to NNK-Ae triggers the phosphorylation of γ-H2AX as observed in western blot, further confirms the reorganization of histone proteins during DSBs. One hour of AF4 pretreatment significantly inhibits ATR/Chk1/p53/γ-H2AX signaling, suggesting the mechanism of protective effect possibly through ATR-dependent manner. Further, we also evaluated AF4's involvement in DNA repair mechanisms. AF4 slightly activates DNA-PKcs along with coexpression of KU80 protein in NNK-Ae-treated BEAS-2B cells. The activation of DNA-PKcs primarily enhances NHEJ repair mechanisms [4]. This effect of AF4 was confirmed by using a DNA-PK inhibitor, NU7026. However, more studies are required to claim DNA repairing efficacies of AF4 against NNK-Ae exposure. Overall, our study enlightens to be the first step in evaluating apple flavonoids against oxidative damage induced by carcinogens in bronchial epithelial cells.

In summary, our studies showed that preexposure of apple flavonoids protect BEAS-2B cells challenged against various carcinogens, especially nicotine-derived nitrosamine ketones, by inhibiting DDR signaling and initiate DNA repair mechanisms. Further studies can also give insights to understand the active constituents of AF4 that can also be developed as potential therapeutic adjuvants to reduce the side effects of various cytotoxic or genotoxic chemotherapeutics.

Abbreviations

AF4: Apple flavonoid fraction
ATM: Ataxia telangiectasia mutated
ATR: ATM-Rad3-related
BEAS-2B: Normal human bronchial epithelial cells
BEGM: Bronchial epithelial cell growth medium
CHK: Check point kinases
DDR: DNA damage response
DMSO: Dimethyl sulfoxide
DNA-PK: DNA-protein kinases
DSBs: DNA double-strand breaks
HR: Homologous recombination
IF: Immunofluorescence
MDC1: Mediators of DNA damage check point 1
MTX: Methotrexate
NHEJ: Nonhomologous end joining
NNK: 4-(Methylnitrosamino)-1-(3-pyridyl-d4)-1-butanone
NNK-Ae: NNK acetate
PI3K: Phosphatidylinositol-3-kinase
ROS: Reactive oxygen species.

Conflicts of Interest

No conflict of interest was declared by authors on this article.

Authors' Contributions

Vazhappilly Cijo George performed all the experiments, analyzed the data, and wrote the preliminary draft of the manuscript. H. P. Vasantha Rupasinghe is the principal investigator who designed the experiments and contributed to the manuscript.

Acknowledgments

The authors kindly acknowledge the financial support provided by the Discovery Grant program of the Natural Sciences and Engineering Research Council (NSERC) of Canada (2016-05269), Mitacs-Accelerate Program (IT07444), and CoraMedical, Toronto, ON, Canada. The authors would also like to thank Dr. Graham Dellaire of Faculty of Medicine, Dalhousie University for his valuable advices and support in the establishment and validation of the γ-H2AX assay.

References

[1] A. J. Davis and D. J. Chen, "DNA double-strand break repair via non-homologous end-joining," *Translational Cancer Research*, vol. 2, pp. 130–143, 2013.

[2] M. R. Lieber, "The mechanism of double-strand DNA break repair by the nonhomologous DNA end-joining pathway," *Annual Review of Biochemistry*, vol. 79, pp. 181–211, 2010.

[3] T. Helleday, E. Petermann, C. Lundin, B. Hodgson, and R. A. Sharma, "DNA repair pathways as targets for cancer therapy," *Nature Reviews Cancer*, vol. 8, pp. 193–204, 2008.

[4] M. Shrivastav, C. A. Miller, L. P. De Haro et al., "DNA-PKcs and ATM co-regulate DNA double-strand break repair," *DNA Repair (Amst)*, vol. 8, pp. 920–929, 2009.

[5] T. Bohgaki, M. Bohgaki, and R. Hakem, "DNA double-strand break signaling and human disorders," *Genome Integrity*, vol. 1, p. 15, 2010.

[6] P. Rajendran, E. Ho, D. E. Williams, and R. H. Dashwood, "Dietary phytochemicals, HDAC inhibition, and DNA damage/repair defects in cancer cells," *Clinical Epigenetics*, vol. 3, p. 4, 2011.

[7] A. Rahal, A. Kumar, V. Singh et al., "Oxidative stress, prooxidants, and antioxidants: the interplay," *BioMed Research International*, vol. 2014, Article ID 761264, 19 pages, 2014.

[8] K. L. Cann and G. G. Hicks, "Regulation of the cellular DNA double-strand break response," *Biochemistry and Cell Biology*, vol. 85, pp. 663–674, 2007.

[9] A. Marechal and L. Zou, "DNA damage sensing by the ATM and ATR kinases," *Cold Spring Harbor Perspectives in Biology*, vol. 5, pp. 1–17, 2013.

[10] J. W. Harper and S. J. Elledge, "The DNA damage response: ten years after," *Molecular Cell*, vol. 28, pp. 739–745, 2007.

[11] H. Yajima, K. J. Lee, and B. P. Chen, "ATR-dependent phosphorylation of DNA-dependent protein kinase catalytic subunit in response to UV-induced replication stress," *Molecular and Cellular Biology*, vol. 26, pp. 7520–7528, 2006.

[12] J. F. Goodwin, V. Kothari, J. M. Drake et al., "DNA-PKcs-mediated transcriptional regulation drives prostate cancer progression and metastasis," *Cancer Cell*, vol. 28, pp. 97–113, 2015.

[13] U. Moll, R. Lau, M. A. Sypes, M. M. Gupta, and C. W. Anderson, "DNA-PK, the DNA-activated protein kinase, is differentially expressed in normal and malignant human tissues," *Oncogene*, vol. 18, pp. 3114–3126, 1999.

[14] V. C. George, G. Dellaire, and H. P. V. Rupasinghe, "Plant flavonoids in cancer chemoprevention: role in genome stability," *The Journal of Nutritional Biochemistry*, vol. 45, pp. 1–14, 2017.

[15] P. G. Keddy, K. Dunlop, J. Warford et al., "Neuroprotective and anti-inflammatory effects of the flavonoid-enriched fraction AF4 in a mouse model of hypoxic-ischemic brain injury," *PLoS One*, vol. 7, article e51324, 2012.

[16] J. Warford, R. Quinton, D. Jones et al., "The flavonoid-enriched fraction AF4 suppresses neuroinflammation and promotes restorative gene expression in a mouse model of experimental autoimmune encephalomyelitis," *Journal of Neuroinflammation*, vol. 268, pp. 71–83, 2014.

[17] S. Sudan and H. P. V. Rupasinghe, "Flavonoid-enriched apple fraction AF4 induces cell cycle arrest, DNA topoisomerase II inhibition, and apoptosis in human liver cancer HepG2 cells," *Nutrition and Cancer*, vol. 66, pp. 1237–1246, 2014.

[18] P. Wang, S. M. Henning, and D. Heber, "Limitations of MTT and MTS-based assays for measurement of antiproliferative activity of green tea polyphenols," *PLoS One*, vol. 5, article e10202, 2010.

[19] H. Wang and J. A. Joseph, "Quantifying cellular oxidative stress by dichlorofluorescein assay using microplate reader," *Free Radical Biology & Medicine*, vol. 27, pp. 612–616, 1999.

[20] A. Ivashkevich, C. E. Redon, A. J. Nakamura, R. F. Martin, and O. A. Martin, "Use of the gamma-H2AX assay to monitor DNA damage and repair in cancer research," *Cancer Letters*, vol. 327, pp. 123–133, 2012.

[21] V. C. George, D. R. Naveen Kumar, P. K. Suresh, S. Kumar, and R. A. Kumar, "Comparative studies to evaluate relative in vitro potency of luteolin in inducing cell cycle arrest and apoptosis in HaCaT and A375 cells," *Asian Pacific Journal of Cancer Prevention*, vol. 14, pp. 631–637, 2013.

[22] V. Lobo, A. Patil, A. Phatak, and N. Chandra, "Free radicals, antioxidants and functional foods: impact on human health," *Pharmacognosy Reviews*, vol. 4, pp. 118–126, 2010.

[23] E. Birben, U. M. Sahiner, C. Sackesen, S. Erzurum, and O. Kalayci, "Oxidative stress and antioxidant defense," *World Allergy Organization Journal*, vol. 5, pp. 9–19, 2012.

[24] E. P. Rogakou, W. Nieves-Neira, C. Boon, Y. Pommier, and W. M. Bonner, "Initiation of DNA fragmentation during apoptosis induces phosphorylation of H2AX histone at serine 139," *The Journal of Biological Chemistry*, vol. 275, pp. 9390–9395, 2000.

[25] A. R. Collins, "The comet assay for DNA damage and repair: principles, applications, and limitations," *Molecular Biotechnology*, vol. 26, pp. 249–261, 2004.

[26] J. P. Silva, A. C. Gomes, and O. P. Coutinho, "Oxidative DNA damage protection and repair by polyphenolic compounds in PC12 cells," *European Journal of Pharmacology*, vol. 601, pp. 50–60, 2008.

[27] E. Willmore, S. de Caux, N. J. Sunter et al., "A novel DNA-dependent protein kinase inhibitor, NU7026, potentiates the cytotoxicity of topoisomerase II poisons used in the treatment of leukemia," *Blood*, vol. 103, pp. 4659–4665, 2004.

[28] S. A. Langie, G. Koppen, D. Desaulniers et al., "Causes of genome instability: the effect of low dose chemical exposures

in modern society," *Carcinogenesis*, vol. 36, Supplement 1, pp. S61–S88, 2015.

[29] S. K. Das, "Free radicals, antioxidants and nutraceuticals in health, disease & radiation biology. Preface," *Indian Journal of Biochemistry & Biophysics*, vol. 49, pp. 291-292, 2012.

[30] K. Wolfe, X. Wu, and R. H. Liu, "Antioxidant activity of apple peels," *Journal of Agricultural and Food Chemistry*, vol. 51, pp. 609–614, 2003.

[31] S. Sekhon-Loodu, S. N. Warnakulasuriya, H. P. V. Rupasinghe, and F. Shahidi, "Antioxidant ability of fractionated apple peel phenolics to inhibit fish oil oxidation," *Food Chemistry*, vol. 140, pp. 189–196, 2013.

[32] A. Murakami, "Dose-dependent functionality and toxicity of green tea polyphenols in experimental rodents," *Archives of Biochemistry and Biophysics*, vol. 557, pp. 3–10, 2014.

[33] E. J. Calabrese, "Converging concepts: adaptive response, preconditioning, and the Yerkes-Dodson law are manifestations of hormesis," *Ageing Research Reviews*, vol. 7, pp. 8–20, 2008.

[34] M. H. Hanigan and P. Devarajan, "Cisplatin nephrotoxicity: molecular mechanisms," *Cancer Therapy*, vol. 1, pp. 47–61, 2003.

[35] J. Xue, S. Yang, and S. Seng, "Mechanisms of cancer induction by tobacco-specific NNK and NNN," *Cancers (Basel)*, vol. 6, pp. 1138–1156, 2014.

[36] V. C. George, D. R. Kumar, P. K. Suresh, and R. A. Kumar, "Antioxidant, DNA protective efficacy and HPLC analysis of *Annona muricata* (soursop) extracts," *Journal of Food Science and Technology*, vol. 52, pp. 2328–2335, 2015.

[37] C. R. Clapier and B. R. Cairns, "The biology of chromatin remodeling complexes," *Annual Review of Biochemistry*, vol. 78, pp. 273–304, 2009.

[38] P. L. Olive and J. P. Banath, "Kinetics of H2AX phosphorylation after exposure to cisplatin," *Cytometry. Part B, Clinical Cytometry*, vol. 76, pp. 79–90, 2009.

[39] T. Tanaka, A. Kurose, X. Huang, W. Dai, and Z. Darzynkiewicz, "ATM activation and histone H2AX phosphorylation as indicators of DNA damage by DNA topoisomerase I inhibitor topotecan and during apoptosis," *Cell Proliferation*, vol. 39, pp. 49–60, 2006.

[40] M. Lohani, M. Ahuja, M. A. Buabeid et al., "Anti-oxidative and DNA protecting effects of flavonoids-rich *Scutellaria lateriflora*," *Natural Product Communications*, vol. 8, pp. 1415–1418, 2013.

[41] R. H. Hussein and F. K. Khalifa, "The protective role of ellagitannins flavonoids pretreatment against N-nitrosodiethylamine induced-hepatocellular carcinoma," *Saudi Journal of Biological Sciences*, vol. 21, pp. 589–596, 2014.

[42] J. Zhang, X. Wang, K. E. Bove, and M. Xu, "DNA fragmentation factor 45-deficient cells are more resistant to apoptosis and exhibit different dying morphology than wild-type control cells," *The Journal of Biological Chemistry*, vol. 274, pp. 37450–37454, 1999.

[43] P. Dong, X. Fu, X. Wang, W. M. Wang, W. M. Cao, and W. Y. Zhang, "Protective effects of sesaminol on BEAS-2B cells impaired by cigarette smoke extract," *Cell Biochemistry and Biophysics*, vol. 71, pp. 1207–1213, 2015.

[44] J. Smith, L. M. Tho, N. Xu, and D. A. Gillespie, "The ATM-Chk2 and ATR-Chk1 pathways in DNA damage signaling and cancer," *Advances in Cancer Research*, vol. 108, pp. 73–112, 2010.

[45] B. N. Cronstein, "Low-dose methotrexate: a mainstay in the treatment of rheumatoid arthritis," *Pharmacological Reviews*, vol. 57, pp. 163–172, 2005.

[46] B. P. Chen, N. Uematsu, J. Kobayashi et al., "Ataxia telangiectasia mutated (ATM) is essential for DNA-PKcs phosphorylations at the Thr-2609 cluster upon DNA double strand break," *The Journal of Biological Chemistry*, vol. 282, pp. 6582–6587, 2007.